Blood Supply and Vascular Reactivity of the Spinal Cord

Under Normal and Pathological Conditions

by

Nikolay Martirosyan

A Dissertation Presented in Partial Fulfillment
of the Requirements for the Degree
Doctor of Philosophy

Approved April 2016 by the
Graduate Supervisory Committee:

Mark C. Preul, Co-Chair
Brent Vernon, Co-Chair
Nicholas Theodore
Gerald Michael Lemole
Eric Vu

ARIZONA STATE UNIVERSITY

May 2016

ABSTRACT

The unique anatomical and functional properties of vasculature determine the susceptibility of the spinal cord to ischemia. The spinal cord vascular architecture is designed to withstand major ischemic events by compensating blood supply via important anastomotic channels. One of the important compensatory channels of the arterial basket of the conus medullaris (ABCM). ABCM consists of one or two arteries arising from the anterior spinal artery (ASA) and circumferentially connecting the ASA and the posterior spinal arteries. In addition to compensatory function, the arterial basket can be involved in arteriovenous fistulae and malformations of the conus. The morphometric anatomical analysis of the ABCM was performed with emphasis on vessel diameters and branching patterns.

A significant ischemic event that overcomes vascular compensatory capacity causes spinal cord injury (SCI). For example, SCI complicating thoracoabdominal aortic aneurysm repair is associated with ischemic injury. The rate of this devastating complication has been decreased significantly by instituting physiological methods of protection. Traumatic spinal cord injury causes complex changes in spinal cord blood flow (SCBF), which are closely related to a severity of injury. Manipulating physiological parameters such as mean arterial pressure (MAP) and intrathecal pressure (ITP) may be beneficial for patients with a spinal cord injury. It was discovered in a pig model of SCI that the combination of MAP elevation and cerebrospinal fluid drainage (CSFD) significantly and sustainably improved SCBF and spinal cord perfusion pressure. In animal models of SCI, regeneration is usually evaluated histologically, requiring animal sacrifice. Thus, there is a need for a technique to detect changes in SCI

noninvasively over time. The study was performed comparing manganese-enhanced

magnetic resonance imaging (MEMRI) in hemisection and transection SCI rat models

with diffusion tensor imaging (DTI) and histology. MEMERI ratio differed among

transection and hemisection groups, correlating to a severity of SCI measured by fraction

anisotropy and myelin load. MEMRI is a useful noninvasive tool to assess a degree of

neuronal damage after SCI.

DEDICATION

I'm dedicating this work to my parents who raised me and taught me what is right

and what is wrong, and two of my mentors who played a crucial role in the development

of my career as a physician-scientist.

Lyova M. Martirosyan and Marieta N. Apresyan

Nicholas Theodore, MD and Mark C. Preul, MD

ACKNOWLEDGMENTS

Maziyar A. Kalani, Edgar E. Babalov, Daniel D. Cavalcanti and Wyatt L. Ramey for

being by my side and unconditional support.

TABLE OF CONTENTS

LIST OF TABLES

LIST OF FIGURES

CHAPTER 1

Introduction

The blood supply of the spinal cord is very complex. Spatial and morphometric

organization of the vascular channels ensure uninterrupted and adequate blood flow to the

eloquent structures of the spinal cord under normal physiological conditions.

There are two main divisions of spinal cord vasculature: extrinsic and intrinsic.

The extrinsic vasculature connects the large vessels (i.e. the aorta, brachiocephalic and

pelvic arteries) to intrinsic spinal cord arteries. (Tveten, 1976, pp. 257-273) The radiculo-

medullary arteries are an important component of the extrinsic spinal cord vascular

system. The intrinsic vessel located on the surface of the spinal cord or within its fissures

and sulci. The terminal branches of the intrinsic arteries supply spinal cord tissue with

blood. The intrinsic system comprised by vasa corona, central and sulcal arteries

(Turnbull, 1973, pp. 56-84).

The arterial basket of conus medullaris (ABCM) is an important vascular

structure of the spinal cord. It consists of two arteries arising from the anterior spinal

artery on the ventral surface of the conus, and circumferentially anastomose with

posterior spinal arteries on the dorsal surface of the conus. The detailed morphometric

analysis of ABCM arteries was performed in the past. Also, it was unknown if the

ABCM gives rise to small perforating branches supplying conus medullaris tissue. We

have performed an anatomical study of ABCM on sixteen human cadaveric spines with

colored rubber silicone injected into spinal cord vascular system. In thirteen specimens

there was bilateral branching pattern of ABCM, and in three specimens there was a

unilateral branching of ABCM. The unilateral branching may be associated with higher

rate of ischemic events at the conus medullaris area. We also found by performing Nissl stain, that there are numerous small feeding arteries to the conus medullaris tissue arising from ABCM. This was the first time such anatomical structures were described.

The functional organization of the spinal cord vasculature allows the formation of the watershed zones. The watershed zones are areas of concurrent blood supply by two or more separate vascular feeders. Such a vascular architecture allows for redundancy of the blood supply to the functionally eloquent spinal cord tissue and provides protection from ischemia in the settings of dynamic blood flow alterations. There is a watershed zone in the anterior spinal artery between two adjacent radiculo-medullary arteries. Also, there is watershed zone between sulcal arteries and terminal branches of the central arteries (Bolton, 1939, pp. 137-148; Sliwa and Maclean, 1992, pp. 365-372). Chapter 1 reviews detailed anatomy and physiology of spinal cord vascular system under normal and different pathological conditions.

The blood flow autoregulation is an important function of the vasculature. The autoregulation allows maintaining constant blood flow to the spinal cord within a normal range of the mean arterial pressure (MAP) and partial arterial pressure of the carbon dioxide (paCO$_2$) (Ducker and Perot, 1971, pp. 413-415). There is delayed loss of autoregulation and ischemia after the spinal cord injury (SCI). The restoration of the autoregulation and ischemia prevention have crucial in the propagation of secondary SCI and results in improved clinical outcomes in experimental settings (Sandler and Tator, 1976, pp. 660-676).

It was also noted in patients undergoing abdominal aneurysm repair that a decrease of intrathecal spinal pressure (ITP) via cerebrospinal fluid drainage (CSFD) was

associated with the decrease of a rate of devastating paraplegia postoperatively (Robertazzi and Cunningham, 1998, pp. 29-34). Thus, our hypothesis was that aggressive elevation of the MAP combined with ITP reduction via CSFD is efficacious in improving SCBF after acute traumatic spinal cord injury. We performed a study in a pig model of spinal cord injury to evaluate our hypothesis. We found that isolated MAP elevation and CSFD lead to short-term improvement in SCBF. The combination of MAP elevation and CSFD resulted in sustained improvement of SCBF. This combined intervention could decrease the extent of spinal cord damage and improve neurologic outcomes.

The research in the spinal cord injury field is crucial for the understanding of pathological mechanisms and designing novel treatment options. The current standard for longitudinal assessment of spinal cord regeneration involves a sacrifice of multiple animals for histological assessment. A recent development of the magnetic resonance imaging (MRI) technology allowed development of in vivo repetitive modality to assess regeneration (Martirosyan NL, 2010, pp. 131-136). The manganese-enhanced MRI (MEMRI) allows for repeatable in vivo real-time imaging assessment of axonal transport in the injured spinal cord. The Mn^{2+} is a paramagnetic neuronal tracer that is transported via voltage-gated Ca^{2+} channels. Its uptake in functional active neuronal tissue allows assessing the regeneration (Tindemans I, 2003, pp. 3352-3360, Walder N, 2008, pp. 277-283). In our previous study, we were able to demonstrate that MEMRI T1-signal intensity correlates with manganese concentration measured by inductively coupled plasma mass spectrometry (Martirosyan NL, 2010, pp. 131-136). Our hypothesis was that MEMRI can be used to assess SCI as effectively as diffusion tensor imaging (DTI) and histology. We compared transection and hemisection SCI models with uninjured animals. We were able

3

to demonstrate that MEMRI correlates to injury severity and histological change in myelin content. MEMRI allows for a longitudinal study of SCI subjects and for reduction of study subjects.

Summary

The anatomy and physiology of spinal cord vascular system are crucial to understand mechanisms of SCI. A tool to assess spinal cord severity longitudinally in vivo could reduce the number of experimental study subjects. This dissertation addresses a means for understanding of anatomy and physiology of spinal cord blood supply, and the imaging of the spinal cord injury:

1. Reviewing current knowledge about anatomy and physiology of spinal cord blood supply.

2. Performing morphometric analysis and identifying branching patterns of ABCM.

3. Identifying a new paradigm to improve SCBF after spinal cord injury

4. Validating novel tool for longitudinal in vivo assessment of spinal cord injury severity

CHAPTER 2

Blood supply and vascular reactivity of the spinal cord under normal and

pathological conditions

The management of spinal cord injury remains challenging, despite intense

research efforts and the ongoing development of technology. Ischemia is recognized as

one of the most important factors determining severity of spinal cord injury and clinical

outcome (Rowland, Hawryluk et al., 2008, p. E2). The following review discusses the

current understanding of the structure and function of the vasculature in normal and

injured spinal cords.

Spinal Cord Vasculature

Arteries of the Spinal Cord

The intrinsic arteries of the spinal cord can be separated into a central and a

peripheral system. The central system, which supplies two-thirds of the spinal cord, is

derived from the anterior spinal artery (ASA) and its blood flow is centrifugal (Tveten,

1976, pp. 257-273). This system supplies the anterior gray matter, anterior portion of the

posterior gray matter and posterior white columns, inner half of the anterior and lateral

white columns, and base of the posterior white columns (Turnbull, 1973, pp. 56-84). In

the peripheral system, the blood flows centripetally from the posterior spinal arteries

(PSAs) and pial arterial plexus (Tveten, 1976, pp. 257-273). This system supplies the

outer portion of the anterior and lateral white columns and the posterior portion of the

posterior gray matter and posterior white columns (Fig. 1) (Turnbull, 1973, pp. 56-84).

The central and peripheral arterial systems have no precapillary interconnections. Their terminal branches, however, overlap allowing parts of the spinal cord to receive blood from both systems. This overlap occurs within the inner first quarter to first third of the white matter and within the outer edge of the gray matter. The exceptions are the posterior halves of the posterior horns, which are supplied entirely by the peripheral system. The widest internal overlap occurs in the posterior and lateral columns (Turnbull, Brieg et al., 1966, pp. 951-965). Extrinsically, the anastomosis between the systems is greatest around the tip of the cauda equina (Fig. 2) (Singh, Silver et al., 1994, pp. 314-322). Although there is some overlap between the systems because the blood flows away from the center in the central system and toward the center in the peripheral systems, their relationship is not truly compensatory.

The various regions of the spinal cord are disproportionately vascularized, and the ratio of blood supplied by the central system to the peripheral system is not constant throughout the cord. The cervical region has a large peripheral and large central arterial supply, the thoracic region has large peripheral and small central supply, and the lumbar and upper sacral regions have a small peripheral and large central supply (Hassler, 1996, pp. 302-307).

Obstruction of an artery feeding the cervical and lumbrosacral regions seldom results in an infarction, because these areas are well vascularized.
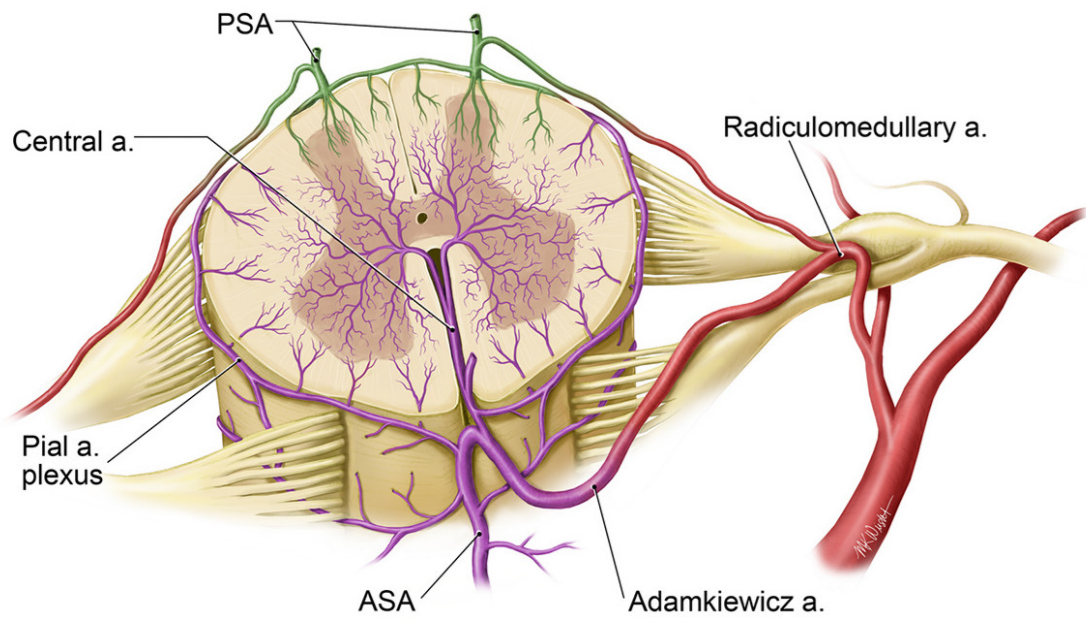
Figure 1. Vascularization of lumbar spinal cord. Contribution of the ASA and PSA in supplying the blood to the spinal cord. a. = artery/arterial. Used with permission from Nicholas Theodore, M.D.

The radicular (radiculomedullary) arteries reaching the upper cervical region are fed by intervertebral branches of the vertebral arteries and their descending rami (Lazorthes, Gouaze et al., 1971, pp. 253-262). In the lower cervical region the segmental arteries (which feed the radiculomedullary arteries) arise from the deep cervical artery, the costocervical artery (from the subclavian artery), or the ascending cervical artery. The many interconnections between these arteries and others in the neck allow blood flow despite occlusion. In the lumbar region arteries extend from the aorta and into the body wall where radicular arteries arise from them, some of which may be radiculomedullary arteries. The segmental arteries in the sacral region are supplied with blood from the lateral sacral arteries. These pelvic arteries form numerous anastomoses with other arteries of the pelvis. Therefore, not unlike in the cervical region, a single occlusion of an artery is unlikely to result in ischemia (Turnbull, 1973, pp. 56-84). Because none of the sacral radicular arteries contribute to the ASA or PSA, their obstruction is less threatening (Lazorthes, Gouaze et al., 1971, pp. 253-262).

The thoracic vascular region, however, is poorly collateralized and compromise of blood flow is creates the greates risk of ischemia. In thoracic cord, the distance between sources of blood supply is considerable. The radiculomedullary arteries feeding the thoracic spinal cord originate from a few intercostal arteries (from the subclavian artery and aorta), and anastomotic connections between the extraspinal arteries supplying this region are scarce (Turnbull, 1973, pp. 56-84). The compensatory support provided in the lumbar and cervical regions does not exist in the thoracic region; consequently, compromise of these arteries results in discreet regions of ischemia.

Extrinsic Spinal Cord Arteries

The ASA

The ASA, the trunk of the central arterial system, supplies most of the intrinsic spinal vasculature. Occlusion of this artery results in infarction of the anterior two-thirds of the spinal cord (Figs. 1 and 2) (Zeitin and Lichtenstein, 1936, pp. 96-111).

Before the vertebral arteries unite to form the basilar artery, each gives off a branch that join together and then descend on the surface of the anterior spinal cord as the ASA. Usually, these branches fuse within 2 cm of their origins, but they can remain separated until C-5 (Turnbull, Brieg et al., 1966, pp. 951-965). The ASA extends over the length of the spinal cord, ventral to the anterior median fissure (Turnbull, 1973, pp. 56-84).

The diameter of the ASA usually decreases gradually from its origin until it reaches the thoracic region. From the thoracic region down, the diameter of the ASA remains fairly constant. At the lower end of the sacral or coccygeal region, branches from the ASA loop caudally around the conus medullaris and join each limb of the PSA. The trunk of the ASA is then reduced to a tiny vessel, which extends along the conus and the filum terminale (Fig. 2) (Tveten, 1976, pp. 257-273).
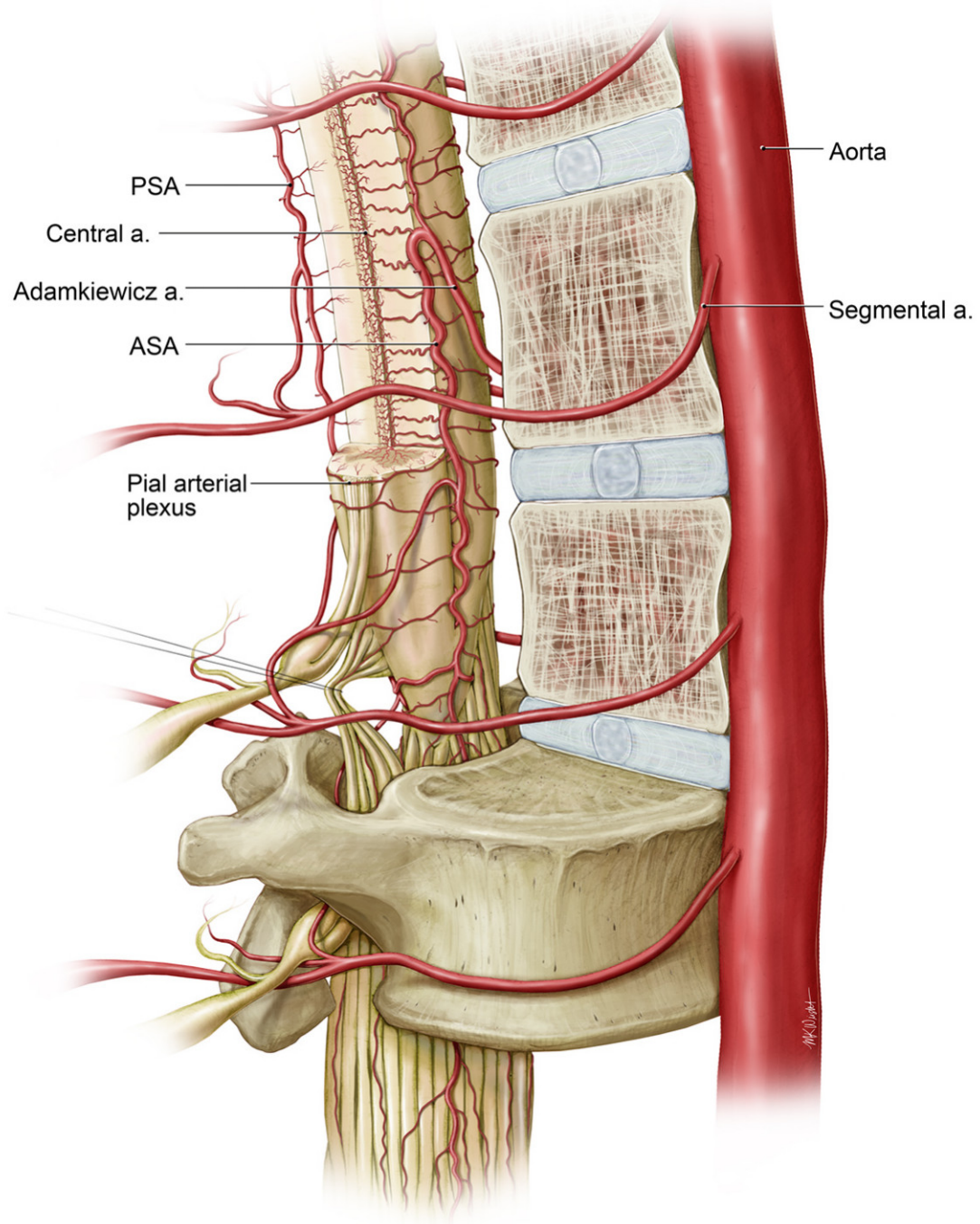
Figure 2. Anterolateral view of lumbar spinal cord. Used with permission from Nicholas Theodore, M.D.

Because the ASA is an anastomotic channel consisting of terminal branches of successive radiculomedullary arteries, its size varies in response to its conjunctions. The most striking example is at its junction with the great radicular artery (artery of Adamkiewicz), often at L-1 or L-2 on the left. In the lower thoracic region, before the vessels merge, the ASA becomes so small that it is almost indistinguishable from other arteries. At its juncture with the artery of Adamkiewicz, however, the ASA reaches its greatest diameter (Figs. 1 and 2) (Gillilan, 1958, pp. 75-103). Although rare, two radiculomedullary arteries may enter a single segment of the ASA from both sides. In this scenario, the shape of the ASA is often rhomboidal, a feature often noted in the cervical region (Tveten, 1976, pp. 257-273). The ASA is frequently duplicated for short distances in the lower cervical region and is singular in other regions (Turnbull, 1973, pp. 56-84).

The PSA

The paired PSA run longitudinally along the posterolateral surface of the spinal cord medial to the posterior nerve roots. The PSA can arise from the vertebral arteries or the posterior inferior cerebellar arteries. Much more rarely, it branches from the posterior radicular artery at C2. The PSAs swing laterally around the brainstem and then veer posteriorly along the surface of the cervical spinal cord (Turnbull, 1973, pp. 56-84). They are distinct single vessels only at their origin. Thereafter, they become anastomosing channels, largely retaining their embryonic plexiform design (Gillilan, 1958, pp. 75-103).

At the lower end of the spinal cord, the PSA sends out small branches to the proximal part of the posterior rootlets and nerve roots, most often in the roots of the

cauda equine (Tveten, 1976, pp. 257-273). The size of the PSAs varies. At times they become incredibly small, making them impossible to identify.

Pial Arterial Plexus

Surface vessels branching from both the ASA and the PSA form an anastomosing network, the pial arterial plexus (vasa coronae), which encircles the spinal cord (Gillilan, 1958, pp. 75-103). Most of the branches from the pial arterial plexus penetrate the dorsal midline of the spinal cord. All of the penetrating branches run directly inward, perpendicular to the surface of the spinal cord. These branches irrigate the outer portion of the spinal cord, including the greater part of the posterior horns, and extend to the substantia gelatinosa (Fig. 1) (Turnbull, Brieg et al., 1966, pp. 951-965).

Radicular Arteries

Among the 31 pairs of radicular arteries, there are three distinct types. Some radicular arteries end within the roots or on the dura mater before reaching the spinal cord. Some radicular arteries do not penetrate beyond the surrounding arterial systems of the spinal cord. Finally, some radicular arteries actually vascularize the spinal cord (i.e., medullary or radiculomedullary arteries). The diversity in the paths of the radicular arteries illustrates their various levels of supply. Radicular arteries supply blood to the dura mater, to the nerve roots that they accompany, to the spinal ganglia, and to the ASA and PSA (Lazorthes, Gouaze et al., 1971, pp. 253-262).

Radiculomedullary arteries are often located on the left side of the thoracic and lumbar regions (where the aorta is left of midline) and are more equally distributed in the

cervical region. Left sidedness dominance is more pronounced among the anterior

radiculomedullary arteries than the posterior radiculomedullary arteries, which

nonetheless are still more dominant on the left (Turnbull, 1973, pp. 56-84).

The typical segmental artery, which can originate from various sources (e.g.,

subclavian, aorta), divides into anterior and posterior rami. The posterior ramus splits into

a spinal arterial branch and a muscular arterial branch. The spinal branch crosses the

intervertebral foramen and divides into anterior and posterior radicular arteries (Sliwa

and Maclean, 1992, pp. 365-372). As noted, not all of these radicular arteries reach the

surface arteries of the spinal cord. The radicular arteries that traverse the nerve roots do

so on the anterior surface. After they reach the nerve root, they become encased in

perineurium and enter the subarachnoid space, where they are loosely attached to the

nerve roots. A single radicular artery can become an anterior or a posterior radicular

(radiculomedullary) artery, or, although rare, divide to become both (Turnbull, 1973, pp.

56-84).

The number of anterior radicular arteries that contribute to the ASA ranges from a

minimum of 2 to a maximum of 17, with an average of 10. The mean diameter of the

anterior radicular artery ranges from 0.2-0.8 mm. When the diameter of the artery is

smaller than 0.2 mm, it seldom reaches the ASA and usually serves to supply the root

(Turnbull, 1973, pp. 56-84).

Each region of the ASA receives different numbers of anterior radicular arteries.

The cervical ASA receives a mean angle of 0 to 6, the thoracic ASA receives 1 to 4, and

the lumbar ASA receives 1 or 2. The smaller arteries accompanying the roots of the

cauda equina are thought to become more important when large radicular arteries enter

the spinal cord at a relatively high position or when they become narrowed. Again, the scarcity of anterior radicular arteries and the extensive distance between them indicate that occlusion of a single artery in the thoracic region can result in ischemia (Turnbull, 1973, pp. 56-84).

Posterior radicular arteries, of which there can be 10 to 23 (range 12 to 16), divide on the posterolateral surface of the spinal cord to supply the ipsilateral PSA. These arteries are smaller than their anterior counterparts. Their diameters range from 0.2-0.5 mm. Posterior radicular arteries can originate as high as C-2 and are more frequent on the caudal portion of the spinal cord, where they are usually narrower. The posterior radicular arteries extend to feed the pial arterial plexus on the lateral aspect of the spinal cord, in addition to the nerve roots, dura mater, spinal ganglia and PSA (Sliwa and Maclean, 1992, pp. 365-372).

The number and position of the posterior radicular arteries do not appear to be related to the number and position of the anterior radicular arteries. When anterior and posterior radicular arteries occur at the same level and side, they unite to form a common stem outside the dura (Hassler, 1966, pp. 302-307).

The artery of Adamkiewicz (the arteria radicularis magna, the great radicular artery, the artery of lumbar enlargement) is the largest vessel that reaches the spinal cord. It is 1.0-1.3 mm in diameter, and it supplies a quarter of the spinal cord in 50% of people (Sliwa and Maclean, 1992, pp. 365-372). In 75% of people, this artery travels with roots T-9–T-12. In 10% it follows roots L-1 or L-2, and in 15% it has a high origin at dorsal roots T-5–T-8. In this final case, a more caudal supplementary artery called the arteria conus medullaris is always present (Lazorthes, Gouaze et al., 1971, pp. 253-262). The

artery of Adamkiewicz is found on the left side 80% of the time. When it joins the ASA, it branches into a small ascending branch (0.231 mm) and into a large descending branch (0.941 mm) (Figs. 1 and 2) (Parke, 1995, pp. 2073-2079, Turnbull, 1973, pp. 56-84).

Fried and Aparcio ligated the artery of Adamkiewicz and the ASA just above and just below the entrance of Adamkiewicz in monkeys to determine how the location of the blockage would alter perfusion of the spinal cord and neurological outcome (45 Fried and Aparicio, 1973, pp. 289-293). When the artery of Adamkiewicz was ligated just above the union of the vessels, neurological deficits were slight. However, ligations above the artery of Adamkiewicz produced mild to moderate chromatolysis and hyperchromatism. When a ligation was placed below the entrance, however, 82% of monkeys became paraplegic (Fried and Aparicio, 1973, pp. 289-293). These findings indicate that more caudal regions of the spinal cord rely heavily on the artery of Admkiewicz for perfusion.

Intinsic Spinal Cord Arteries

Central Arteries

Adults have a mean of 210 central arteries (Hassler, 1966, pp. 302-307). The central arteries feed the central area of the spinal cord, which consists of the white matter bordering the central sulcus, the gray matter of anterior horn, and the deep gray matter of posterior horn (Lazorthes, Gouaze et al., 1971, pp. 253-262). Central arteries arise from the ASA and penetrate the spinal cord posteriorly in the anterior median fissure. When central arteries stem from a duplicated portion of the ASA (often in the lower cervical region), they only pass to the side of the ASA from which they arise. Otherwise, when the artery reaches the anterior white commissure, it continues to either side of the spinal

cord. Less commonly, it bifurcates and each limb of the vessel retreats to the contralateral side of the spinal cord (Sliwa and Maclean, 1992, pp. 365-372). Successive central arteries usually alternate sides, but they also can extend to the same side. On reaching the anterior gray matter, the arteries divide into short ascending and descending branches and into horizontal branches, which often traverse the periphery of the gray matter before they transition into capillaries (Fig. 1) (Tveten, 1976, pp. 257-273).

If the central artery bifurcates, it always does so in the sagittal plane. It cannot be seen in transverse sections. Such bifurcations are least common in the cervical and thoracic regions (9% and 7%, respectively) and slightly more common in the lumbar and upper sacral regions (14% and 13%, respectively) (Fig. 2) (Hassler, 1966, pp. 302-307).

The dispersal and configuration of the central arteries, much like the radicular arteries, can be explained by the relative paucity of gray matter in the thoracic spinal region (Turnbull, 1971, pp. 141-147). There are fewer central arteries in the thoracic region, and they are smaller than those in the cervical and lumbosacral regions. The cervical region has 5-8 central arteries/cm of ASA compared to 2-6 and 5-12 in the lumbosacral region (Turnbull, 1971, pp. 141-147). The mean diameter of the central arteries is 0.21 ± 0.05 mm in the cervical region, 0.14 ± 0.04 mm in the thoracic region, 0.23 ± 0.6 mm in the lumbar region, and 0.2 ± 0.5 mm in the upper sacral region (Hassler, 1966, pp. 302-307).

In the less crowded cervical and thoracic regions, an acute angle is formed by the emerging central arteries and the ASA. In the lumbosacral region, a right angle is formed. As a result the central arteries in the lumbosacral region extend both horizontally and deeper into the spinal cord than the central arteries in the other regions. This difference is

the result of the angles, because the lengths of the central arteries are almost the same (cervical 4.5 ± 1.0 mm, thoracic 4.3 ± 0.9 mm, lumbar 4.7 ± 1.2 mm, and upper sacral 4.4 ± 1.1 mm) (Hassler, 1966, pp. 302-307). In the cervical region, and even more so in the thoracic region, the trunks of the central arteries traverse the spinal cord at an angle, covering the considerable longitudinal distance between arteries. Terminal branches of the central arteries stretch along the length of the spinal cord, overlapping with the territories of neighboring arteries. In the thoracic region the central arteries send most of their branches longitudinally, while those in the cervical and lumbosacral region mainly branch horizontally (Tveten, 1976, pp. 257-273). A central¬¬ artery in the thoracic region can cover as much as 3.0 cm. In contrast, it can cover no more than 1.2 cm in the cervical region and no more than 1.7 cm in the lumbosacral region (Turnbull, 1971, pp. 141-147).

Capillaries of the Spinal Cord

As is common in the vasculature of the spinal cord, the white matter is not served by capillary beds as abundantly as by the gray matter. In fact, the density of the capillary bed is 5 times greater in gray matter than in white matter. The capillary beds in white matter are also fairly uniform, stretching longitudinally in the direction of the nerve fibers. Where the gray and white matter meet, the capillary beds are denser than those in white matter alone. Within the gray matter, the density of the beds depends on the location of the cell bodies. This arrangement reflects the greater metabolic requirements of cell bodies compared to axons (Turnbull, 1971, pp. 141-147).

The lateral horns, anterior horns, and base of the posterior horns (especially the substantia gelatinosa) have the thickest capillary beds, although the remainder of the posterior horns is not well supplied (Turnbull, 1973, pp. 56-84). Knots of vessels (glomeruli) exist in and around the capillary beds of the anterior and posterior horns. These glomeruli consist of many different vessels entwined with one another as well as single coiled channels. The capability of these glomeruli to act as sensors to direct autonomic blood flow of the spinal cord is supported by the presence ot muscular cushions in the intima of the lower (inferior thoracic, and lumbrosacral) ASA and their sensory (afferent and efferent) junctions (Parke, 2004, pp. 558-563).

Direction of Arterial Blood Flow

The watershed effect occurs when two streams of blood flowing in opposite directions meet, as is common in the vascular system of the spinal cord. In a watershed area the likelihood of the surrounding tissues suffering from occlusion increases. Local pressure from a space occupying lesion which may not cause any vascular compromise elsewhere can result in ischemia in the watershed region (Bolton, 1939, pp. 137-148).

At the union of a radicular artery and the ASA, the blood courses upward and downward from the entry point. Therefore, in the area of the ASA between neighboring radicular arteries, there is a dead point where blood flows in neither direction, that is, a watershed area. The location of this dead point fluctuates constantly. In the midthoracic area, where the distance between radicular arteries is the greatest, the watershed effect is at its maximum (Sliwa and Maclean, 1992, pp. 365-372).

The blood flow in the PSA does not mirror that of the ASA. The PSA does not narrow like the ASA and thus does not provide a mechanical barrier to upward flow. When Bolton injected a solution with Indian ink into the vertebral arteries of human corpses and followed its path, the blood running down the PSA reached the highest thoracic segments (Bolton, 1939, pp. 137-148). At this point the vertebral blood met the blood flowing up from the caudal part of the ASA via two terminal braches. These terminal branches pass caudal to the fifth anterior sacral roots, and each one joins with a single PSA, lateral to the fifth posterior sacral roots (Fig. 2). The ascending blood flow of the caudal portion of the PSA is often reinforced by posterior lumbar radicular arteries (Bolton, 1939, pp. 137-148).

As noted, the artery of Adamkiewicz, the most notable of the radicular arteries, joins the ASA with a small ascending branch and a larger descending branch. Resistance to flow through the upper branch is 278 times greater than in the downward branch, because the diameter of the ascending branch is much smaller (0.231 mm) than that of the descending branch (0.941 mm) (Hitchon, Lobosky et al., 1987, pp. 849-857). Under normal conditions in humans, the ascending branch of the artery of Adamkiewicz is required to supply the arterial domain of the upper one to three thoracolumbar segments, and its relatively small blood flow is sufficient. It is likely, however, that under the collateral demands of aortic cross-clamping during surgery, the quantity of blood flow to the higher midthoracic area is unreliable. In the ASA the blood flow may be modified by contraction of the conventional circular musculature of the tunica media, the generally longitudinally disposed layer of the intimal musculature, and the intimal cushions near

and in the critical vascular junction just below the boundary between the thoracolumbar and midthoracic arterial domains (Hitchon, Lobosky et al., 1987, pp. 849-857).

Autoregulation

Autoregulation is the process that assures constant blood flow when systemic blood pressure or CO2 concentrations rise or fall. While the blood flow in the spinal cord is 40-60% that of the brain, the tissue oxygen levels are the same (35-39 mm Hg) (Ducker and Perot, 1971, pp. 413-415). The volume of blood perfusing the spinal cord increases when arterial CO2 tension increases and falls when it decreases. Vasodilation and constriction enable these changes to occur without altering the spinal cord blood flow (SCBF) (Smith, Pender et al., 1969, pp. 1158-1163).

Effect of Mean Arterial Pressure and CO2 Pressure on SCBF

Research has been done on various animals to determine the ranges of mean arterial pressure (MAP) and CO2 pressure in which autoregulation is maintained. In sheep blood flow in the gray and white matter in both the cervical and lumbar regions remains steady when MAP ranges between 40 and 100 mm Hg (Lobosky, Hitchon et al., 1984, pp. 264-267).

Hitchon and associates used lambs to measure SCBF, because the white and gray matter in their spinal cords are markedly distinct (Hitchon, Lobosky et al., 1987, pp. 849-857). When MAP was between 100 and 40 mm Hg, SCBF in the cervical gray and white matter (124-141 ml/100g/min and 22-26 ml/100g/min, respectively) and in the lumbar gray and white matter (74-104 ml/100g/min and 15-24 ml/100g/min, respectively) all

20

remained fairly stable. When MAP fell below 40 mm Hg, SCBF dropped significantly

(Hitchon, Lobosky et al., 1987, pp. 849-857).

Kobrine and associates found that when CO2 pressure was between 10 to 50 mm

Hg in monkeys, SCBF stayed constant (Kobrine, Doyle et al., 1975, pp. 573-581). When

the pressure of CO2 surpassed 50 mm Hg, SCBF increased. Further increases above 90

mm Hg had no effect on SCBF, which had reached a physical maximum (Kobrine, Doyle

et al., 1975, pp. 573-581). In another study, Kobrine and associates found that SCBF

remained constant when MAP was between 50 and 135 mm Hg (Kobrine, Evans et al.,

1977, pp. 54-55). Below 50 mm Hg vascular resistance decreased maximally, and SCBF

became a function of MAP. When MAP exceeded 135 mm Hg, vascular resistance

decreased, vasodilatation occurred, and SCBF increased markedly. These findings are

clinically relevant because the capillary endothelium responsible for the normal blood-

brain barrier can be disrupted in this hypertensive environment and high SCBF can result

in the formation of edema, which can be detrimental to neural function (Kobrine, Evans

et al., 1977, pp. 54-55).

Mechanism of autoregulation

In research by Young and associates, cats received paravertebral

sympathectomies, adrenalectomies, or both to determine whether paravertebral

sympathetic ganglia or the adrenal gland was involved in autoregulation (Young,

DeCrescito et al., 1982, pp. 706-710). There was no autoregulation of SCBF in response

to systemic pressure changes in cats with sympathectomies, and there was a linear

relationship between MAP and SCBF. In the control and adrenalectomy groups, SCBF

did not correlate with MAP between 80 to 160 mm Hg. Therefore, the sympathetic

ganglia are a necessary component of spinal cord autoregulation (Young, DeCrescito et

al., 1982, pp. 706-710). In contrast, Iwai and Monafa (1992) found only moderate effects

on regional SCBF after they performed lower lumbar sympathectomies in rats.

Proximal transections have been performed to help determine the location of the

sensory control center for autoregulation. These procedures do not influence the response

of MAP and CO2, indicating that the sensory control center for autoregulation lies caudal

to the medulla (Kindt, 1971, pp. 19-23, Kobrine, Evans et al., 1977, pp. 54-55).

Glomeruli found in capillary beds within the spinal cord may act as sensors within the

spinal cord (Kindt, 1971, pp. 19-23). One reason for this supposition is that these

glomeruli resemble arteriovenous glomerular clumps, which are found in fingers, toes,

the penis, and other parts of the body, act as components of nerve root circulation capable

of shunting blood from arteries to veins and bypassing the capillaries. Such shunting can

also occur in the spinal cord. Further research is needed to cement this theory (Kindt,

1971, pp. 19-23).

Both alpha and beta components of the sympathetic nervous system influence

autoregulation of SCBF. When alpha components were blocked, Kobrine and associates

found that autoregulation of the spinal cord ceased and MAP and SCBF displayed a

linear relationship (Kobrine, Evans et al., 1977, pp. 54-55). When beta components were

blocked, autoregulation was sustained at a higher than normal threshold, signaling the

affect of the beta components of decreasing the MAP in which autoregulation occurs

(Kobrine, Evans et al., 1977, pp. 54-55).

Aortic Cross-Clamping

During repair of thoracoabdominal aortic aneurysms, temporary aortic cross-clamping (AXC) decreases SCBF and distal organ perfusion (Barone, Joob et al., 1988, pp. 535-540). After an hour of AXC, thoracolumbar SCBF has been reported to decrease from 20 to 1.8 ml/100g/min (Gharagozloo, Neville et al., 1998, pp. 73-86) AXC causes distal hypotension (below the clamp), proximal hypertension (above the clamp), left ventricle afterload, and an increase in cerebrospinal fluid pressure (CSFP) and central venous pressure (CVP). AXC also elevates intracranial pressure to a magnitude that cannot be reproduced by phenylephrine, nor that can be deferred by sodium nitroprusside (D'Ambra, Dewhirst et al., 1988, pp. III198-III202). The induction of proximal hypertension and intracranial pressure during AXC prompts the autoregulatory mechanisms of the cerebral and spinal vasculature to increase CSFP reflexively, effectively lowering spinal cord perfusion pressure (SCPP) and diminishing the blood supply to the spinal cord (Robertazzi and Cunningham, 1998, pp. 29-34). Systemically, a spinal cord injury causes hypotension not only by interrupting sympathetic fibers but also by direct myocardial dysfunction. With its limited blood supply and the most deleterious watershed effect, the thoracolumbar spinal cord is the portion of the spinal cord at greatest risk for ischemic injury (Svensson, Stewart et al., 1988, pp. 823-829).

Understanding the relationships among distal and proximal blood pressure, CSFP, SCPP, and MAP is necessary to solve the problems that can arise during AXC. SCPP is a key measure used to evaluate the circulation of the spinal cord. SCPP is equal to the

23

difference between the mean distal aortic pressure (DAP) and CSFP (Robertazzi and Cunningham, 1998, pp. 29-34). SCPP must stay above 50-60 mm Hg to protect the spinal cord from ischemia (Kazama, Masaki et al., 1994, pp. 112-115, Mauney, Blackbourne et al., 1995, pp. 245-252).

Several studies have supported the notion that SCPP is more relevant in determining SCBF than are CSFP and MAP. Griffiths and associates exemplified this point when they raised SCPP significantly (from 5 to 123 mm Hg) in dogs while maintaining CSFP and observed a stealthy rebound of the SCBF (Griffiths, Pitts et al., 1978, pp., 1145-1151). In this study SCBF autoregulation was lost when SCPP fell below 50 mm Hg. As the SCPP was lowered from baseline to 50 mm Hg, the vascular resistance decreased. Below 50 mm Hg the resistance was unchanged, perhaps because the vessels were fully dilatated and compressed by the CSFP (Griffiths, Pitts et al., 1978, pp., 1145-1151).

Taira and Marsala correlated proximal aortic pressure (PAP) with DAP during AXC and with proportional decreases in DAP and SCBF after the aorta was unclamped (Taira and Marsala, 1996, pp. 1850-1858). When PAP was held above 100 mm Hg during AXC, DAP was 19 ± 4 mm Hg. When PAP was held at 40 mm Hg, DAP fell to 7 ± 1 mm Hg. After the clamp was released while PAP slowly decreased so did the SCBF. The decrease in SCBF was 8 ± 4% of baseline values when PAP was held above 100 mm Hg and 2.5 ± 1.6% of baseline values when PAP was 40 mm Hg. Therefore, SCBF can increase as a result of increasing PAP during and after AXC. This point is clinically relevant because at lower PAPs neurological deficits were incurred more quickly than at higher PAPs (Taira and Marsala, 1996, pp. 1850-1858). In dogs Laschinger et al. showed

that a DAP of 60-70 mm Hg was adequate to maintain spinal cord function during AXC (Laschinger, Cunningham et al., 1983, pp. 417-426). When DAP fell below 40 mm Hg, somatosensory evoked potentials (SSEPs) were often lost and a spinal cord injury was incurred (66% paraplegia). Maintaining DAP above 70 mm Hg uniformly preserved SCBF as long as critical intercostal arteries remained intact.

The direct relationship between CSFP and CVP has been shown in various studies (Clark, Mutch et al., 1992, pp. 357-364). In dogs, Piano and Gewertz showed that although CSFP and CVP both increased significantly with AXC, the increase in CSFP was always equal to or more than the venous increase (Piano and Gewertz, 1990, pp. 695-701). With volume loading this trend continued, supporting the relationship between CSFP and CVP. The mechanism that links the CSFP and CVP relies on the structure of the venous system of the spinal cord. Radicular veins extend from the sinusoidal channels of the spinal cord and travel through dural space, dura, and epidural fat before joining the larger veins. As the veins traverse this labyrinthine route, they narrow. When CSFP within the tissue of the spinal cord becomes higher than venous pressure, the vein collapses. Outflow resistance and venous pressure then increase (Piano and Gewertz, 1990, pp. 695-701).

In humans the normal range of CSFP is 13 to 15 mm Hg, while its range during AXC is 21 to 25 mm Hg. Berendes et al. (1982) found that when CSFP remained below 20 mm Hg in patients during thoracic aortic operations (87.5%, n=8), no postoperative neurologic deficits were evident. When CSFP exceeded 40 mm Hg during the operation (12.5%), paraparesis developed postoperatively (Kazama, Masaki et al., 1994, pp. 112-

115). Blaisdell and Cooley found that when CSFP was higher than DAP, the incidence of paraplegia increased by 17% (Blaisdell and Cooley, 1962, pp. 351-355).

Molina and associates observed that when the clamp was released after an hour of AXC, CSFP remained elevated for 5 minutes and returned to normal only after another 25 minutes. After the clamp was released, hyperemia was observed in both the gray and white matter from T-12 down. The degree of hyperemia, however, was much greater in the gray matter (Molina, Cogordan et al., 1985, pp. 126-136).

Risks and Neurological Deficits

Neurologic deficits are a considerable risk associated with surgeries that employ AXC. Svensson and colleagues reviewed 1509 patients who underwent repairs to treat thoracoabdominal aortic disease of varied severity. Among these patients, the incidence of paraplegia or paraparesis was 16% (Mauney, Blackbourne et al., 1995, pp. 245-252). In a study of 121 cases of thoracoabdominal aortic aneurysms repair cases by Cinà and associates, neurological deficits were recorded in 6.2% of patients, and the hospital mortality rate was 21.4% (Cinà, Lagana et al., 2002, pp. 631-638).

The complexity of the repair is a significant predictor of spinal cord injury. The Crawford classification system organizes thoracoabdominal aortic aneurysms repairs based on the extent and position (Crawford ES, Crawford JL et al., 1986, pp. 389-404). Type I aneurysms extend from the proximal descending thoracic aorta to the upper abdominal aorta. Type II aneurysms extend from the proximal descending thoracic aorta to below the renal arteries. Type III aneurysms extend from the distal half of the descending thoracic aorta into the abdomen. Type IV aneurysms involve most or all of

the abdominal aorta. Repairs of types I, II, III and IV were associated with rates of

paraplegia or paraparesis of 15%, 31%, 7%, and 4%, respectively (Mauney, Blackbourne

et al., 1995, pp. 245-252). In a randomized study, Crawford and associates found that

there was a 32% incidence of neurological deficits (of varied severity and duration)

affecting the legs associated with type I and II repairs (Mathé, Roger et al., 1998, pp.

110-116).

In the 1970s the first attempts at improving thoracoabdominal aortic aneurysm

surgery focused on decreasing the duration of surgery (Winnerkvist A, Bartoli S et al.,

2002, pp. 6-10). Time is clearly an important indicator of neurological outcome. Repairs

requiring more than 60 minutes of aortic occlusion were reported to carry a 20% risk of

paraplegia and paraparesis, whereas the risk for 30 minutes of occlusion was less than

10% (Mauney, Blackbourne et al., 1995, pp. 245-252). When spinal cord ischemia was

sustained for 50 minutes, the incidence of spastic paraplegia in dogs was 87.5% (Clark,

Mutch et al., 1992, pp. 357-364).

During the last 40 years, however, it has become clear that numerous factors

influence the neurologic outcome of thoracoabdominal aortic aneurysm repairs in

addition to the duration of AXC: the extent of the aneurysm, acute dissection, and

preoperative problems (i.e., renal condition, previous aortic surgery, diabetes) (Coselli,

Lemaire et al., 2002, pp. 631-639). Preoperative hypotension, distal aortic hypotension

after aortic occlusion, the interruption of critical intercostal arteries, and postoperative

hypotension or hypoxia can all result in injury (Mauney, Blackbourne et al., 1995, pp.

245-252). Each of these factors can affect SCBF, the oxygen delivery system to the spinal

cord, which is crippling to neurological function. Gharagozloo and colleagues found that

SCBF held at 10 ml/100g/min during AXC resulted in no paraplegia, while SCBF reduced to 4 ml/100g/min resulted in universal paraplegia (Gharagozloo, Neville et al., 1998, pp. 73-86). This finding illustrates the neurological impact of decreased SCBF.

Not all neurological deficits reveal themselves immediately. The incidence of postoperative paraplegia was documented as 10% by Schepens et al. (1995), as 21% by Cox et al. (1992) and as 13% by Crawford et al. (1991) Crawford (1998) et al. and associates found that 68% of patients who had undergone type I and II repairs developed neurological deficits. In 32% of the patients with neurological deficits, the paralysis did not manifest for several days (Crawford ES, Crawford JL et al., 1985, pp. 439-455). Immediate neurological deficits are a result of the hypoxic environment induced by prolonged AXC and minimal SCBF. Delayed neurological deficits can materialize 1 to 21 days after surgery. These deficits may be a result of ischemia arising from low SCBF as a result of high vascular resistance and regional hypotension restricting blood flow through the high-resistance vascular plexus of spinal cord or a result of reperfusion hyperemia and free radicals causing spinal cord edema (Robertazzi and Cunningham, 1998, pp. 29-34).

Barone and associates compared the SCBF and blood pressure of paraplegic and normal dogs during and after surgery (Barone, Joob et al., 1988, pp. 535-540). The thoracolumbar SCBF in both paraplegic and nonparaplegic dogs was 10-20% of baseline after 30 minutes of AXC. Thirty minutes after the cross-clamp was released, significant hyperemia was present. After AXC the nonparaplegic dogs had reperfusion flows approximately twice their baseline, while the paraplegic dogs had flows approximately eight times their baseline (Barone, Joob et al., 1988, pp. 535-540).

Thoracic endovascular aneurysm repair is a less invasive alternative to traditional surgical repair. The associated rate of spinal cord injury is 3 to 6%. In a review of thoracoabdominal aortic aneurysm repairs done using this endovascular technique, Hnath et al. found that draining CSF concurrently decreased the rate of spinal cord injury (Hnath, Mehta et al., 2008, pp. 836-840).

Avoiding Complications

Various methods have been conceived to improve the neurological outcomes of AXC. On their own none of these methods can address all the possible causes of spinal cord injury and neurological deficits.

Monitoring and Imaging

Monitoring spinal cord function and using imaging to avoid displacing key radicular arteries are important factors in improving the outcomes of thoracoabdominal aortic aneurysm repair. In patients undergoing surgery to treat thoracoabdominal aortic artery disease and aneurysms, Dong and colleagues found that using motor evoked potentials (MEPs) to follow spinal cord function was more effective than using SSEPs. The MEPs of 28.6% of their patients (n=56) showed evidence of spinal cord injury, while the SSEPs of only 25% showed such signs. In 81.3% of the 28.6% patients, ischemic changes in MEPs were reversed by reimplanting segmental arteries, increasing DAP, or using hypothermic conditions (Dong, MacDonald et al., 2002, pp. S1873-S1876). Kieffer and colleagues found that using spinal cord arteriography to identify the location of the artery of Adamkiewcz before thoracoabdominal aortic surgeries was very useful.

When the artery of Adamkiewcz was visualized and originated above or below the clamp area, the duration of surgery decreased and no spinal cord complications occurred. When the artery of Adamkiewicz originated in the clamped section, revascularization was attempted. When revascularization was successful, only 5% sustained ischemic injury. When it was unsuccessful, 50% developed ischemic injuries. Of the group in whom the artery of Adamkiewicz could not be visualized, 60% became paraplegic (Kieffer, Ammar et al., 1987, pp. 353-358).

Distal Aortic Perfusion

Distal aortic shunting, as provided by left atrium-to-femoral artery (LA-to-FA) bypass or a simpler arterial-to-arterial shunt aims to provide effective control of proximal blood pressure and to avoid a decrease in distal aortic flow (Robertazzi and Cunningham, 1998, pp. 29-34). Still ischemia can occur if the arteries supplying the ASA rely on excluded segments of the aorta (Tabayashi, 2005, pp. 1-6).

CSF Drainage

Manipulating the CSF compartment whether by pressure or content alteration remains an enticing goal for its potential effect on SCI. CSF drainage has been heavily investigated to identify whether drainage is effective and, if so, when it should be initiated and in conjunction with what other protection mechanisms. Proximal hypertension induced by AXC prompts the spinal cord vasculature to increase CSFP reflexively, lowering SCPP and thereby diminishing blood supply to the spinal cord.

Drainage of CSF reduces CSFP, offsetting the gradient and improving SCPP (Robertazzi and Cunningham, 1998, pp. 29-34).

In dogs Kazama and associates found that draining CSF an hour into a 2-hour AXC procedure was of limited efficacy (Kazama, Masaki et al., 1994, pp. 112-115). It only increased SCPP by 8-10 mm Hg, not enough to ensure the safety of the spinal cord. Only when CSFP was elevated abnormally (40 mm Hg) did drainage of CSF significantly increase SCBF (from 12 to 17ml/100g/min) and prevent damage to the spinal cord (Kazama, Masaki et al., 1994, pp. 112-115). Blaisdell and Cooley found that the incidence of paraplegia associated with AXC in dogs decreased from 50% to 8% when CSFD was performed during the operation (Blaisdell and Cooley, 1962, pp. 351-355).

McCullough and associates found that draining CSFD before 40 minutes of AXC had elapsed increased SCPP from 22 mm Hg to 30 mm Hg during aortic occlusion and that the incidence of paraplegia decreased by 90% (McCullough, Hollier et al., 1988, pp. 153-160).

Elmore and colleagues found that draining CSF before an hour of AXC had elapsed eliminated paraplegia in dogs, although 44% were paraparetic after surgery (Elmore, Gloviczki et al., 1991, pp. 131-139). Bower and associates showed that draining CSF before an hour of AXC had elapsed improved SCPP (from 13.5 mm Hg without CSF drainage to 21.1 mm Hg) and improved SCBF (from 2.5 ml/100gm/min without CSFD to 15.1 ml/100gm/min) in the gray matter of the lumbar spinal cord. Furthermore, reperfusion hyperemia in the lower portions of the spinal cord was not present when CSF was drained (34.1 ml/100gm/min) but was present when CSF was not drained (136.6 ml/100gm/min). Of the dogs undergoing CSF drainage (n=7), 57.1% exhibited no

31

neurological deficit and none became paraplegic. Of the dogs undergoing CSF drainage, 62.5% developed spastic paraplegia and none were neurologically normal (Bower, Murray et al., 1988, pp. 135-144). In contrast when Horn and associates drained CSF in rabbits after inducing a spinal cord injury, there was no indication that perfusion of the spinal cord improved. The different outcomes may reflect different methods: complete spinal cord injury versus AXC (Horn, Theodore, et al., 2008, p. E12).

LA-to-FA bypass performed in conjunction with CSF drainage (as opposed to no drainage) reduces the incidence of neurological complications associated with type I and II thoracoabdominal aortic aneurysm repairs by almost one-third (Robertazzi and Cunningham, 1998, pp. 29-34). Animals undergoing LA-to-FA shunting and CSF drainage had significantly higher SCBF than animals undergoing CSF drainage alone (Elmore, Gloviczki et al., 1991, pp. 131-139).

Pathophysiology of Spinal Cord Blood Flow After Trauma

Basics of Spinal Cord Injury

To address spinal cord injuries and how to minimize their deleterious effects, an understanding of the pathophysiological mechanisms that follow spinal cord injury must first be understood. Two types of zones define the spinal cord after injury. One zone completely lacks vasculature able to perfuse the tissue, while the other is capable of capillary perfusion within a week of injury. This second zone contains glial cells, macrophages, necrotic tissue, damaged neurons, and swollen axons. The zone with worthless vasculature often consists of the posterior central gray matter and posterior

columns at and below the trauma site. The size and extent of the zones vary, depending on the severity of the trauma (Fairholm and Turnbull, 1970, pp. 453-455).

Microangiograms showing vascular changes over various time frames have been used to construct a fairly consistent postinjury timeline. During compression the extrinsic arteries (ASA, PSA) remain intact, while the arteries within the traumatized region become constricted (Vlajic, 1978, pp. 451-460). Five minutes after injury, muscular venules in the gray matter appear distorted and develop holes. Muscular venules in white matter, however, appear to be unaffected (Dohrmann, Wagner et al., 1971, pp. 6-8). Hemorrhages emerge from capillaries and venules in the border zone between gray and white matter and in the gray matter itself (Sasaki, 1982, pp. 360-363). In these hemorrhagic areas the vessels do not perfuse blood. Fifteen minutes after injury, there is further leakage from gray matter venules and less than a third of the gray matter vessels perfuse properly. As a result, hemorrhagic areas in the gray matter continue to grow. Although white matter hemorrhages become more pronounced, the number of functioning vessels increases after 30 minutes (Dohrmann, Wick et al., 1973, pp. 52-58, Dohrmann, Wagner et al., 1971, pp. 6-8). One hour after injury, the hemorrhages in the gray matter coalesce and neurons are clearly damaged (Fairholm and Turnbull, 1970, pp. 453-455). Furthermore, most of vessels near the gray-white border cannot perfuse blood. The larger extrinsic vessels (ASA, PSA), however, continue to remain functional. Four hours after injury, leakage from vessels is considerable in both the gray and white matter. The only functional intrinsic vessels are limited to the peripheral half of the white matter (Dohrmann, Wick et al., 1973, pp. 52-58, Dohrmann, Wagner et al., 1971, pp. 6-8). After 24 hours, the central arteries at the site of injury and adjacent areas were markedly

displaced, often occluded, and had narrowed (Koyanagi, Tator, et al., 1993, pp. 260-268).

Reports on the state of white matter vessels 24 hours after injury have differed. In rats

Sasaki found that hemorrhages originating from ruptured vessels in the dorsal white

matter were present (Sasaki, 1982, pp. 360-363). In contrast, Dohrmann found that the

white matter vessels of cats were almost restored to normal (Dohrmann, Wick et al.,

1973, pp. 52-58).

Still, the implications are fairly clear. Gray matter is severely injured soon after

injury, while damage in white matter is slower to appear and more likely to recover. The

predominance of hemorrhages in gray matter may be the result of its rich capillary

network, which is highly susceptible to mechanical stress because of its complex texture

(Tator and Koyanagi, 1997, pp. 483-492). This stress can induce clotting, which

decreases or halts blood flow, and causes venous hypertension, which can disrupt vessel

walls (Koyanagi, Tator, et al., 1993, pp. 260-268). Edema, a result of vessel leakage, may

increase interstitial fluid pressure, causing vessel closures, and creating a snowball effect

(Rivlin and Tator, 1978, pp. 844-853). Damage to central arteries and their branches

causes hemorrhaging and ischemia in their areas of distribution, which includes the gray

matter (Koyanagi, Tator, et al., 1993, pp. 260-268). The pia mater is a strong membrane.

Therefore, the large vessels on the surface of the spinal cord and in the anterior median

sulcus are relatively spared from major damage due to mechanical stress. The ASA and

PSA possess heavier mesenchymal-supporting investment, and electron microscopic

studies suggest that white matter vasculature possesses denser glial packing than vessels

of gray matter (Bingham, Goldman et al., 1975, pp. 162-171).

Autoregulation with injury

Spinal cord injury is associated with vasculature changes. After the initial blockage of blood vessels, disruption of veins, and diapedesis of blood cells, the blood vessels in gray matter become necrotic. White matter is not usually affected as severely, and blood vessels there remain intact. Only when the injury is severe will edema of the white matter occur, resulting in irreparable neurological deficits.

To further understand chronic changes as a result of spinal injury, cats with various degrees of spinal cord injury (control, mild 200 g-cm; severe, 400 g-cm) were observed over a 14-day period after injury. In cats with mild trauma, SCBF and CO_2 responsiveness were not significantly different from those of uninjured cats, although there was a trend toward hyperemia. In cats with severe spinal cord trauma, the hyperemia was significantly different from that of uninjured cats on the 11th and 14th days. In this group, CO_2 responsiveness was strikingly impaired (0.03ml/min/100g/torr compared with 0.47 ml/min/100g/torr in the controls) (Smith, McCreery et al., 1978, pp. 239-251). One explanation for this delayed increase in SCBF is that hypotension causes transient ischemia leading to a local decrease in pH, both intra- and extracellularly. The hydrogen ions then act directly on blood vessels, causing vasodilatation. Other ions and substances, such as potassium and histamine, could employ a similar mechanism (Kobrine, Doyle et al., 1975, pp. 573-581).

Relations Among MAP, SCBF and Spinal Cord Function After Injury

To better understand how treatments should address spinal cord trauma, considerable research has been directed toward defining relationships among MAP, SCBF, SSEPs, and neurological outcomes after injury, both at and around the trauma site.

Various studies have examined the effect of changing MAP after trauma in an attempt to normalize SCBF. Dolan and Tator found that by increasing the MAP in rats after trauma (175 gm–1-min cord clip-compression), SCBF also increased (Dolan and Tator, 1982, pp. 350-358). Thirty minutes after injury, SCBF in the white and gray matter were a fraction of control values (3.42 from 18.7 ± 6.7 and 15.6 from 74.2 ± 22.3 ml/100gm/min, respectively). After MAP was increased by blood transfusion, SCBF almost doubled in both white (6.3 ± 6.4 ml/100gm/min) and gray (25.6 ± 30.2 ml/100gm/min) matter. Despite this increase in flow, no blood leaked from the injured vessels, implying occlusions of injured vessels and perfusion only through uninjured vessels (Dolan and Tator, 1982, pp. 350-358).

The results of Guha and associates' study of rats implied that restoring MAP to its baseline after severe injury was the best option when altering MAP (Guha, Tator et al., 1989, pp. 372-377). With hypotension, posttraumatic ischemia persisted and worsened, while with extreme hypertension, (180 mmHg) SCBF increased to 31.3 ± 3.5 ml/100gm/min (from 16.2 ± 4.4 ml/100gm/min). Raising MAP this much, however, could be deleterious to less injured portions of the spinal cord. Consequently, normotension was identified as the ideal pressure after trauma (Guha, Tator et al., 1989, pp. 372-377). Wallace and Tator found that by increasing MAP in rats after trauma by adding whole blood or dextran to the system, SCBF also increased (Wallace and Tator,

1987, pp. 710-715). The dextran decreased the hematocrit by about 50% and was twice as effective as whole blood in increasing SCBF. This finding implied that hemodilution improved perfusion after injury. The combination of restoration to normotension and hemodilution improved SCBF optimally (Wallace and Tator, 1987, pp. 710-715). SCBF can differ above and below the trauma site (Dolan and Tator, 1982, pp. 350-358). Ohasi and associates found a potential correlation between arterial diameter and autoregulation when they examined differences between zones distal and proximal to the trauma site in rats after trauma (50 gm – 1 min spinal cord clip-compression). Although arterial diameter decreased overall, it did so most significantly distally. In contrast, SCBF decreased to a greater extent proximally. CO_2 reactivity and autoregulation also were both impaired, although more so distally; perhaps, this finding indicates that arterial diameter affects CO_2 reactivity and autoregulation more so than SCBF after injury (Ohashi, Morimoto et al., 1996, pp. 322-329).

After trauma, SCBF and SSEPs can be used to distinguish between extreme neurological outcomes (uninjured or paraplegic animals); identification of partially injured animals is more difficult. Ducker and associates' research in monkeys support this idea. The SCBF of monkeys with slight or no neurological deficits steadily increased for a week after injury, reaching 170% of normal SCBF (from 15 to 25.5 ml/min/100g) and SSEPs reappeared within 5-120 min. When monkeys became paraplegic, their SCBF fell to 30% of their baseline values in a week (15 to 4.5 ml/min/100g). SSEPs rarely returned with stability. Partially injured animals maintained their baseline SCBF, and SSEPs returned in 60% of subjects, perhaps a result of white matter hyperemia (Ducker, Salcman et al., 1978, pp. 64-70). Similarly, Carlson and associates found that

37

neurological recovery in dogs was related to higher SCBF during spinal cord compression (Carlson, Gorden et al., 2003, pp. 95-101).

Severity and Duration of Trauma

After injury MAP first quickly increases and then falls. Depending on the severity of the trauma, hypotensive tissue is reperfused. Based on the reperfusion and on the effect of the initial impact, the microscopic appearance of the spinal cord can vary. Such variations can be used to illustrate the resulting neurological deficits.

Lohse and associates found that MAP spiked and then fell below baseline values after light (100 gm-cm) and moderate (260 gm-cm) trauma in cats (Lohse, Senter, 1980, pp. 335-345). After light trauma, MAP immediately increased to 137% of pretrauma values. After 15 minutes it decreased to 77% of the pretrauma value and remained low for the 6 hours of the experiment. After moderate trauma, the MAP rose to 144% of its pretrauma value, decreased to 72% of that value, and remained low for the duration of the experiment. Five minutes after severe trauma (300 gm-cm) in monkeys, SCBF in the gray matter fell to 62% of baseline, while in the white matter it fell to 93% of baseline. After 15 minutes, SCBF in gray and white matter rose (to 92% and 141%, respectively). During the next 45 minutes, SCBF in the gray and white matter again fell (21% and 90%, respectively). After this point, SCBF in white matter increased slowly, while the SCBF of gray matter did not. These data show that as severity of trauma increases so do fluctuations in SCBF (Bingham, Goldman et al., 1975, 162-171).

Another obvious result of increasing the force of spinal cord injury is depression of SCBF gray matter (Fehlings, Tator et al., 1989, pp. 241-259). Holtz and associates'

38

research support this finding. They showed that post-trauma motor function likewise declines (Holtz, Nystrom et al., 1990, pp. 952-957). Griffiths found similar results using CO_2 sensitivity as a measure of neurological deficit. After moderate injury (300 gm-cm), CO_2 sensitivity was considerably reduced and was nonexistent after severe injury (500 gm-cm) (Griffiths, 1976, pp. 247-259).

Carlson and associates addressed the question of reperfusion after injury in dogs and found that duration of spinal cord compression (30, 60 and 180 minutes) and reperfusion after decompression was inversely related (Carlson, Minato et al., 1997, pp. 951-962). Five minutes after compression, SCBF increased from baseline (21.4 ± 2.2 ml/100gm/min) in both the 30-minute (49.1 ± 3.1 ml/100gm/min) and 60-minute groups (≈44 ml/100gm/min) but fell slightly in the 180-minute group (19.8 ± 6.2 ml/100gm/min). Fifteen minutes after compression, the 30- and 60-minute groups remained above baseline (32.3 ± 4 and 32.4 ± 3.7 ml/100gm/min, respectively), while SCBF in the 180-minute group did not change significantly (Carlson, Minato et al., 1997, pp. 951-962). Similar results have been found in other animals, including pigs and monkeys (Bingham, Goldman et al., 1975, pp. 162-171, Palleske, Kivelitz et al., 1970, pp. 29-41).

These differences in SCBF after trauma have a direct impact on vascular resistance. After trauma, SCBF, vascular resistance, and MAP all depend on one another (SCBF = MAP/VR). Therefore, when moderate and light trauma decrease MAP and increase SCBF, vascular resistance will decrease. Because severe trauma decreases SCBF, vascular resistance increases. This is a clear distinction between traumatic injuries that do and do not cause paraplegia. The mechanisms that might mediate such changes in

local vascular resistance are unknown, but several possibilities exist. Changes in hydrogen and potassium ions, the release of biologically active substances, or primary injury to the microvasculature could affect vascular resistance (Lohse, Senter et al., 1980, pp. 335-345).

Vascular resistance and other microvasculature features are well depicted in studies using microangiograms of the spinal cord. Using contrast material to capture extravasation, Allen and associates evaluated microangiograms of cats after moderate and severe injury (300 gm-cm and 500 gm-cm) (Allen, D'Angelo et al., 1974, pp. 107-115). There were many similarities in the vasculature changes after moderate and severe injuries. Immediately after moderate injury, several small areas of extravasation were present in the central gray matter of the traumatized region. Fifteen minutes after injury, blood flow was markedly reduced in the gray matter arterial network, as were the size and number of the peripheral arteries serving the posterior horns, especially in the posterior columns. Thirty minutes after injury, the appearance of the peripheral arteries began to approach normal and continued to improve. Over time the degree of extravasation in the central gray matter became more pronounced. After severe injury there were more areas of extravasation than after moderate trauma. Leakage again appeared in the gray matter, but there were also areas of extravasation in the gray and white border region. Fifteen minutes after injury, the SCBF of both gray and white matter was reduced markedly. Over time the central gray matter filled with extravasated contrast material as it had after moderate injury. Perfusion of the white matter improved after one hour but remained below control values (Allen, D'Angelo et al., 1974, pp. 107-115). Reed et al. found that 90 minutes after severe trauma (500 gm-cm), microangiography showed

severe narrowing of vessels in the gray and white matter (Reed, Allen et al., 1979, pp. 391-397). After 2 hours there was almost no filling of the peripheral vessels supplying the white matter. After 3 hours the entire gray matter was hemorrhagic and there was no blood flow.

Gray to White Injury

Primary damage directly inflicts injury on neurons and axons. Edema, ischemia, and inflammatory responses are common mechanisms that accelerate damage. Ischemia and reperfusion induce the release of inflammatory cytokines, free radicals, and excitatory amino acids (Hamamoto, Ogata et al., 2007, pp. 1955-1962). Vascular disruption and local tissue ischemia are features of secondary damage.

In the mid 1970s, the prevailing theory concerning the pathophysiology of acute spinal cord injuries relied on two steps. First, there was hemorrhage in the central gray matter, which specifically included endothelium separating from the basement membranes, recanalization, blood clotting and disruption of vessel walls. Ischemia in the lateral white matter followed but included no changes comparable to those in the gray matter. Consequently, gray matter was thought to be the origin of the damage, which slowly spread to the surrounding white matter (Bingham, Goldman et al., 1975, pp. 162-171). Wallace and associates found that ischemia in the white matter of rats, especially in the dorsal columns and anterior and lateral funiculi, was common when fed by arteries that traversed hemorrhagic gray matter. This finding further supports the secondary nature of injury in the white matter, stemming from trauma to the gray matter (Wallace, Tator et al., 1986, pp. 433-439).

41

Kobrine and associates' (1975) experimental data investigating the impact of severe injury (600 gm-cm) in monkeys opposes this theory. SCBF in the lateral white matter more than doubled ($p < .01$) within 1 hour of injury and returned to normal after 8 hours. SCBF in the central gray matter fell for 4 hours after injury. Cawthon and associates found similar results in cats after severe trauma (500 gm-cm). White matter SCBF almost rebounded to baseline values within 8 hours (Cawthon, Senter et al., 1980, pp. 801-807). An hour after trauma, SCBF in the white matter at the trauma site was near control values (10.99 ± 0.89 ml/min/100 gm), while rostral and caudal blood flow was depressed for approximately 1 cm. Four hours after trauma, flow blood through white matter was depressed at the trauma site. Two cm rostral and caudal (2 cm) to the site, blood flow was also depressed to a lesser extent. Eight hours after trauma, blood flow through white matter was 90% that of the controls 3 mm caudal to the trauma center, and 16 mm caudal to the trauma center it was 97% (Cawthon, Senter et al., 1980, pp. 801-807).

These findings suggest that the initial trauma disrupts the ability of the white matter to function and that injury is not simply a result of spreading from gray to white matter. These data show that autoregulation in white matter is maintained through the first hour after injury and then lost. The reappearance of normal blood flow 5 to 7 hours later indicates that autoregulation is regained. The return of blood flow may depend on clearing the tissue of toxins, vasospasm, or other mechanisms that restore vasoconstriction (Senter and Venes, 1979, pp. 198-206). The increase in SCBF in white matter after injury also could be a response to increased metabolic demand or loss of autoregulation and subsequent vascular dilation as a direct result of trauma (Kobrine,

Doyle et al., 1975, pp. 144-149). A documented increase in histamine levels at the site of trauma, known to cause vascular dilatation by weakening vascular tone, also explains the increased blood flow in white matter (Naftchi, Demeny et al., 1974, pp. 52-57). Segmental loss of gray matter is functionally tolerated because it involves only a small portion of total neuronal pool in gray matter. Loss of segmental white matter, however, is more serious because all distal functioning neurons cannot operate and neurological deficit occurs. If treatment could be initiated before white matter is destroyed (within 3-4 hours of severe injury), paralysis might be avoided in some cases (Ducker, Salcman et al., 1978, pp. 60-63).

White Matter Issues

The severity of trauma within white and gray matter varies but is greatest in the white matter. Understanding how specific areas of the spinal cord react to traumatic injury clarifies the ability of the vasculature to function. Sandler and Tator found that after moderate trauma was induced in monkeys by inflating an extradural cuff to 400 mm Hg for 5 min, the SCBF in the dorsal columns and dorsolateral white matter rebounded slower than in other areas of the white matter. SCBF in the lateral ventral areas was significantly different from that of the controls for 30 minutes after trauma, but the SCBF in the dorsal columns and in the left lateral dorsal white matter was still significantly lower after 6 hours compared to controls. After 24 hours, blood flow in all of the white matter was significantly higher than in the controls (Sandler and Tator, 1976, pp. 660-676).

Conclusion

Spinal cord vasculature has unique anatomical and physiological properties. Variability in the direction of blood flow and in the diameter of arteries assure a constant and sufficient blood supply. The pathophysiology of spinal cord blood flow under normal conditions has been investigated in several studies, and a consensus has been reached on the key mechanisms of the blood supply to the normal spinal cord. Although numerous experiments have attempted to investigate the principles elucidating the blood supply in the injured spinal cord, these mechanisms remain unclear. Techniques that would allow continuous precise measurement of blood flow in different spinal cord regions could potentially answer many of the questions regarding how the blood flow is altered. Manipulating physiological parameters such as MAP and intrathecal pressure may have potential benefit in improving the blood supply to ischemic areas of the injured spinal cord.

CHAPTER 3

Microsurgical anatomy of the arterial basket of conus medullaris

Introduction

During embryonic development, the vascular supply of the spinal cord undergoes

significant modification and pruning. The differential growth of the spinal cord and

spinal column results in the descent of the spinal nerve roots and ascent of the spinal cord

into its adult configuration by the first year of life (Altman and Bayer, 2001). The blood

supply to the spinal cord consists of an anterior spinal artery (ASA) and paired smaller

posterior spinal arteries (PSAs) (17,22,23 Martirosyan, Feuerstein et al., 2011, pp. 238–

251, Turnbull, 1973, pp. 56–84, Turnbull, 1971, pp. 141–147). The arterial blood supply

to the spinal cord consists of several anastomoses that allow for redundancy of supply to

the spinal cord (Lazorthes, Gouaze et al., 1971, pp. 253–262, Martirosyan, Feuerstein et

al., 2011, pp. 238–251, Turnbull, 1973, pp. 56–84, Turnbull, 1971, pp. 141–147, Tveten,

et al., 1976, pp. 257–273). One critical anastomotic connection is the arterial basket of

the conus medullaris (ABCM). Initially described by Adamkiewicz in the 1880s, it has

subsequently been studied using angiography by Djindjian and Lasjaunias

(Adamkiewicz, 1882, pp. 101–130, Adamkiewicz, 1881, p. 469, Bolton, 1939, pp. 137–

148, Djindjian M, Ribeiro et al., 1988, pp. 201–209, Djindjian R, 1974, pp. 179–185,

Lasjaunias and Berenstein, 1990, Lazorthes, Gouazé et al., 1966, pp. 109–122, Lazorthes,

Poulhes et al., 1958, pp. 3–19).

The ABCM consists of one or two arterial branches connecting the ASA and

PSAs at the level of the conus medullaris. Although initially thought of as a fail-safe

mechanism for providing alternative vascular supply to the conus, the ABCM has also

been noted to be a critical component of vascular malformations of the conus medullaris (Djindjian M, Ribeiro et al., 1988, pp. 201–209, Parke, Gammell et al., 1981, pp. 53–62, Stein, Ommaya et al., 1972, pp. 649–651). To the best of our knowledge, this is the first detailed microsurgical anatomical study of the ABCM with emphasis on the morphometric characteristics and branching pattern of the arteries forming the anastomosis between the ASA and PSAs.

Materials and Methods

We used 16 human cadaveric thoracolumbar spines up to 24 hours post mortem with no known vascular disease of the spinal cord. The anterior corpectomies and foraminotomis were performed utilizing high-speed drill and rongeurs. The ventral aspect of entire thoracolumbar spinal thecal sac and nerve toot were fully exposed. Utilizing operating microscope longitudinal midline durotomy was performed and ventral spinal cord and cauda equina were defined. The artery of Adamkiewicz was identified and cannulated with 32 gauge plastic canula. Continuous room temperature normal saline irrigation was used to purge the vascular system until no gross blood clots could be seen in vessels. Next, a red-colored silicone-rubber mixture was injected into the artery of Adamkiewicz (Alleyne, Cawley et al., 1998, pp. 791–795). This injection was performed under moderate pressure to avoid contrast extravasation and ensure adequate latex filling into distal small caliber vessels. Macrosocpically, there was no evidence of vascular malformations or pathology (including atherosclerosis which could alter the latex injection) involving the spinal cords. The specimens were fixed in a 5% formalin solution. One week after formalin fixation, we carried out microsurgical dissection of the

samples (Djindjian, Ribeiro et al., 1988, pp. 201-209, Parke, Gammell et al., 1981, pp. 53-62). We identified and measured the course, diameter and branching angle of the arteries comprising the ABCM. After all measurements were taken, spinal cords were sent for histologic sections to identify smaller caliber perforating vessels arising from ABCM.

Histology

Embedding & Sectioning:

Spinal cords were treated with 20% glycerol and 2% dimethylsulfoxide to prevent freeze-artifacts. Spinal cord was embedded in a gelatin matrix using MultiCord Technology™ (NeuroScience Associates, Knoxville, TN) as used in previous studies (Fix, Ross, et al., 1996, pp. 291-304, Ross, Switzer et al., 1996, pp. 137-154). The block of embedded spinal cord was allowed to cure and was then rapidly frozen by immersion in isopentane chilled with crushed dry ice. The block was mounted on a freezing stage of an AO 860 sliding microtome and sectioned in the coronal and sagittal plane at 40μ. All sections cut were collected sequentially into a 4x6 array of containers. These containers were filled with Antigen Preserve solution (50% PBS pH 7.0, 50% Ethylene glycol, 1% Polyvinyl Pyrrolidone) for sections to be stained immunohistochemically. At the completion of sectioning, each container held a serial set of one-of-every-24th section (or, one section every 960μ). Each of the large sections cut from the block is actually a composite section holding individual sections from the spinal cord embedded in each block. With such composite sections, uniformity of staining was achieved.

47

Nissl (thionine) Stain:

Every 6th section (every 240 microns) was used for staining. For Nissl staining, 40μ sections were first mounted onto gelatinized (subbed) slides. They were then dehydrated through alcohols prior to defatting in a chloroform/ ether/ alcohol solution. The slides were then rehydrated and stained in 0.05% Thionine/ 0.08M acetate buffer, pH 4.5. Following deionized water rinses, the slides were differentiated in 95% alcohol/ acetic acid and dehydrated in a standard alcohol series, cleared in xylene and coverslipped.

Results

Characteristics of the Arterial Basket of the Conus Medullaris

The ASA tapers distally at the level of the conus medullaris. The pre-conus diameter of the ASA measures 0.7 ± 0.12 mm. At the level of the conus, the diameter of the artery narrows to 0.38 ± 0.08 mm. The ASA forms an anastomotic basket with the posterior spinal artery (PSA) via one or two anastomotic branches (See Table 1 for measurements). In most specimens (n= 13; 81.3%), we identified two anastomotic branches connecting the ASA and PSA (Figs 3 A-D). In the remaining specimens (n=3, 18.7%), a unilateral right-sided anastomotic artery was identified (Fig. 4 D). We measured the diameter of the anastomotic arteries in all specimens. The mean diameter of the right anastomotic branch was 0.49 ± 0.13 mm, and the mean diameter of the left anastomotic branch was 0.52 ± 0.14 mm. The branching angle of the arteries forming the anastomotic basket was 95.8 ± 36.6 degrees on the right side, and 90 ± 34.3 degrees on the left side.
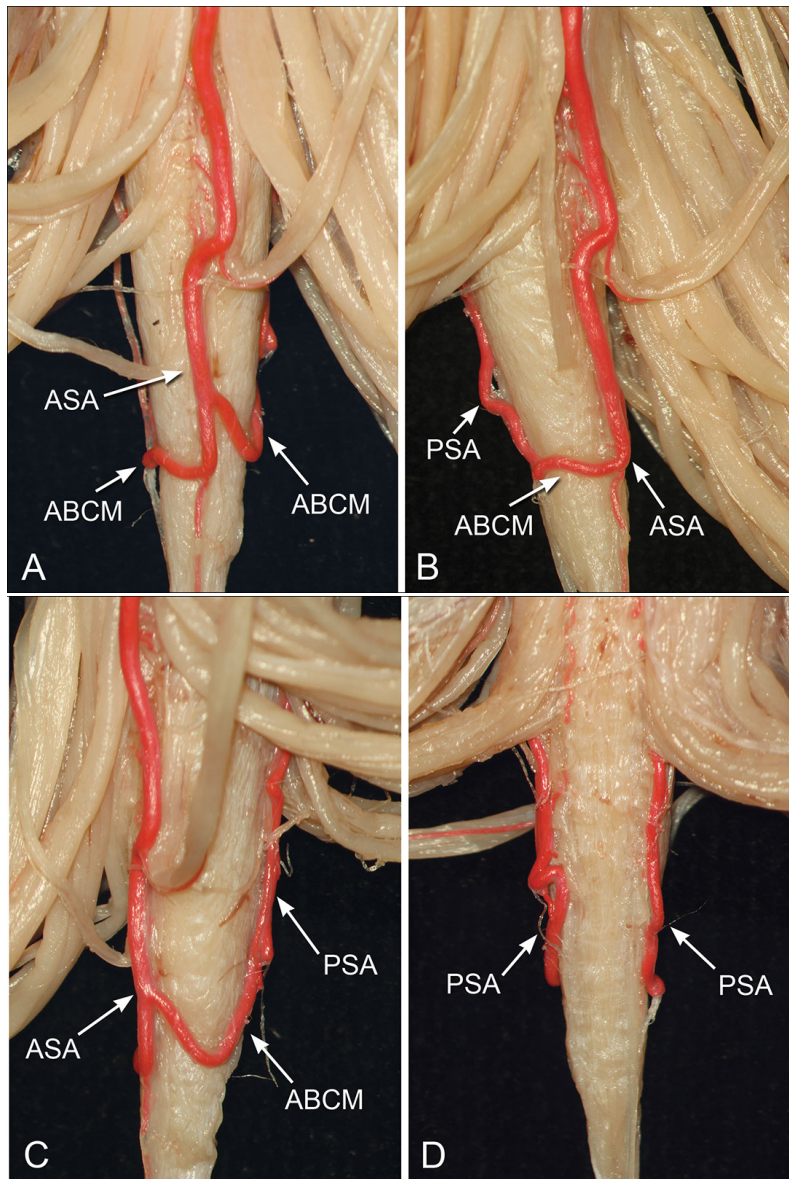
Figure 3. The anatomy of the ABCM. (A) Anterior view of a gross anatomical specimen demonstrating bilateral networks connecting the anterior spinal artery (ASA) to the paired posterior spinal arteries (PSAs). (B) Lateral right and (C) left views of gross anatomical specimens at the level of the conus medullaris demonstrate the connection of the ASA to the PSAs via the arterial branches of the basket of the conus. (D) Posterior view of the arterial branches of the basket draining into the PSA.
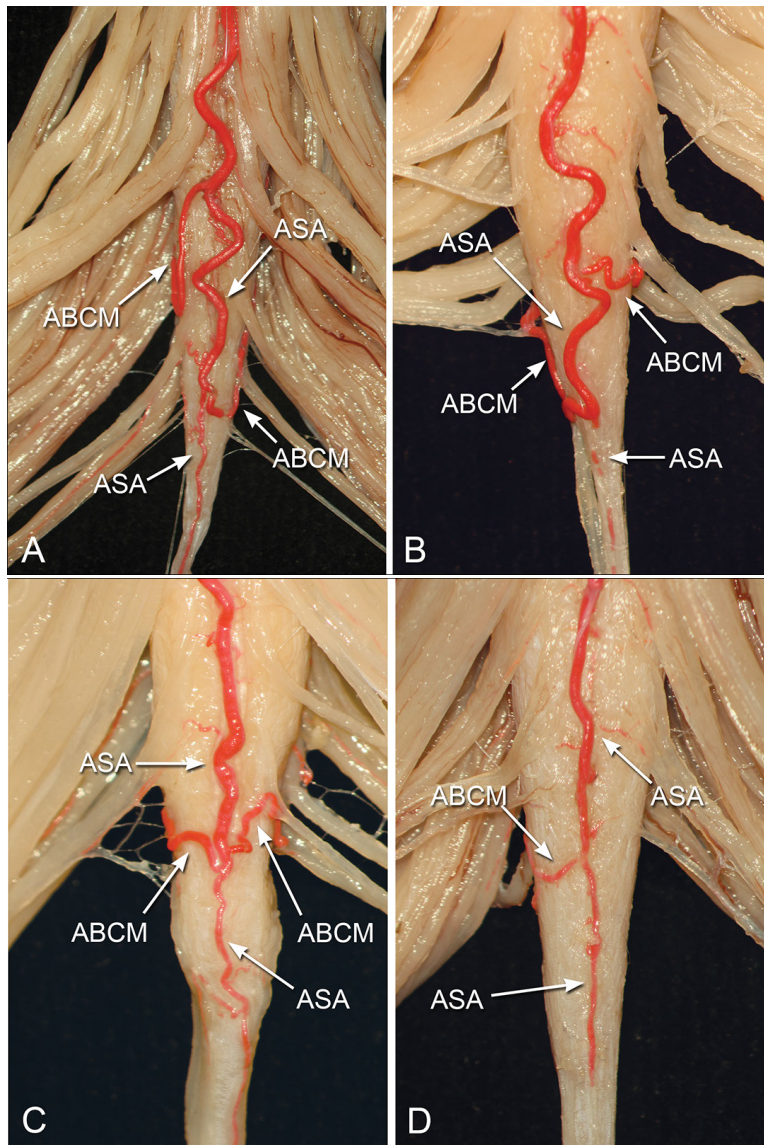
Figure 4. Branching of the ABCM (A) Anterior gross anatomical specimen at the level of

the conus medullaris demonstrates early right- and (B) left-sided branching from the

ASA. (C) Alternatively, bilateral branches from the ASA may occur simultaneously,

although this is a rare arrangement. (D) Unilateral right-sided branching from the ASA

Branching Orientation and Anastomosis Between ASA and PSA

In most specimens, the arterial basket connecting the ASA and PSA consisted of two arterial connection points. In these instances, we noted that in 6 cases the right vessel branched first (Fig. 4A), in 5 cases the left vessel branched first (Fig. 4B), and in 2 cases both vessels branched simultaneously (Fig. 4C). These three differing branching orientations constitute the spectrum of patterns seen in the ABCM. In cases of bilateral arterial anastomoses between the ASA and PSA, the mean distance between the origins of the arteries was 4.5 ± 3.3 mm.

Histology

We were able to identify small caliber (< 0.5mm) centripetal perforating branches arising from ABCM (Fig 5). Due to limitations of histological sections we were not able to identify precisely number of these branches and their length.

Discussion

Anastomotic Contribution of the Arterial Basket of the Conus Medullaris

The ABCM functions as an anastomotic connection between the ASA and PSA. The arterial basket was symmetric in most specimens (n=13), meaning that the ASA is connected to paired PSAs via right and left branches. This symmetric configuration allows for continuity of circulation between the anterior and posterior spinal circulations. In rare cases (n=3), the anastomotic network was asymmetric with a dominant artery connecting the ASA to one of the PSAs. This rare arrangement resulted in one PSA receiving all of the ASA flow. This arrangement may result in a watershed zone on the

51
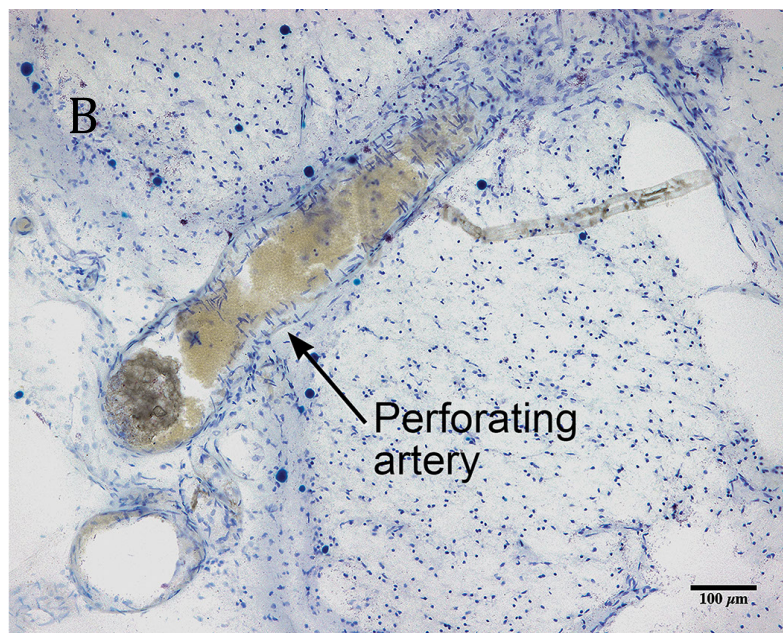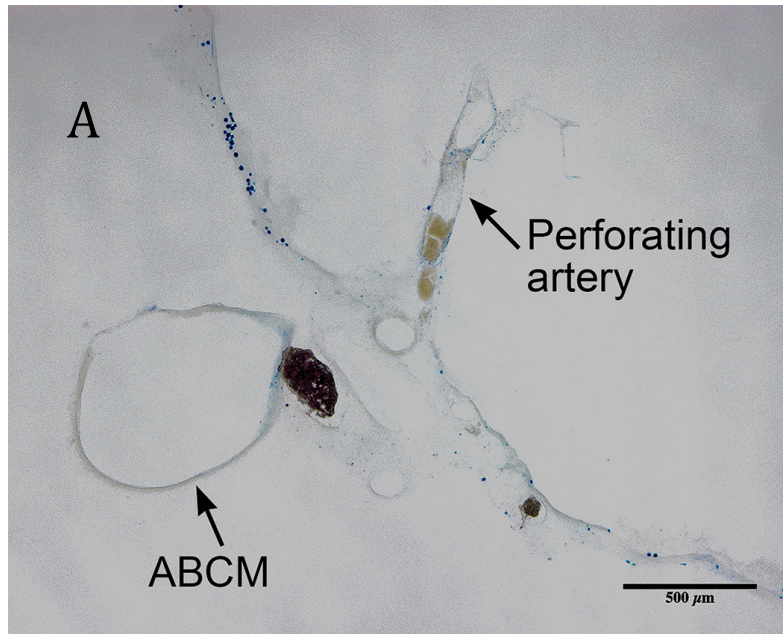
Figure 5. Perforating artery of ABCM. (A) Nissl stain image from the axial section
through conus medullaris shows perforator branch arising from ABCM; (B) Nissl stain
image of small perforator branch surrounded with spinal cord tissue.

contralateral dorsal surface of the spinal cord. Given the limitations of our current technique, it is possible that in these asymmetric cases, finer anastomotic networks between the ASA and the other PSA exist but are not visualized with the injection technique.

Branching Orientation and Anastomosis Between ASA and PSA

We identified three branching orientations connecting the ASA and PSAs. In the two most common scenarios, the ASA was connected to the PSA via bilateral branching arteries, which branched from the ASA at different levels of the conus (Figs 4A-B). In a more uncommon orientation, the bilateral branching arteries branched simultaneously from the ASA to connect to the paired PSAs. These branching orientations do not appear to have functional significance, but the anatomic description of these branching patterns is novel and has not been previously described.

Arterial Basket of the Conus and Conus Medullaris Arteriovenous Malformations

The ABCM is frequently involved in vascular malformations of the conus (Figs 6, 7) (Hsu, Rodesch et al., 2002, pp. 47-53, Kalani, Ahmed et al., 2012, pp. 348–354, Kim and Spetzler et al., 2006, S3-195–S3-201, Krings, Lasjaunias et al., 2007, pp. 57–72, Spetzler, Detwiler et al., 2002, pp. 145–156, Wilson, Abla et al., 2012, pp. 100–108). The angiography provides a robust means of obtaining anatomical information about vasculature at the conus. However spinal angiography is a rarely performed, time-consuming procedure that is only performed to evaluate pathological conditions. For this
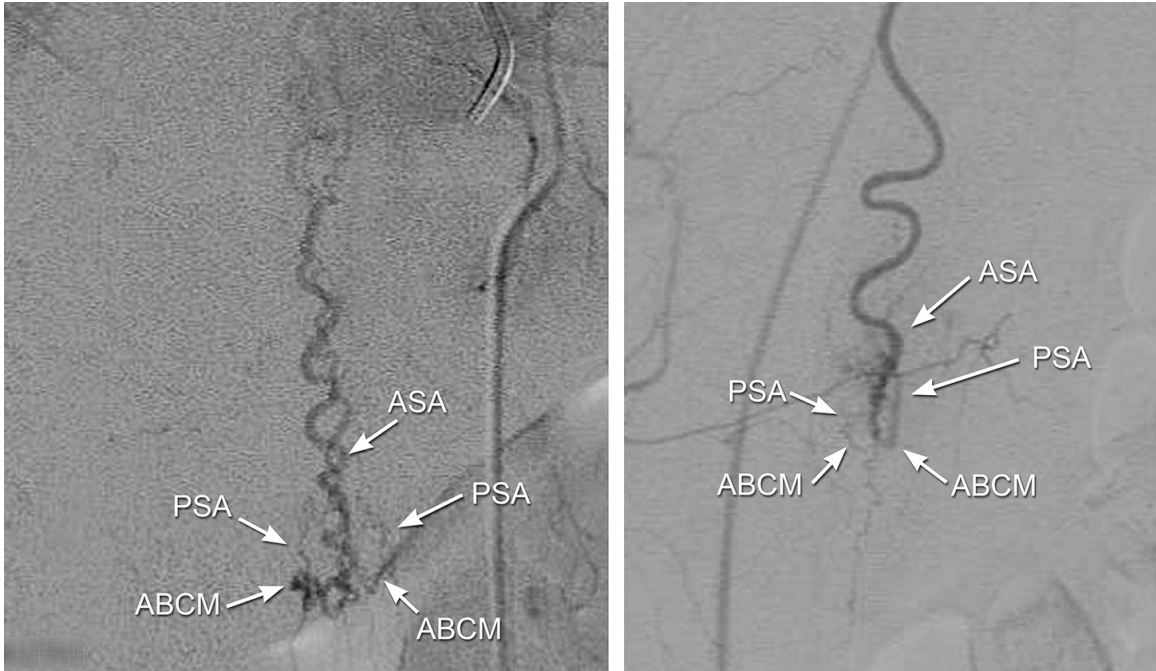
Figure 6. Simple arteriovenous malformations of the conus medullaris. (A, B) Anteroposterior (AP) angiogram at the level of the conus medullaris demonstrates the involvement of the ABCM in a conus medullaris AVM. ASA, PSA and ABCM can be identified.
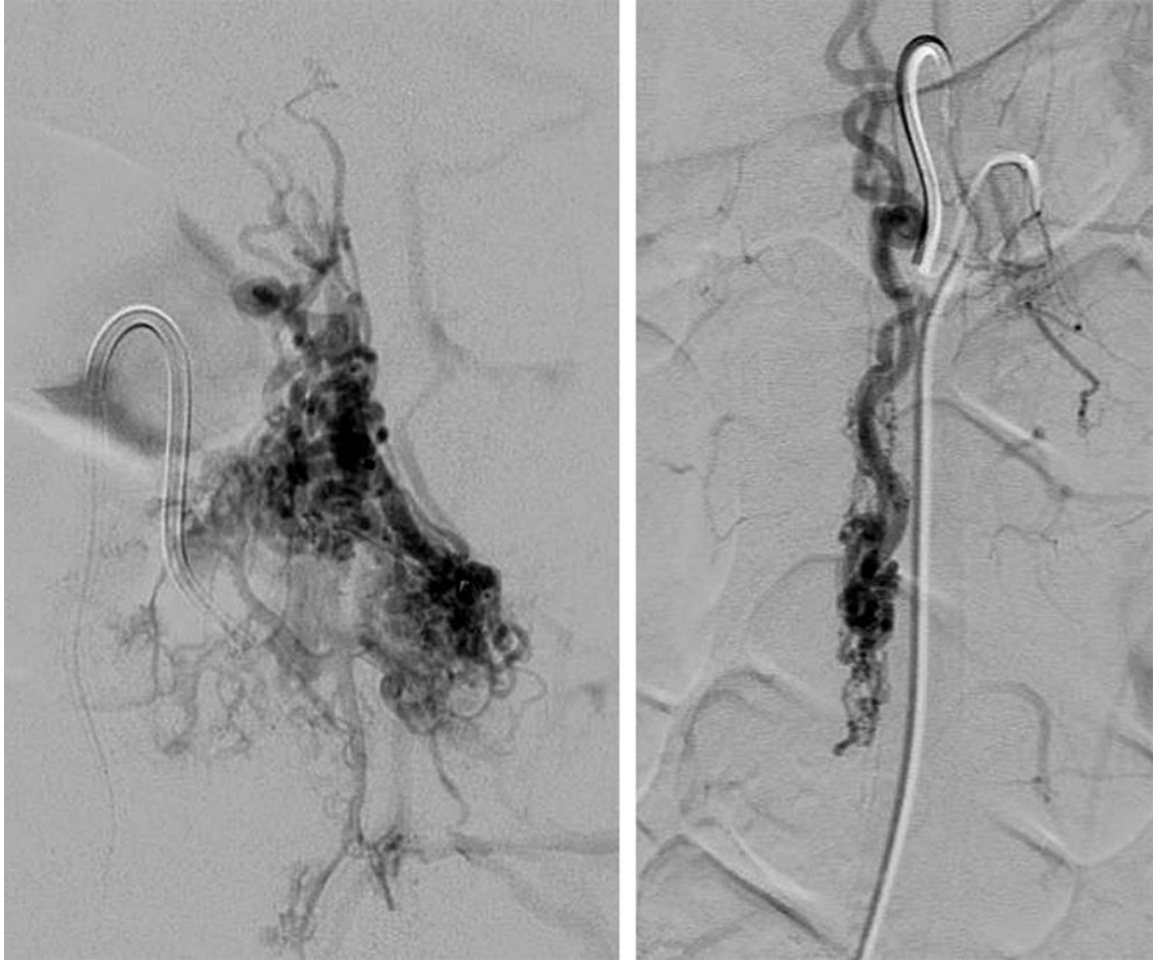
Figure 7. Complex arteriovenous malformations of the conus medullaris. (A, B) AP

angiograms of the complex cases of AVM of the conus medullaris involving of the

ABCM. Large size of the nidus obscures proper delineation of the ASA, PSA and ABCM

reason we were not able to perform additional correlation between anatomical findings with angiographic data.

The ABCM is ill defined or un-definable on spinal angiography (Wilson, Abla et al., 2012, pp. 100–108   ) In many cases of AVMs of the conus, the large size of the nidus obscures proper delineation of the ABCM. (Fig 7)

Understanding of the anatomy of the basket and its variations is critical for addressing vascular malformations in this location. The presence of perforating vessels feeding the conus that arise from this ABCM have clinical implications for the resection of vascular lesions as well as other pathologies in this region. This anatomy if often not well described or studied; our study adds a new dimension, highlighting the importance of perforating vessels arising from the ABCM to the vasculature of the conus medullaris.

Conclusion

The ABCM is an anastomotic network connecting the ASA and PSAs. We identified three different branching patterns connecting the ASA and PSAs. In the majority of the cases, bilateral arteries connected the ASA and PSA allowing for redundancy in vascular supply to the spinal cord and conus. Small perforating arteries arising from ABCM provide blood supply to the conus medullaris tissue. The ABCM is involved in vascular malformations and tumors at the level of the conus. The physiological role of the ABCM in the vascular malformation of the conus is unclear and requires further investigation. Practitioners treating vascular lesions tumors of the conus medullaris must have a solid understanding of the anatomy of this critical anastomotic network.

Table 1. Morphometric parameters of ABCM branches.

N	ASA above origin, mm	ASA below origin, mm	Right branch, mm	Right angle, deg	Left branch, mm	Left angle, deg	Distance between origins, mm
1	0.8	0.3	0.4	120	0.5	85	2
2	0.5	0.4	0.4	115	n/a	n/a	n/a
3	0.6	0.4	0.15	100	0.25	130	6.4
4	0.75	0.5	0.5	85	0.45	120	6.1
5	0.55	0.35	0.5	160	n/a	n/a	n/a
6	0.55	0.4	0.5	50	n/a	n/a	n/a
7	0.75	0.3	0.6	90	0.5	85	2.5
8	0.9	0.45	0.75	90	0.8	150	0
9	0.8	0.35	0.5	77	0.6	55	6.3
10	0.55	0.4	0.5	85	0.5	35	5
11	0.8	0.4	0.6	155	0.6	120	12.7
12	0.8	0.5	0.55	30	0.5	90	0.9
13	0.65	0.5	0.4	47	0.4	80	2.4
14	0.8	0.4	0.4	140	0.7	100	6
15	0.7	0.2	0.6	90	0.65	40	2.45
16	0.75	0.3	0.5	100	0.4	80	5.3
Mean	0.70	0.38	0.49	95.88	0.53	90.00	4.47
SD	0.12	0.08	0.13	36.57	0.14	34.28	3.31

CHAPTER 4

Cerebrospinal fluid drainage and induced hypertension improve spinal cord

perfusion after acute spinal cord injury in pigs

Introduction

Acute spinal cord injury (SCI) from blunt trauma affects 10,000 to 14,000 persons

per year in the United States (Hadley, Walters et al., 2013, pp. 40-53, Burke, Linden et

al., 2001, pp. 274-278). The goals of treatment are to overcome the physiologic barriers

imposed by the spinal injury itself and to allow patients to regain their pre-injury level of

neurologic function (Rowland, Hawryluk et al., 2008, p. E2).

The role of ischemia in the secondary injury cascade has been well studied in

animal models. The mechanisms of secondary injury after SCI have been well defined:

loss of spinal cord microcirculation, loss of autoregulation, and ischemia are all important

in the pathogenesis of secondary spinal cord damage (Guha, Tator et al., 1989, pp. 372-

377, Martirosyan, Feuerstein et al., 2011, pp. 238-251, Kobrine, Doyle et al., 1975, pp.

573-581, Smith, McCreery et al., 1978, pp. 239-251, Dohrmann, Wick et al., 1973, pp.

52-58). One of the basic tenets of management of acute spinal cord injury is the

prevention of spinal cord ischemia by avoiding systemic hypotension and hypoxia. Rapid

decompression of the compressed spinal cord with stabilization of the spine to prevent

further injury and aggressive medical resuscitation with mean arterial blood pressure

(MAP) elevation has become common practice (Casha and Christie, 2011, pp. 1479-

1495, Ploumis, Yadlapalli et al., 2010, pp. 356-362, Fehlings, Vaccaro et al., 2012, p.

e32037). Although no Class I evidence supports its effectiveness, MAP elevation is now recommended for routine use after cervical SCI (Ryken, Hurlbert et al., 2013, pp. 84-92, Vale, Burns et al., 1997, pp. 239-246).

Other potential non-pharmacologic interventions include cerebrospinal fluid (CSF) drainage and hypothermia (Horn, Theodore et al., 2008, p.E12, Dididze, Green et al., 2013, pp. 395-400). The neuroprotective strategy of CSF drainage has been used in patients undergoing abdominal aortic aneurysm surgery, decreasing the neurologic dysfunction after aortic occlusion (Svensson, Crawford et al., 1993, pp. 357-368; discussion 368-370, Khan and Stansby, 2012, p. CD003635). Furthermore, in animal studies, CSF drainage has been shown to decrease spinal cord damage following acute injury (Horn, Theodore et al., 2008, p. E12, Francel, Long et al., 1993, pp. 742-751). However, in humans with SCI, CSF drainage alone did not result in clinical improvement (Kwon, Curt et al., 2009, pp. 181-193).

Characterizing the physiologic changes induced in the spinal cord by MAP elevation and CSF drainage could help clinicians better understand the mechanisms of ischemia after SCI, with the ultimate goal of ameliorating the detrimental effects of ischemia. In our study, we sought to determine the efficacy, in pigs, of aggressive MAP elevation combined with intrathecal pressure (ITP) reduction via CSF drainage; our primary objective was to improve spinal cord blood flow (SCBF) after blunt SCI, in order to decrease or even prevent ischemia.

Materials and Methods

Animal Care

All methodologies concerning the use of animals for scientific study have been approved by the Institutional Animal Care and Use Committee at Barrow Neurological Institute in Phoenix and St. Joseph's Hospital and Medical Center.

Study Groups

For these nonsurvival experiments, we used 15 pigs (adult Yorkshire swine). All 15 pigs underwent laminectomy. We divided them evenly into 5 groups: *control* (n = 3); *SCI* only (n = 3); SCI combined with MAP elevation (*SCI + MAP*, n = 3); SCI combined with CSF drainage (*SCI + CSFD*, n = 3); and SCI combined with both MAP elevation and CSF drainage (*SCI + MAP + CSFD*, n = 3).

Preparation and Monitoring

Each pig was anesthetized with an intramuscular injection of ketamine (40 mg/kg) and xylazine (10 mg/kg). After adequate anesthesia was achieved, the pigs were intubated and maintained under general anesthesia with 2%-3% isoflurane and propofol (0.1 to 0.5 mg/kg/min continuous intravenous IV infusion). A femoral artery was cannulated for blood pressure recordings, and an ear vein was cannulated for administration of drugs. Body temperature was maintained with a heating pad and monitored by rectal temperature probe.

For the surgery, the animals were positioned prone on the operating table. To expose the T3-T8 and L5-S1 spinal levels, we made a midline incision and performed a

subperiosteal dissection. Next, to expose the dura mater at those levels, we performed a laminectomy. A laser Doppler flow monitoring TSD143 probe (Biopac Systems, Inc., Goleta, CA) was then placed over the dura mater at the T5 level. During all procedures, we measured SCBF in blood perfusion units (BPU) and recorded the results. To ensure identical placement of each probe after SCI, we marked the underlying dura mater. This technology allows measurement of blood flow from 1.5 mm tissue depth.

For the pigs with cerebrospinal fluid (CSF) drainage, we placed a lumbar drain (Medtronic, Inc., Minneapolis, MN)—under direct visualization, using an operating microscope—at the lumbosacral junction level intrathecally. To avoid uncontrolled CSF leakage, we used a minimal durotomy (up to 1 mm). We chose the L5-S1 level because of the anatomy of the pig spinal cord, which typically terminates just above the lumbosacral junction. Throughout the procedure, we monitored ITP and recorded the total amount of drained CSF.

Next, 1 hour after the laminectomy (in all groups except the *control* group), we induced mild SCI by delivering a force of 300 gm/cm^2 (20gm weight 15 cm above the spinal cord).

In the pertinent study groups, we also initiated MAP elevation and CSF drainage 1 hour after SCI, to allow the pigs to recover from the procedural stress. MAP was elevated by a continuous infusion of phenylephrine (at a rate of 0.2 mcg/kg/min). This concentration and rate resulted in doubling of MAP.

All relevant physiologic parameters (SCBF, ITP, MAP, and body temperature) were monitored in real time for all animals using the Biopac MP150 unit with additional

LDF100C, DA100C, and SKT100C amplifiers. To display and store data, we used a

Windows personal computer with AcqKnowledge 3.8.2 software (Biopac Systems, Inc.).

Data Analysis

We acquired data immediately before SCI and then 30 minutes, 1, 2, 3, and 4

hours after SCI. In treatment groups, measurements at 1 hour were taken immediately

after treatment initiation. For data processing, we used Excel (Microsoft Corporation,

Redmond, WA). For data analysis, we used the 1-tailed Student *t* test, with results

considered significant if $P < 0.05$.

SCBF

To standardize and compare SCBF, we recorded the value immediately before

SCI as zero. SCBF was then calculated at the set time points after SCI as the percent

difference from the value immediately before SCI. Thus, a negative value represented a

decrease in SCBF; a positive value represented an increase in SCBF.

Intrathecal Pressure

We analyzed ITP, at the set time points after SCI, by comparing it with the value

taken immediately before SCI (in mm Hg).

Study Design

All 15 pigs underwent T5 laminectomy and monitoring as described above. The

control group was not subjected to SCI or any additional interventions (beyond

62

laminectomy and monitoring). In the other 4 study groups, we induced mild SCI 1 hour

after the laminectomy. In the 2 *MAP* groups, a phenylephrine drip was begun 1 hour after

SCI. In the 2 *CSFD* groups, CSF drainage was begun 1 hour after SCI, with the lumbar

drain open at 5 mm Hg. The total experiment time was 6 hours, including 1 hour of

preparation and a total of 5 hours of monitoring time. At the end of the procedures, the

pigs were euthanized per institutional guidelines.

Results

SCBF

SCBF in the *SCI* group decreased by 56% (range, 47.5% to 61.1%) after SCI

compared with baseline (Fig. 8, Table 2). This gradual decrease was reached 1 hour after

SCI and persisted throughout the experiment. MAP elevation after SCI (the *SCI + MAP*

group) decreased SCBF by 34% (range, 25.5% to 34.1%) at 2, 3, and 4 hours after SCI;

interestingly, at 1 hour after SCI (when the phenylephrine drip began), SCBF increased

by an average of 12.6%. However, the difference in SCBF between the *SCI* group and the

SCI + MAP group was not statistically significant ($P > 0.05$; Table 2).

In the *SCI + CSFD* group, SCBF decreased by an average of 16.8% one hour

after SCI and continued to decrease at later time points (range, 50.2% to 60.1%). The

difference was not statistically significant ($P= 0.42$) compared with the *SCI + MAP*

group, but it was statistically significant compared with the *SCI + MAP + CSFD* group

($P < 0.05$; Table 2).

In the *SCI + MAP + CSFD* group, SCBF increased at 2, 3, and 4 hours after SCI

(range, 24.5% to 61.6%) —a statistically significant difference compared with the
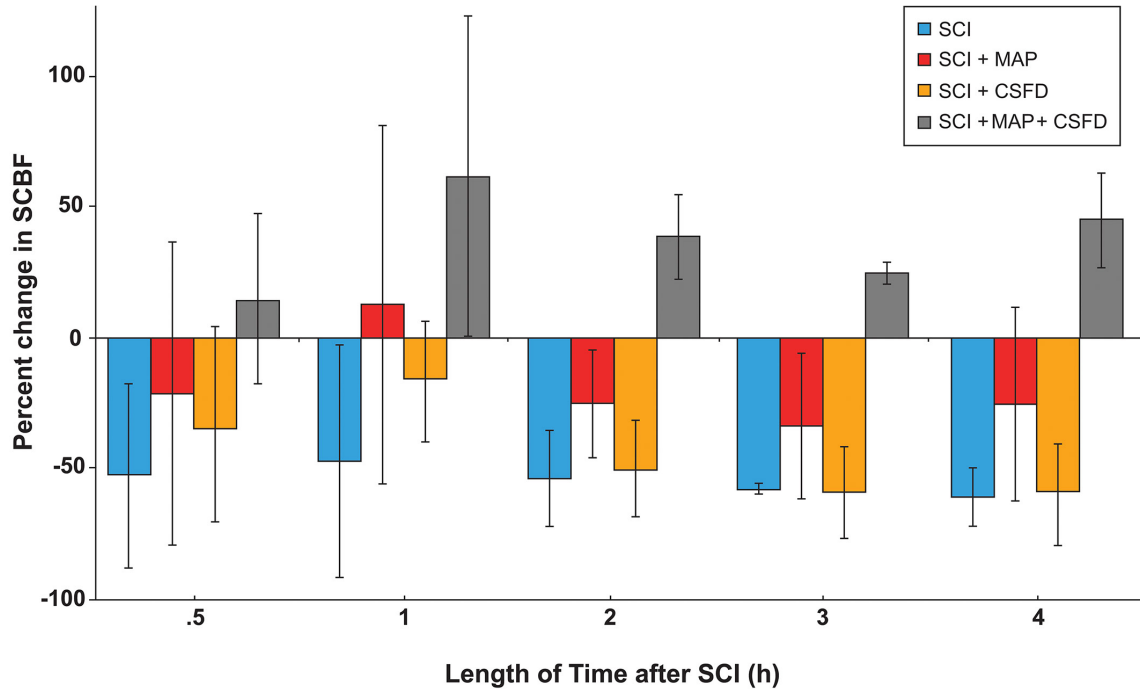
Figure 8. Percentage of change in SCBF at different time points after SCI compared with baseline for the control and treatment groups. In treatment groups, measurements at 1 hour were taken immediately after treatment initiation. There was overall hypoperfusion in SCI, SCI+MAP, and SCI+CSFD groups after SCI. In contrast, SCBF was elevated in comparison with the pre-SCI level in the SCI+MAP+CSFD group. CSFD, cerebrospinal fluid drainage; MAP, mean arterial pressure; SCBF, spinal cord blood flow; SCI, spinal cord injury. Used with permission from Barrow Neurological Institute.

Figure 9. Mean ITP changes at different time points after SCI compared with baseline.

ITP, intrathecal pressure; MAP, mean arterial pressure; SCI, spinal cord injury. Used

with permission from Barrow Neurological Institute.

decrease in both the *SCI* and *SCI + MAP* groups ($P < 0.05$; Table 2). Furthermore, 1 hour after SCI (when both the phenylephrine drip and CSF drainage began), SCBF increased by an average of 61.6%. (Fig. 8).

SCBF in the *control* group decreased only slightly, by 2.4% to 5%, throughout the experiment

Intrathecal Pressure

In the *SCI* group, ITP decreased by 0.8 to 2.35 mm Hg after SCI (Fig. 9). In the *SCI + MAP* group, ITP increased by 4.9 to 5.45 mm Hg. (Fig. 9). In the *control* group, ITP remained stable throughout the experiment. Mean CSF drainage was 32.3 ml in the *SCI + CSFD* group and 55.4 ml in the *SCI + MAP + CSFD* group.

Dynamics

In all 4 study groups (not counting the *control* group), SCBF increased for a short period immediately after acute SCI (Figs. 10, 11). In the *SCI* group, the SCBF remained low throughout the experiment (Fig. 10B)., and ITP varied only slightly, without significant changes.

In the *SCI + MAP* group, SCBF increased immediately after the phenylephrine drip began, but decreased below the baseline level within the next 1 to 1.5 hours (Fig. 10C). The SCBF remained low for the remainder of the experiment. ITP increased immediately after the phenylephrine drip began and remained elevated throughout the experiment.

66
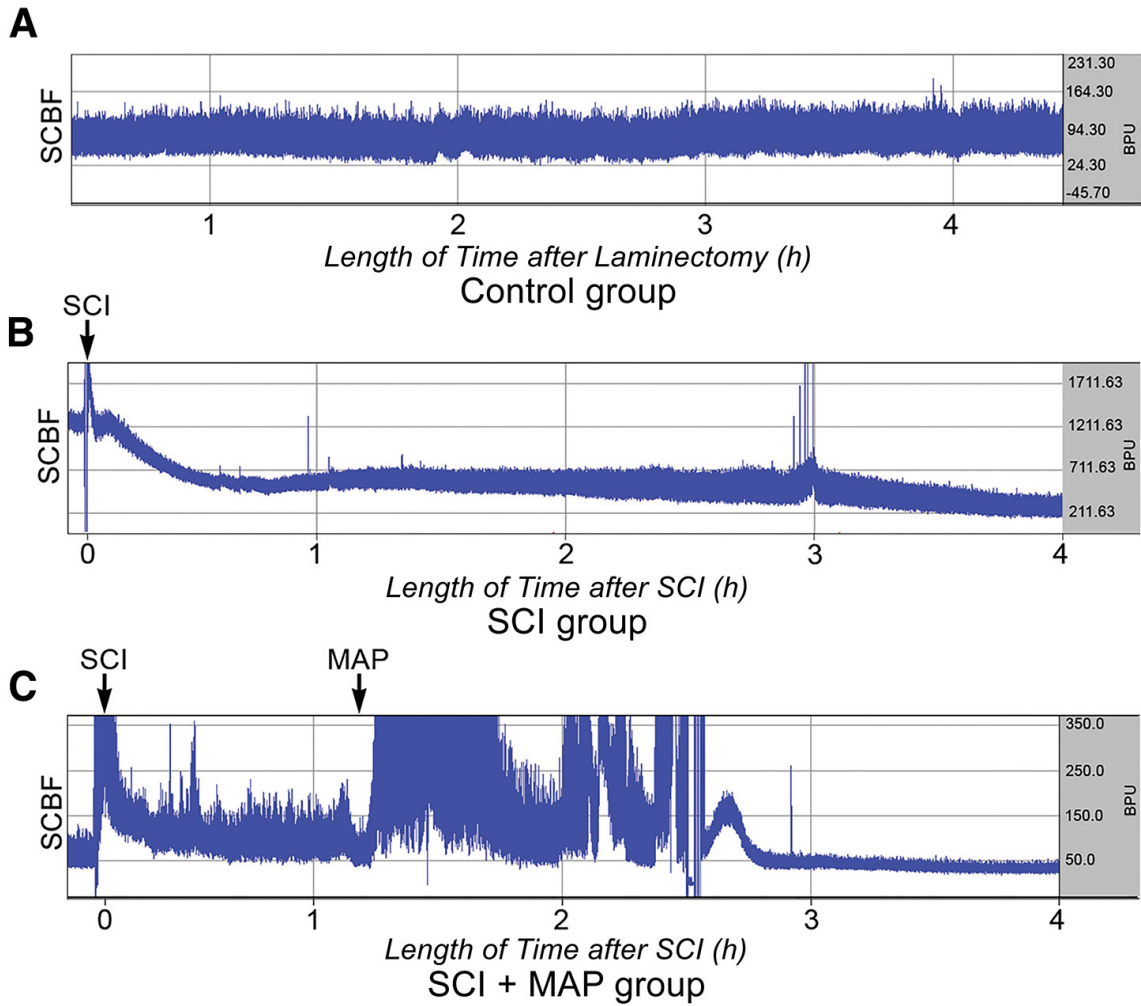
Figure 10. Snapshot of SCBF in the control group (A), SCI group (B), and

SCI+MAP group (C). Arrows indicate the SCI and MAP elevation time points. BPU,

blood perfusion unit; SCBF, spinal cord blood flow; SCI, spinal cord injury; MAP, mean

arterial pressure. Used with permission from Barrow Neurological Institute.
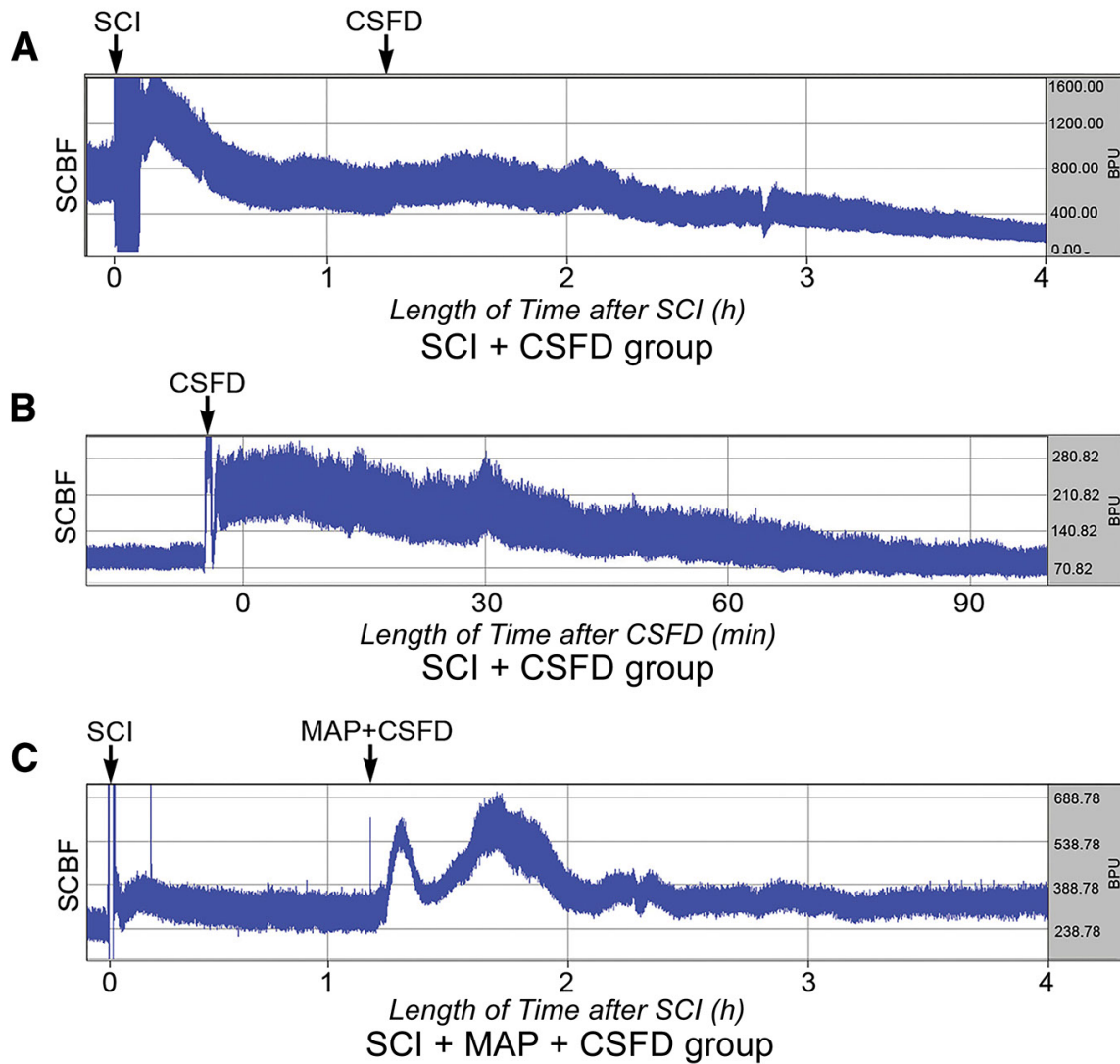
Figure 11. Snapshot of SCBF for entire experiment in the SCI+CSFD group (A)

and SCI+MAP+CSFD group (C). B, effect of CSFD on SCBF after SCI within 90

minutes after CSFD initiation. The shorter timeline allows for finite observation of the

SCBF pattern. Arrows indicate the SCI, MAP elevation and CSFD time points. BPU,

blood perfusion unit; CSFD, cerebrospinal fluid drainage; MAP, mean arterial pressure;

SCBF, spinal cord blood flow; SCI, spinal cord injury. Used with permission from
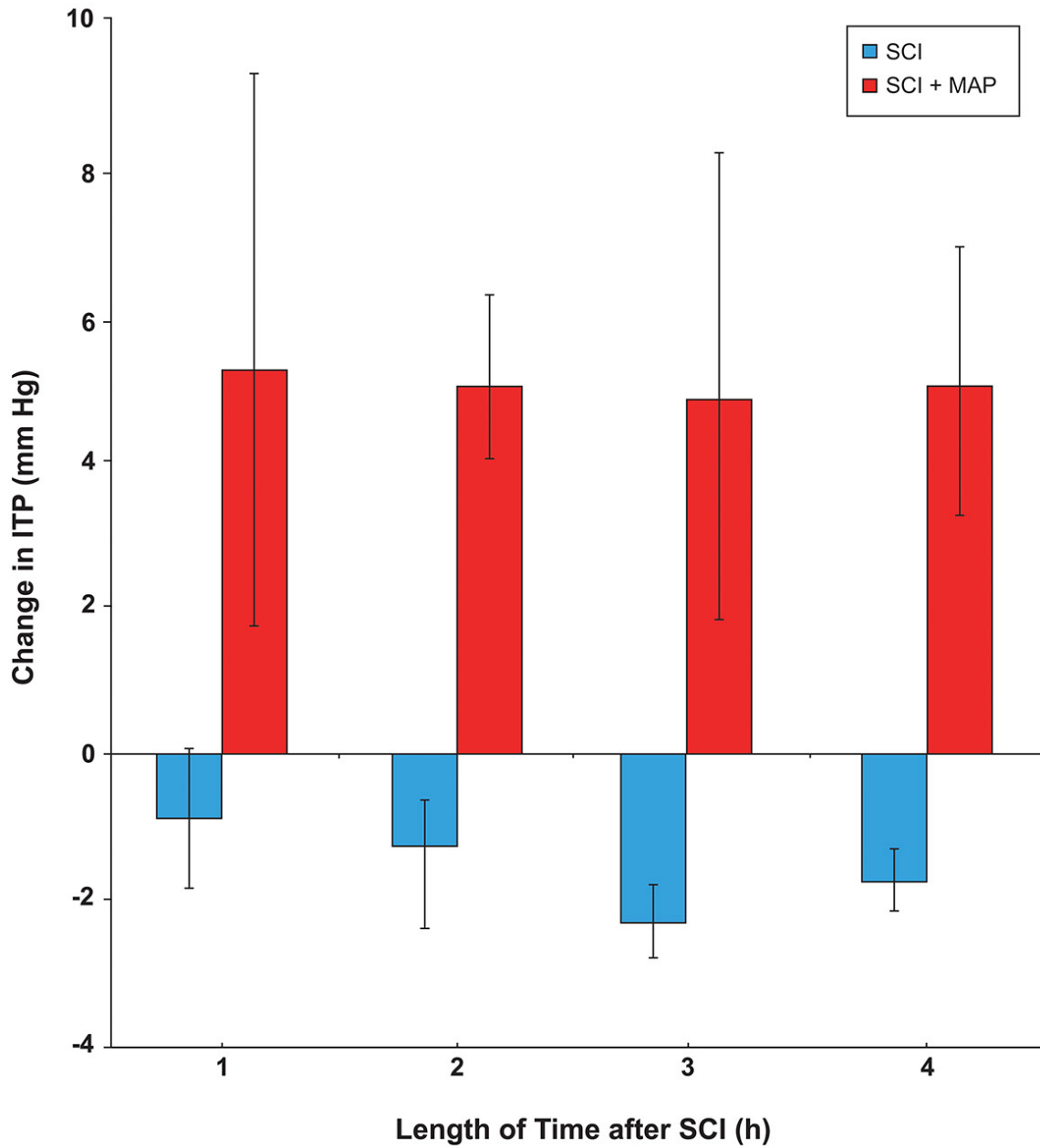
Barrow Neurological Institute.

In the *SCI + CSFD* group, SCBF increased somewhat. However, as in the *SCI +*
MAP group, this effect was temporary: after CSF drainage began at 1 hour, SCBF
decreased and remained at the level below baseline (Figs. 11 A, B). In the *SCI + MAP +*
CSFD group, SCBF increased and remained elevated throughout the experiment (Fig.
11C). In the *control* group, all parameters remained stable throughout the experiment
(Fig. 10A).

In a separate test procedure to define dynamic CSF changes with changing ITP,
we began MAP elevation and CSF drainage 1 hour after SCI. As a result, SCBF
increased. However, about 40 minutes later, we stopped CSF drainage; over the next 3
hours, ITP increased and SCBF gradually decreased, despite MAP elevation. After 3
hours, we again began CSF drainage, which resulted in a noticeable increase in SCBF
(Fig. 12).
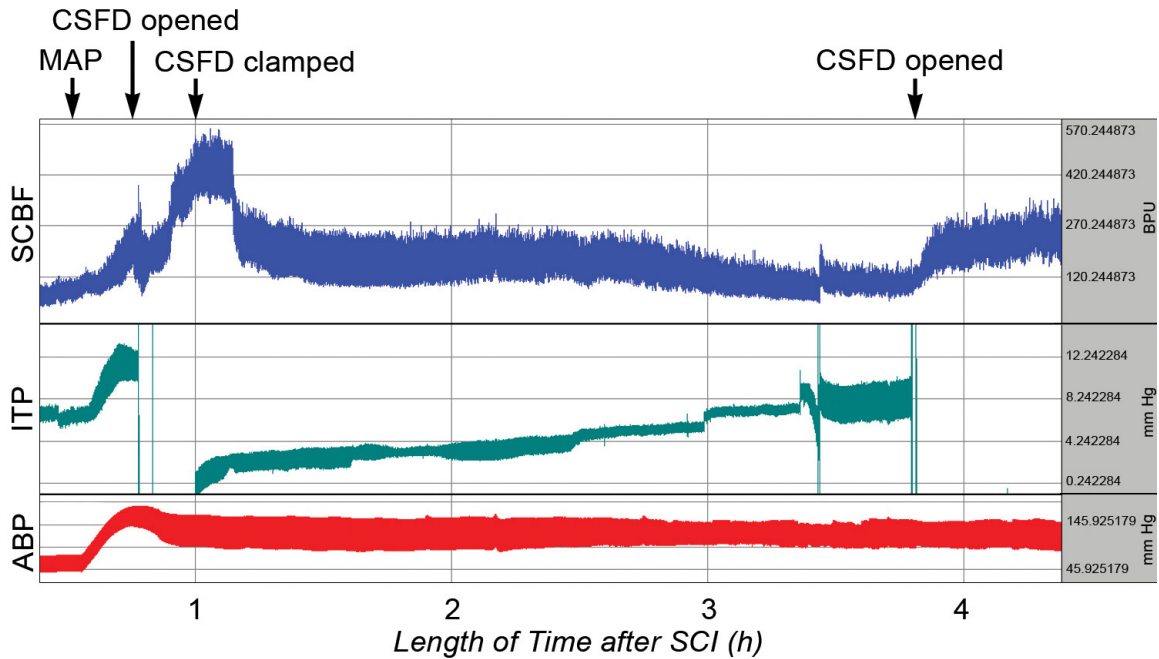
Figure 12. Effect of cerebrospinal fluid drainage (CSFD) and MAP elevation on typical monitoring parameters after SCI. In this test procedure, CSFD was stopped after 40 minutes, and restarted 3 hours later. Arrows indicate the MAP elevation and consecutive initiation and termination of CSFD time points. ABP, arterial blood pressure; BPU, blood perfusion unit; CSFD, cerebrospinal fluid drainage; ITP, intrathecal pressure; MAP, mean arterial pressure; SCBF, spinal cord blood flow; SCI, spinal cord injury. Used with permission from Barrow Neurological Institute.

Discussion

This study describes effects of ITP and MAP changes on SCBF in the settings of mild SCI. The results of our study suggest that combination of elevated MAP and CSFD improves SCBF.

Blood flow in the normal spinal cord is maintained within a normal range (i.e., is autoregulated) when the MAP is 60 to 120 mm Hg and the $paCO_2$ is 10 to 50 mm Hg (Kobrine, Doyle et al., 1975, pp. 573-581, Hickey, Albin et al., 1986, pp. 1183-1189, Kindt, 1971-1972, pp. 19-23). One study has suggested that sympathetic control plays an important role in autoregulation (Kobrine, Evans et al., 1977, pp. 54-55). Loss of autoregulation greatly contributes to ischemia after SCI (Guha, Tator et al., 1989, pp. 372-377, Senter and Venes, 1979, pp. 198-206). Moreover, experimental data have demonstrated delayed onset (by 1 to 2 hours) of ischemia after SCI, which is coincident with loss of autoregulation (Senter and Venes et, 1979, pp. 198-206). Thus, at least theoretically, MAP elevation should address the hypoperfusion experienced after loss of autoregulation after SCI. We also know that according to the Monro-Kellie doctrine any MAP elevation beyond the limit of autoregulation causes increases in cerebral blood flow, intracranial pressure, and, subsequently, ITP (Mokri , 2001, pp. 1746-1748, Piano and Gewertz, 1990, pp. 695-701). However, CSF is produced via an active secretory process and does not change with alterations in MAP (Brown, Davies et al., 2004, pp. 957-970).

Another suggested mechanism of ischemia after SCI is increased vascular resistance. Vascular resistance increases in inverse ratio to SCBF. One of the proposed mechanisms of increased vascular resistance is increased ITP. The spinal cord is encased

71

within the dura mater, which, in turn, is surrounded by rigid bony and ligamentous structures. Thus, increased ITP causes compression of neural elements and vasculature (in a manner analogous to the effects of increased intracranial pressure as predicted by the Monro-Kellie doctrine). Venous outflow compromise results in congestion, increased vascular resistance, and decreased SCBF (Piano and Gewertz, 1990, pp. 695-701). Thus CSF drainage decreases ITP, and therefore should improve spinal cord perfusion pressure after acute SCI.

In our study, we used a mild injury model. This type of SCI provides more opportunities for successful therapeutic interventions with better functional outcome. With this type of SCI, autoregulation of the spinal cord blood supply is altered. However, elements of autoregulation are still present. In contrast, severe SCI results in significantly decreased SCBF and potentially a total loss of autoregulation (Guha, Tator et al., 1989, pp. 372-377).

Measurements of SCBF at 30 minutes provided nonconsistent data with no statistically significant difference (Fig. 8, Table 2). This observation could be explained by complex alterations in spinal cord vasculature after injury. Hyperperfusion has been shown to be the first response to spinal cord injury, followed by hypoperfusion (Smith, McCreery et al., 1978, pp. 239-251, Kobrine, Doyle et al., 1975, pp. 144-149). It is possible that our measurements registered different stages of early post SCI changes in SCBF in different animals. Similar observations were made for the 1-hour measurements, taken immediately after treatment initiation. However the measurements taken 2, 3, and 4 hours after SCI represent homogeneous and comparable data after stabilization of physiological parameters.

72

In our *SCI* group, the pigs showed typical ischemic changes in SCBF after injury; overall, ITP and arterial blood pressure remained stable (Figs. 8, 9B). In our other 3 study groups (the *SCI + MAP* group, the *SCI + CSFD* group, and the *SCI + MAP + CSFD* group), our interventions were intended to address ischemia. In the *SCI+MAP* group, elevation of MAP was initiated 1 hour after SCI, which according to previous research, corresponds to the time course of loss of autoregulation and ischemia (Kobrine, Doyle et al., 1975, pp. 573-581, Senter and Venes, 1979, pp. 198-206). We implemented aggressive elevation of MAP to reach levels beyond autoregulation limits. This allowed us to maximize the effect on SCBF. However, as described previously, elevation of MAP beyond autoregulation level resulted in elevation of ITP. Overall, treatment with induced hypertension resulted in short-term improvement of SCBF. However, SCBF did not reach pre-SCI levels. As ITP pressure continued to rise, SCBF decreased and the spinal cord was left relatively ischemic (Figs. 8, 9, 10C, 12). Addition of CSF drainage to MAP therapy in the *SCI+MAP+CSFD* group 1 hour after SCI resulted in significant improvement of SCBF. The SCBF improved and stayed above pre-SCI levels throughout the experiment. Furthermore, there was a statistically significant difference in SCBF between the *SCI/SCI+MAP* and the *SCI+MAP+CSFD* groups (Figs. 8, 10, 11; Table 2). Analysis of the effect of CSF drainage on SCI (*SCI+CSFD)* revealed short-term improvement of SCBF without reaching pre-SCI values, similar to the *SCI+MAP* group (Figs. 11C, 12). This effect could be attributed to the decompression of the venous system, improving outflow and decreasing vascular resistance. However, alteration of autoregulation and worsening of ischemia resulted in overall decrease in SCBF. According to our results, neither sustained MAP (*SCI group)*, nor its elevation

(*SCI+MAP group)* resulted in lasting improvement in SCBF in the setting of acute SCI

(Figs. 8, 10B and C; Table 2). Moreover, the spinal cord remained relatively

hypoperfused.

The main purpose of this study was to perform an observation of physiological

parameters following acute spinal cord injury. In our experiments, animals were

sacrificed four hours after spinal cord injury (immediate and early acute phase).

According to previous reports, we could expect differences on the molecular level

(Rowland, Hawryluk et al., 2008, p. E2). However, given the relatively short time of

observation, we did not expect to detect significant histological differences between study

groups in this experiment.

Our initial experiment was intended to investigate short-term pathophysiological

changes with a combination of CSF drainage and MAP. These experiments are very

cumbersome and require substantial financial and infrastructural resources. It would not

be feasible to perform experiments with as long a monitoring time for as many animal

groups as was presented in the current investigation. Based on the results of this study,

we plan to conduct an investigation exploring the long term effects of CSFD and MAP in

pigs. We are planning to monitor animals for 24 hour after injury. The animal will be

under general anesthesia for the time of experiment. This will allow more prominent

histological changes occur in the injured spinal cord. We are planning to use advanced

methods of SCBF monitoring in our future experiments. Very recent advances in

technology allow for continuous/repetitive SCBF monitoring deeper into the parenchyma

of the spinal cord (Mesquita, D'Souza et al., 2013, p. e83370, Soubeyrand, Laemmel et

al., 2012, pp. E1376-E1382). Due to local regulation we will not be able to perform long-term survival study on pigs with SCI.

Limitations

Laser Doppler flowmetry (LDF) was used to assess SCBF in our study. This technique was the only reliable and validated method available for continuous SCBF monitoring when we designed and started our experiments. It has been used in multiple studies previously (Pesek, Kibler et al., 2014, pp. 163-170; discussion 169-170, Brady, Lee et al., 2009, pp. 1278-1283, Soubeyrand, Laemmel et al., 2013, pp. 1810-1819, Blaser, Lang et al., 2012, pp. 221-227, Modi, Suh et al., 2011, pp. 1781-1789. Phillips, Cibert-Goton et al., 2013, p. 037005, Lindsberg, O'Neill JT et al., 1989, pp. H674-H680, Lindsberg, Jacobs et al., 1992, pp. H285-H292, Yamada, Morimoto et al., 1998, pp. 626-634, Olive, McCully et al., 2002, pp. 639-645, Westergren, Farooque et al, 2001, pp. 74-84).

Other more precise methods to measure SCBF require animal sacrifice and provide data at a single time point (Cawthon, Senter et al., 1980, 801-807, Ross, Koyanagi et al., 1999, pp. 739-746). The goal of our study was monitor SCBF changes after each step of experiment (baseline before SCI, 1h, 2h, 3h and 4h time points). This would require using five times more animals (75 pigs instead of 15). Therefore these methods (hydrogen clearance, microspheres etc) would not be feasible to implement in our study. Our data represent superficial SCBF, and therefore could not assess the SCBF deep within the parenchyma. LDF allowed measurement of blood flow at a comparably small depth (up to 1.5 mm), which is a limitation of this technology (Lips, de Haan et al.,

2002, pp. 531-538, Simonovich, Barbiro-Michaely et al., 2008, pp. 2495-2502). The pattern of superficial SCBF changes that we observed in the treatment groups may potentially be applicable to deep structures. Nevertheless, the majority of the spinal cord contains eloquent tissue and the protection of any tissue from secondary injury may greatly affect a patient's functional recovery.

Conclusion

In our study of 15 pigs, we found that SCI did not increase ITP, but that the elevation of MAP did, leading to a decrease in SCPP. Both MAP elevation alone and CSF drainage alone led to only short-term improvement of SCBF followed by hypoperfusion. However, the combination of MAP elevation and CSF drainage improved SCBF at the injury site—appearing to prevent hypoperfusion of the spinal cord after SCI. Such an outcome, if replicated in human patients, could potentially decrease spinal cord damage and improve clinical outcomes. Although laser Doppler flowmetry provides flow measurements from 1.5 mm tissue depth, these results may represent pattern of blood flow changes in entire spinal cord after injury. We are currently contemplating a clinical trial based on a review of the literature and the results of our experiments.

Table 2. Statistical difference of changes (positive or negative) in SCBF after SCI (%). Comparison between SCBF in SCI+MAP+CSFD group and SCI, SCI+MAP, SCI+CSFD groups.

Time after SCI	SCI+ MAP+ CSFD SCBF	SCI SCBF	*P* Value	SCI+MAP SCBF	*P* Value	SCI+CSFD SCBF	*P* Value
30 min	14.7 ± 32.7	-53.0 ± 35.4	0.1	-21.3 ± 58.0	0.3	-33.2 ± 37.2	0.1
1h	61.6 ± 61.2	-47.5 ± 44.3	0.03	-12.6 ± 68.4	0.2	-16.8 ± 23.3	0.07
2h	38.4 ± 16.0	-53.9 ± 18.3	0.001	-25.5 ± 20.7	0.007	-50.3 ± 18.3	0.002
3h	24.6 ± 4.2	-58.0 ± 2.2	<0.001	-34.0 ± 28.0	0.03	-59.2 ± 17.5	0.005
4h	44.9 ± 18.1	-61.1 ± 11.2	0.001	-25.5 ± 37.0	0.03	-60.0 ± 19.5	0.001

77

CSFD: cerebrospinal fluid drainage; MAP: mean arterial blood pressure; SCBF: spinal cord blood flow; SCI: spinal cord injury.

P < 0.05 considered significant.

CHAPTER 5

Manganese Enhanced MRI Offers Correlation with Severity of Experimental

Models of Spinal Cord Injury

Introduction

Every year, 12,500 cases of spinal cord injury (SCI) occur in the United States.

The majority of patients are young, active individuals in their fourth decade of life

(Center NSCIS, 2015). Despite significant scientific and clinical effort over past century,

no known treatment paradigm improves SCI outcome beyond natural history (Dobkin B,

et al., 2007, pp. 25-35, Rowland JW, et al., 2008, p. E2). Ongoing and future

experimental studies are anticipated to improve our understanding of mechanisms of SCI

or to suggest therapeutic interventions.

Currently, histologic assessment is the gold standard for evaluating the severity of

an SCI and for determining effectiveness of investigated treatment modalities (Feron F, et

al., pp.2951-2960, Alto LT, et al., 2009, pp. 1106-1113). Thus, in laboratory studies, a

substantial number of animals are required for sacrifice at different time points during the

experiment for longitudinal analyses of histologic changes. Magnetic resonance imaging

(MRI) techniques, such as diffusion tensor imaging (DTI), have the potential to provide

information on the functional status of the spinal cord, as well as fiber integrity, without

or with minimal animal sacrifice. For example, DTI has been used to demonstrate neural

tract integrity after SCI (Schwartz ED, 2003, pp. 570-589, Mulcahey MJ, et al. 2012, pp.

E797-803).

Manganese-enhanced MRI (MEMRI) has been widely implemented to assess different fiber tracts in the brain (Pautler RG, 2002, pp. 441-448, Van der Linden A et al, 2004, pp. 602-612). Mn^{2+} exhibits electrochemical properties similar to Ca^{2+} and is transported via calcium voltage-gated channels (Drapeau P, 1984, pp. 493-510, Lin YJ, 1997, pp. 378-388). As manganese distributes along the functionally active tracts, tracts can be visualized on T1-weighted MRI as a hyperintense signal (Aoki I, 2004, pp 1046-1059, Watanabe T, 2002, pp. 852-859). Our previous study showed a correlation of T1-weighted signal intensity and manganese concentration in the setting of SCI (Martirosyan NL, 2010, pp. 131-136).

A correlation between MEMRI, DTI, and histology has not yet been shown. To determine whether MEMRI could be used to assess SCI as effectively as histology, we compared MEMRI with DTI and histologic assessment in hemisection and transection animal models of SCI.

Materials and methods

Eighteen adult female Sprague-Dawley rats (8 weeks old, weight = 300 g) were used in this study. All animal experiments were performed in accordance with the National Institutes of Health Office of Laboratory Animal Welfare guidelines and were approved by the Institutional Animal Care and Use Committee of Barrow Neurological Institute and St. Joseph's Hospital and Medical Center, Phoenix, Arizona.

Study groups

Rats in this study were evenly distributed among 6 groups with 3 rats per group: transection SCI with manganese chloride ($MnCl_2$) injection (SCIT+Mn); transection SCI without $MnCl_2$ injection (SCIT-Mn); hemisection SCI with $MnCl_2$ injection (SCIH+Mn); hemisection SCI without $MnCl_2$ injection (SCIH-Mn); control rats without SCI and with $MnCl_2$ injection (Control+Mn); control rats without either SCI or $MnCl_2$ injection (Control-Mn). Control animals underwent T9 laminectomy without SCI.

Animal surgery and Spinal Cord Injury Models

Rats were adequately anesthetized with an intramuscular injection of ketamine, xylazine, and acepromazine cocktail. Hairs above the spine were clipped and the skin was cleansed with iodine. The T9 spinal level was localized with intraoperative fluoroscopy and marked with a skin marker. Each rat was placed in a supine position on a heating pad to maintain core body temperature. Oxygen was supplied via nasal cannula. The skin was prepped and draped in standard sterile fashion. An operative microscope was used for the procedure. A midline incision was performed and muscle dissection was carried out to expose the lamina of the T9 level. A laminectomy was performed with a 2-mm bone rongeur. The dura was opened longitudinally in the midline with a scalpel and reflected laterally with forceps. Hemisection and transection models of SCI were used. For the hemisection model (SCIH±Mn groups), the left hemicord was transected with a scalpel, leaving the right hemicord intact. For the transection model (SCIT±Mn groups), the spinal cord was fully transected (Fig. 13). A meticulous hemostasis was achieved with irrigation and application of small wet cotton balls. The wound was closed in multiple

layers and animals were observed until they recovered from anesthesia. Animals received antibiotic injection and pain control in the immediate postoperative period. Their urinary bladders were expressed every 8 hours.

Manganese chloride injection

Twenty-four hours after SCI, the animals in the SCIT+Mn, SCIH+Mn, and Control+Mn groups were anesthetized again and prepared for $MnCl_2$ injection. Cranial hair was clipped and the scalp was cleansed with iodine. The head was affixed to a stereotactic frame. A longitudinal midline scalp incision was performed to expose the bregma. A high-speed drill was used to place two boreholes 2 mm caudal from the bregma and 2 mm lateral to both sides. An automatic microinjector with a 5-µL Hamilton syringe was affixed to the stereotactic frame. The needle was slowly advanced to a depth of 3 mm at each borehole sequentially, which provided access to the lateral ventricle in all animals. A 2-µL volume of 0.2 mol/L $MnCl_2$ was injected into each lateral ventricle over a period of 5 minutes to allow accommodation of the injected fluid into the ventricle. The needle was slowly removed to avoid cerebrospinal fluid (CSF) or $MnCl_2$ backflow.

Sixty hours after $MnCl_2$ injection (84 hours post-SCI surgery), all animals were anesthetized and received a transcordal perfusion of a mixture of 50 mL of normal saline and 1,000 units of heparin, followed by 50 mL of 4% paraformaldehyde. Spinal columns were removed for further imaging and preserved in 4% paraformaldehyde solution.
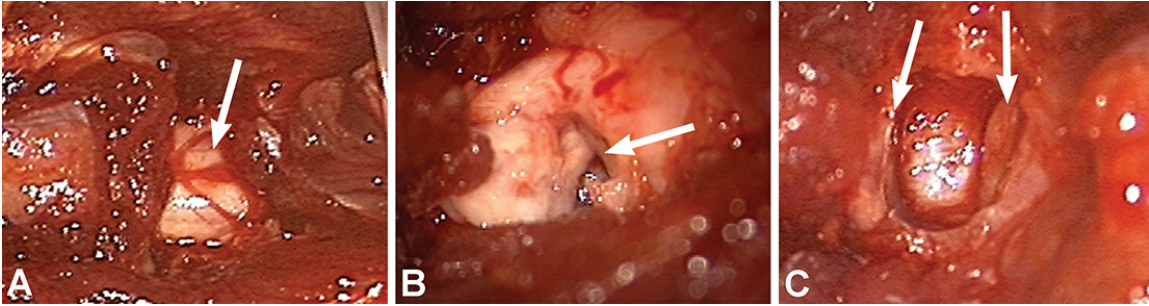
Figure 13. Intraoperative photographs showing spinal cord. A, Control (arrow shows intact spinal cord); B. hemisection (arrow shows hemisected spinal cord); and C, transection animals (arrows show transected edges of spinal cord).

Magnetic Resonance Imaging and Image analysis

Ex vivo MRI was performed using a 7-T, small-animal, 30-cm, horizontal-bore magnet and BioSpec Avance III spectrometer (Bruker, Billerica, MA) with a 116-mm high-power gradient set (600 mT/m) and a 30-mm whole-body quadrature volume coil. Prior to imaging, each spinal column was secured in a custom-made holder, which was then filled with a perfluoropolyether fluid, Galden (Solvay Solexis, Houston, TX), which is invisible on MRI and produces no background signal.

T1-weighted spoiled gradient-echo images were acquired 60 hours after $MnCl_2$ injection (repetition time [TR] = 361 ms, echo time [TE] = 6.7 ms, flip angle = 40°, matrix = 1,024 × 1,024, 78 × 29 ×500 micron voxels, number of excitations [NEX] = 2). DTI imaging was performed in animals without $MnCl_2$ injection (spin-echo, TR = 12.5 s, TE = 27 ms, matrix = 128 × 128, 195 × 195 × 1,000 micron voxels, NEX = 2, 16 diffusion direction, b-value = 2,000 s/mm2).

MEMRI T1-signal intensities of the spinal cord 10 mm rostral from the SCI epicenter (T9 level in control anumals) were calculated and normalized to the paravertebral muscle intensities using ImageJ software. The ratio between spinal cord signal intensity above and below the SCI was calculated. A ratio value approaching 1 signified minimal signal change between areas of spinal cord where measurements were taken (Fig. 14).

DTI fractional anisotropy (FA) measurements were taken 10 mm rostral to the SCI epicenter. The FA in the dorsal column lesion area was normalized to the lateral white matter area that showed no change in FA (Fig. 15).

83

Histology

After MRIs were performed, the spinal specimens were further processed for histologic analysis. In each specimen, the bony elements were removed and the segment of the spinal cord corresponding to the SCI area (T9 level in control anumals) and 10 mm rostral was excised for paraffin embedding. Tissues from the SCI epicenter and approximately 10 mm rostral were cut into 15-μm sections. Luxol fast blue myelin stain was used to assess myelin damage (Margolis G, 1956, pp. 459-474). The optical density of luxol fast blue staining in the rat spinal cord was determined in the SCI epicenter. The optical density at 10 mm rostral to the T9 injury epicenter was also measured as a control. The percentage difference of myelin load at the injury epicenter between SCI and control animals was calculated in groups with the $MnCl_2$ Injection

Data analysis

MEMRI T1-signal intensity ratio, DTI FA, and myelin load percentage differences were calculated and compared among study groups. Data were processed using Microsoft Excel. The 1-tailed Student t-test was used for data analysis, with results considered significant if $P < 0.05$. Pearson's correlation coefficient was calculated to evaluate the correlation between the MEMRI T1-signal intensity ratio, DTI FA, and myelin load percentage differences.
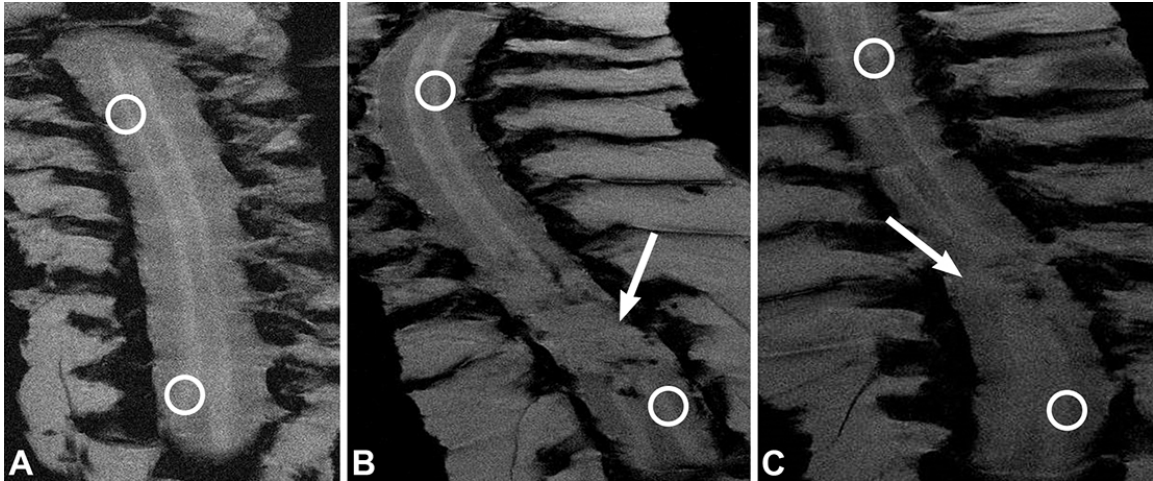
Figure 14. Coronal MEMRI images of spinal cords. A, Control+Mn animal; B,

SCIH+Mn animal; and C, SCIT+Mn animal. Circles indicate areas of spinal cord rostral

and caudal to SCI epicenter where T1-signal intensities were measured. Arrows indicate

regions of SCI.
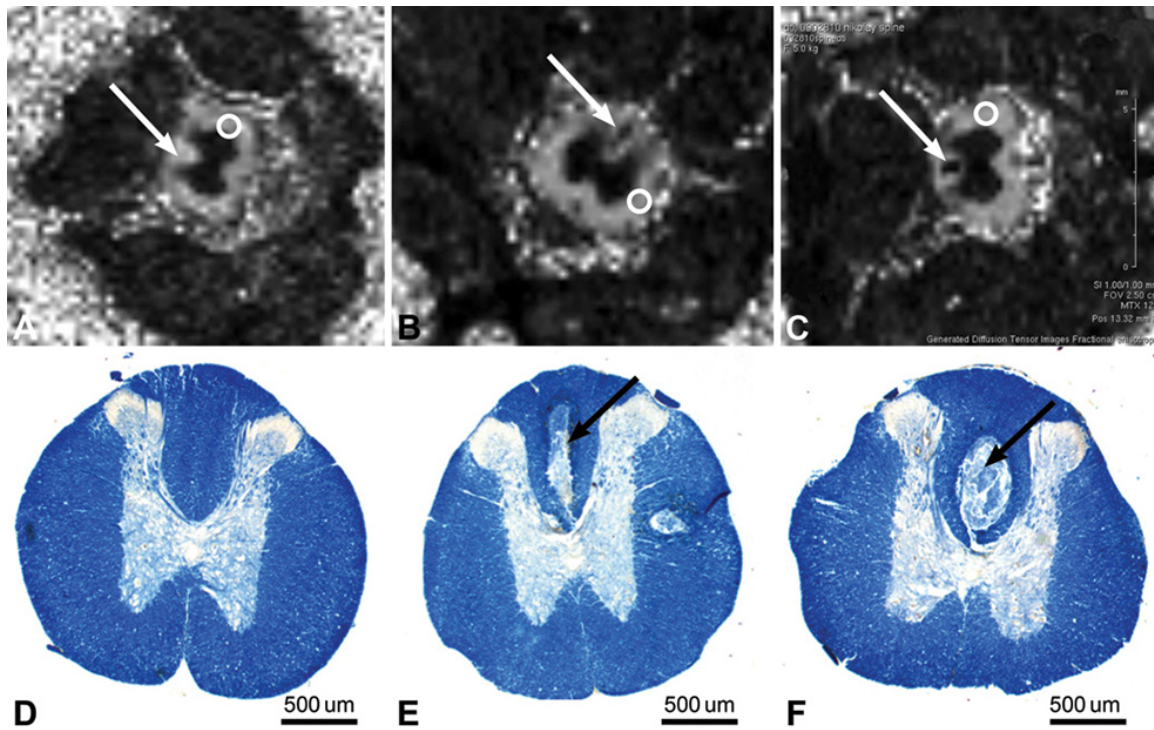
Figure 15. Axial DTI images of spinal cord 10 mm rostral to injury epicenter. A, FA map of spinal cord of control animal. Arrow shows dorsal column. Circle indicates area of lateral white matter that served as FA control. FA map of spinal cord of SCIH animal (B) and SCIT animal (C). Arrows show dorsal column lesion. Circles indicate area of lateral white matter that served as FA control. D-F, Photomicrographs of spinal cord sections 10 mm rostral to injury epicenter: D, control animal; E, hemisection animal; and F, transection animal. Arrow shows dorsal column lesion. Luxol fast blue myelin stain. Scale bar 500 μm.

Results

The mean T1-signal intensity ratio in the Control+Mn group was 0.99, which was significantly higher than in the SCIT+Mn 0.62 and SCIH+Mn 0.87 groups (P <0.05). The mean T1-signal intensity ratio in the groups without $MnCl_2$ injection did not show statistically significant differences (P >0.05): Control-Mn (0.98); SCIT-Mn (0.97); SCIH-Mn (0.98) (Fig. 16, Table 3).

The mean FA percentage increase in Control-Mn animals was 6.1%. The SCIT-Mn and SCIH-Mn groups had 67.5% and 40.12% FA percentage decreases, respectively (Fig. 16, Table 3)

The myelin loads in all animals at the spinal cord level 10 mm rostral to T9 were only minimally different. The SCIT+Mn and SCIH+Mn animals showed 38.7% and 51.8% myelin loads, respectively, compared to similar T9 spinal cord of Control+Mn animals (P<0.05) (Fig. 16, Table 3).

The Pearson correlation coefficients were 0.87 for MEMRI T1-signal intensity ratio and myelin load, -0.98 for FA percentage change and myelin load, and -0.94 for MEMRI T1-signal intensity ratio and FA percentage change.
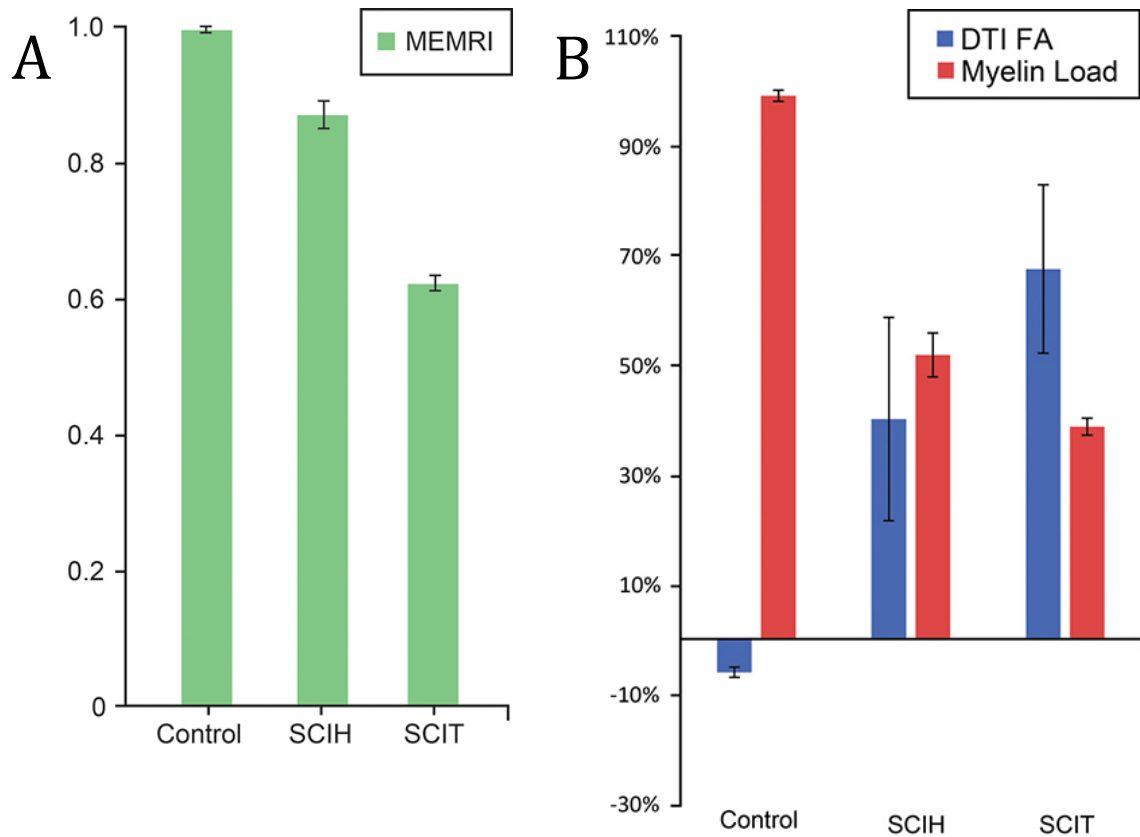
Figure 16. A, MEMRI T1-signal intensity ratio; B, DTI FA percentage change and myelin load in control, hemisection (SCIH) and transection (SCIT) groups. In transection and hemisection groups, MEMRI ratios were lower than in control animals. In transection and hemisection groups, there was an FA decrease and in the control group the FA increase was calculated ($p<0.05$). In the transection and hemisection groups, there was decrease in myelin load compared to the control group.

Discussion

While neuronal degeneration and regrowth is often evaluated by histologic means, noninvasive methods that provide functional assessments over time are needed for a more complete understanding of SCI status. The use of MEMRI T1-signal intensity ratio in rat transection and hemisection SCI models in this study demonstrates that MEMRI offers a correlation with severity of SCI.

Successful research on SCI requires a well-defined and efficient animal model (i.e., a model that uses the fewest possible animals) for studying the basic mechanisms of cord injuries as well as potentially effective clinical therapies. Traditionally, rodent SCIs are modeled using a mid-thoracic (~T9) cord lesion of various types. Lesions are typically either contusive/compressive or trans-sectional, with the latter including both incomplete and complete dissections (Erbayraktar Z, 2013, pp. 103-112). Spinal hemisections can be a particularly useful and efficient approach to studying SCIs, because there is an internal control on the side contralateral to the lesion (Nossin-Manor R, 2002, pp. 231-241). In our experiments, we used the transection model as the most extreme injury severity and the hemisection model to represent moderate SCI. The hemisection and transection models provide consistent and controlled spinal cord tissue damage. Contusion SCI models would also be applicable to such imaging study techniques, although greater variance in outcome would be expected.

Histologic examination of rat spinal cord tissue has revealed differences in gray and white matter injury progression at multiple time points post-injury in a controlled contusion rat model (Ek CJ, 2010, p. e12021). There was a significant loss of gray and white matter 24-hours post injury in our study. We performed imaging in rat specimens

89

84 hours after SCI, which is sufficient time to cause significant spinal cord tissue damage that can be detected by histology and potentially with MRI techniques.

MEMRI can provide information on the functional activity of neural tissue. The chemical properties of Mn^{2+} resemble those of Ca^{2+}, allowing it to be transported through voltage-gated Ca^{2+} channels in neurons (Pautler RG, 2004, pp. 595-601, Pautler RG, 1998, pp. 740-748, Silva AC, 2008, pp. 595-604). Mn^{2+} is paramagnetic and causes robust T1 shortening in tissue water that shows up as strong enhancement on MRI (Lin YJ, 1997, pp. 378-388). Systemic injection of $MnCl_2$ into the CSF allows for assessment of activity-dependent uptake (Aoki I, 2004, pp. 1046-1059, Martirosyan NL, 2010, pp. 131-136, Stieltjes B, 2006, pp. 1124-1131). The uptake depends on the functional activity of the spinal cord: uptake by functionally active neurons is greater than uptake in damaged or inactive neurons (Tindemans I, 2003, pp. 3352-3360, Walder N, 2008, pp. 277-283). A previous study has shown that MEMRI signal from Mn^{2+} injected into the ventricles correlated to functional assessment in a rat SCI model (Stieltjes B, 2006, pp. 1124-1131). The rate of transport is much higher than axonal transport could account for, indicating that the transport occurred through the CSF, with local activity-dependent uptake into the gray matter. The comparison of MEMRI results to images acquired after injection of a different, non-Ca^{2+}-like contrast agent, gadolinium-DTPA, showed that MEMRI results could not be explained by simple disruption of the CSF system due to the injury. MEMRI was compared to total Mn^{2+} content measured by inductively coupled plasma mass spectrometry (ICP-MS) in a full transection SCI rat model (Martirosyan NL, 2010, pp. 131-136). The intensity of the gray matter signal in T1-weighted MRI and the ICP-MS-measured Mn^{2+} was significantly decreased below the injury site. The MRI

signal intensity corresponded with Mn^{2+} levels from the cervical to the lumbar sections of the spine.

MEMRI can also be used to study axonal transport by injecting the agent directly into the white matter (Bilgen M, 2006, p. 15). However, these images also contain a strong gray matter enhancement that indicates that significant gray matter uptake must also play a role in these results. Also, performing a focal injection into the spinal cord can be challenging and requires an additional laminectomy.

Another MRI method that can be used to assess white matter status is DTI, which provides a method to measure directional water diffusion in the white matter tracts (Hagmann P, 2006, pp. S205-223, Bazley FA, 2012, pp. 82-85, Greenberg G, 2008, pp. S45-50, Kim JH, 2007, pp. 253-260). While normal water diffusion is isotropic in all directions in an unbounded space, in a case where there is structure that restricts the water molecule's movement, the diffusion will become more anisotropic. An example of this restricted diffusion is that within an axon, where the diffusion can travel along the distance of the axon with relative freedom, while the membrane walls restrict diffusion along the width of the axon. DTI can measure the degree of anisotropy that is quantified by the parameter FA. In the spinal cord, FA has been shown to correspond to axonal integrity and can be used to follow white matter injury progression. (Bazley FA, 2012, pp. 82-85, Greenberg G, 2008, pp. S45-50, Kim JH, 2007, pp. 253-260). Further assessment of how our imaging results relate to the underlying tissue pathology was performed with histologic staining for myelin. The change in myelin load was then compared to the imaging results and all three measures were correlated to injury severity.

91

In our study, MEMRI, DTI, and myelin load showed strong correlations with severity of SCI.

In addition to the alterations in white matter FA due to injury, DTI also revealed focal lesions in the dorsal columns, both caudal and rostral of the injury site. Other groups have previously reported similar lesions revealed by DTI (Bilgen M, 2006, p. 15). Similar lesions appeared in tissue stained for myelin content, providing evidence that the FA alteration corresponds to myelin content.

Manganese overdose results in damage to the nervous system, liver, and heart. The most common symptom of manganese intoxication is tremor caused by damage of basal ganglia. Thus, cautious use of manganese is warranted (Silva AC, 2008, pp. 595-604, Dobson AW, 2004, pp.115-128).

Conclusion

A major advantage of the MEMRI approach is the ability to study spinal cord injury longitudinally through the injury and recovery period of a laboratory animal. This technique may not only provide a more accurate picture of injury evolution, but it may also reduce the number of animals necessary to perform a particular experiment. Our results showed that MEMRI correlates to injury severity, and histology at a single time point.

Table 3. Mean MEMRI T1-1 signal intensity ratio, DTI FA percentage increase, and myelin load percentage change.

	Control	SCIH	P value (Control vs. SCIH)	SCIT	P value (Control vs. SCIT)
MEMRI*	0.99±0.003	0.87±0.02	<0.001	0.62±0.01	<0.001
DTI FA†	-6.09%± 0.91%	40.12%±18.50%	0.024	67.5%±15.3%	0.003
Myelin load*	99.10%±1.01%	51.83%±4.02%	<0.001	38.72%±1.50%	<0.001

*Performed on experimental/control groups injected with $MnCl_2$.
†Performed on experimental/control groups not receiving $MnCl_2$ injections.
Abbreviations: DTI FA, diffusion tensor imaging fractional anisotropy; MEMRI, manganese-enhanced MRI; SCIH, hemisection spinal cord injury; SCIT, transection spinal cord injury.

CHAPTER 6

Discussion

Spinal cord vascular anatomy and physiology

Spinal cord vasculature exhibits complex anatomical physiological properties. Variability in the direction of blood flow and in the diameter of arteries assure a constant and sufficient blood supply. The pathophysiology of spinal cord blood flow under normal conditions has been investigated in several studies, and a consensus has been reached on key mechanisms of the blood supply to the normal spinal cord. Chapter 2 provides a comprehensive review on the current understanding of the anatomy and physiology of the spinal cord blood supply. Although numerous experiments have attempted to investigate the principles elucidating the blood supply in the injured spinal cord, these mechanisms remain unclear. Techniques that would allow continuous precise measurement of blood flow in different spinal cord regions could potentially answer many of the questions regarding how the blood flow is altered. Manipulating physiological parameters such as MAP and ITP may have potential benefit in improving the blood supply to ischemic areas of the injured spinal cord.

Arterial basket of conus medullaris

The ABCM functions as an anastomotic connection between the ASA and PSA. The arterial basket was symmetric in most specimens (n=13), meaning that the ASA is connected to paired PSAs via right and left branches. This symmetric configuration allows for continuity of circulation between the anterior and posterior spinal circulations. In rare cases (n=3), the anastomotic network was asymmetric with a dominant artery

94

connecting the ASA to one of the PSAs. This rare arrangement resulted in one PSA receiving all of the ASA flow. This arrangement may result in a watershed zone on the contralateral dorsal surface of the spinal cord.

Understanding of the anatomy of the ABCM and its variations is critical for addressing vascular malformations in this location. The presence of perforating vessels feeding the conus that arise from this ABCM has clinical implications for the resection of vascular lesions as well as other pathologies in this region. This anatomy if often not well described or studied; our study adds a new dimension, highlighting the importance of perforating vessels arising from the ABCM to the vasculature of the conus medullaris.

Cerebrospinal fluid drainage and induced hypertension improve spinal cord perfusion after acute spinal cord injury in pigs

In our study of 15 pigs, we found that SCI did not increase ITP, but that the elevation of MAP did, leading to a decrease in SCPP. Isolated MAP elevation or CSFD led to an only short-term improvement of SCBF followed by hypoperfusion. However, the combination of MAP elevation and CSFD improved SCBF at the injury site—appearing to prevent hypoperfusion of the spinal cord after SCI. Such an outcome, if replicated in human patients, could potentially decrease spinal cord damage and improve clinical outcomes. Although laser Doppler flowmetry provides flow measurements from 1.5 mm tissue depth, these results may represent a pattern of blood flow changes in entire spinal cord after injury.

Manganese Enhanced MRI Offers Correlation with Severity of Experimental Models of

Spinal Cord Injury

A major advantage of the MEMRI approach is the ability to study spinal cord injury longitudinally through the injury and recovery period of a laboratory animal. This technique may not only provide a more accurate picture of injury evolution, but it may also reduce the number of animals necessary to perform a particular experiment. Our results showed that MEMRI correlates to injury severity, and histology at a single time point.

Conclusions

This dissertation uses interdisciplinary approaches to further investigate the anatomy of the normal spinal cord and pathophysiology of the blood supply after acute spinal cord injury. Understanding of complex vascular anatomy of the ABCM is important during surgical and endovascular treatment of conus vascular malformations.

Manipulating physiological parameters such as MAP and ITP may be beneficial for patients with a spinal cord injury. Further experiments to assess neurologic function after such intervention.

MEMRI can be as reliable to assess the severity of the spinal cord injury as histology. Although manganese cannot be used in the clinical settings because of its toxicity, MEMRI is an excellent research tool for longitudinal assessment of the spinal cord regeneration. This will potentially decrease the number of the study subjects.

REFERENCES

Adamkiewicz, A. *Die blutgefässe des menschlichen rückenmarkes. I. II. Die gefässe der rückenmark ssubstanz. Die gëfasse der rückenmarksoberflache* [in German]. Wien, 1881.

Adamkiewicz, A. *Die Blutgefässe menschlichen Rückenmarkes : 2. Theil Die Gefässe der Rückenmarksoberfläche* [in German], 1882.

Allen, W. E., 3rd, C. M. D'Angelo, and E. L. Kier. "Correlation of microangiographic and electrophysiologic changes in experimental spinal cord trauma." *Radiology* 111, no. 1 (Apr 1974): 107-15.

Alleyne, C. H., Jr., C. M. Cawley, G. G. Shengelaia, and D. L. Barrow. "Microsurgical anatomy of the artery of Adamkiewicz and its segmental artery." *J Neurosurg* 89, no. 5 (Nov 1998): 791-5.

Alto, L. T., L. A. Havton, J. M. Conner, E. R. Hollis, 2nd, A. Blesch, and M. H. Tuszynski. "Chemotropic guidance facilitates axonal regeneration and synapse formation after spinal cord injury." *Nat Neurosci* 12, no. 9 (Sep 2009): 1106-13.

Aoki, I., Y. J. Wu, A. C. Silva, R. M. Lynch, and A. P. Koretsky. "In vivo detection of neuroarchitecture in the rodent brain using manganese-enhanced MRI." *Neuroimage* 22, no. 3 (Jul 2004): 1046-59.

Barone, G. W., A. W. Joob, T. L. Flanagan, C. E. Dunn, and I. L. Kron. "The effect of hyperemia on spinal cord function after temporary thoracic aortic occlusion." *J Vasc Surg* 8, no. 4 (Oct 1988): 535-40.

Bazley, F. A., A. Pourmorteza, S. Gupta, N. Pashai, C. Kerr, and A. H. All. "DTI for assessing axonal integrity after contusive spinal cord injury and transplantation of oligodendrocyte progenitor cells." *Conf Proc IEEE Eng Med Biol Soc* 2012 (2012): 82-5.

Berendes, J. N., J. J. Bredee, J. J. Schipperheyn, and Y. A. Mashhour. "Mechanisms of spinal cord injury after cross-clamping of the descending thoracic aorta." *Circulation* 66, no. 2 Pt 2 (Aug 1982): I112-6.

Bilgen, M. "Imaging corticospinal tract connectivity in injured rat spinal cord using manganese-enhanced MRI." *BMC Med Imaging* 6 (2006): 15.

Bingham, W. G., H. Goldman, S. J. Friedman, S. Murphy, D. Yashon, and W. E. Hunt. "Blood flow in normal and injured monkey spinal cord." *J Neurosurg* 43, no. 2 (Aug 1975): 162-71.

Blaisdell, F. W., and D. A. Cooley. "The mechanism of paraplegia after temporary thoracic aortic occlusion and its relationship to spinal fluid pressure." *Surgery* 51 (Mar 1962): 351-5.

Blaser, A., J. Lang, D. Henke, M. G. Doherr, C. Adami, and F. Forterre. "Influence of durotomy on laser-Doppler measurement of spinal cord blood flow in chondrodystrophic dogs with thoracolumbar disk extrusion." *Vet Surg* 41, no. 2 (Feb 2012): 221-7.

Bolton, B. "The blood supply of the human spinal cord." *J Neurol Psychiatry* 2, no. 2 (Apr 1939): 137-48.

Bower, T. C., M. J. Murray, P. Gloviczki, T. L. Yaksh, L. H. Hollier, and P. C. Pairolero. "Effects of thoracic aortic occlusion and cerebrospinal fluid drainage on regional spinal cord blood flow in dogs: correlation with neurologic outcome." *J Vasc Surg* 9, no. 1 (Jan 1989): 135-44.

Brady, K. M., J. K. Lee, K. K. Kibler, R. B. Easley, R. C. Koehler, M. Czosnyka, P. Smielewski, and D. H. Shaffner. "The lower limit of cerebral blood flow autoregulation is increased with elevated intracranial pressure." *Anesth Analg* 108, no. 4 (Apr 2009): 1278-83.

Brown, P. D., S. L. Davies, T. Speake, and I. D. Millar. "Molecular mechanisms of cerebrospinal fluid production." *Neuroscience* 129, no. 4 (2004): 957-70.

Burke, D. A., R. D. Linden, Y. P. Zhang, A. C. Maiste, and C. B. Shields. "Incidence rates and populations at risk for spinal cord injury: A regional study." *Spinal Cord* 39, no. 5 (May 2001): 274-8.

Carlson, G. D., C. D. Gorden, S. Nakazawa, E. Wada, J. S. Smith, and J. C. LaManna. "Sustained spinal cord compression: part II: effect of methylprednisolone on regional blood flow and recovery of somatosensory evoked potentials." *J Bone Joint Surg Am* 85-a, no. 1 (Jan 2003): 95-101.

Carlson, G. D., Y. Minato, A. Okada, C. D. Gorden, K. E. Warden, J. M. Barbeau, C. L. Biro*, et al.* "Early time-dependent decompression for spinal cord injury: vascular mechanisms of recovery." *J Neurotrauma* 14, no. 12 (Dec 1997): 951-62.

Casha, S., and S. Christie. "A systematic review of intensive cardiopulmonary management after spinal cord injury." *J Neurotrauma* 28, no. 8 (Aug 2011): 1479-95.

Cawthon, D. F., H. J. Senter, and W. B. Stewart. "Comparison of hydrogen clearance and 14C-antipyrine autoradiography in the measurement of spinal cord blood flow after severe impact injury." *J Neurosurg* 52, no. 6 (Jun 1980): 801-7.

Center, National Spinal Cord Injury Statistical. *Facts and Figures at a Glance.* Birmingham, A, 2015.

Cina, C. S., A. Lagana, G. Bruin, C. Ricci, B. Doobay, J. Tittley, and C. M. Clase. "Thoracoabdominal aortic aneurysm repair: a prospective cohort study of 121 cases." *Ann Vasc Surg* 16, no. 5 (Sep 2002): 631-8.

Clark, F. J., W. A. Mutch, I. R. Sutton, J. M. Teskey, K. McCutcheon, D. B. Thiessen, M. Rosenbloom, and I. R. Thomson. "Treatment of proximal aortic hypertension after thoracic aortic cross-clamping in dogs. Phlebotomy versus sodium nitroprusside/isoflurane." *Anesthesiology* 77, no. 2 (Aug 1992): 357-64.

Coselli, J. S., S. A. LeMaire, C. Koksoy, Z. C. Schmittling, and P. E. Curling. "Cerebrospinal fluid drainage reduces paraplegia after thoracoabdominal aortic aneurysm repair: results of a randomized clinical trial." *J Vasc Surg* 35, no. 4 (Apr 2002): 631-9.

Cox, G. S., P. J. O'Hara, N. R. Hertzer, M. R. Piedmonte, L. P. Krajewski, and E. G. Beven. "Thoracoabdominal aneurysm repair: a representative experience." *J Vasc Surg* 15, no. 5 (May 1992): 780-7; discussion 87-8.

Crawford, E. S., J. L. Crawford, H. J. Safi, and J. S. Coselli. "Redo operations for recurrent aneurysmal disease of the ascending aorta and transverse aortic arch." *Ann Thorac Surg* 40, no. 5 (Nov 1985): 439-55.

Crawford, E. S., J. L. Crawford, H. J. Safi, J. S. Coselli, K. R. Hess, B. Brooks, H. J. Norton, and D. H. Glaeser. "Thoracoabdominal aortic aneurysms: preoperative and intraoperative factors determining immediate and long-term results of operations in 605 patients." *J Vasc Surg* 3, no. 3 (Mar 1986): 389-404.

Crawford, E. S., K. R. Hess, E. S. Cohen, J. S. Coselli, and H. J. Safi. "Ruptured aneurysm of the descending thoracic and thoracoabdominal aorta. Analysis according to size and treatment." *Ann Surg* 213, no. 5 (May 1991): 417-25; discussion 25-6.

D'Ambra, M. N., W. Dewhirst, M. Jacobs, B. Bergus, L. Borges, and A. Hilgenberg. "Cross-clamping the thoracic aorta. Effect on intracranial pressure." *Circulation* 78, no. 5 Pt 2 (Nov 1988): Iii198-202.

Dididze, M., B. A. Green, W. D. Dietrich, S. Vanni, M. Y. Wang, and A. D. Levi. "Systemic hypothermia in acute cervical spinal cord injury: a case-controlled study." *Spinal Cord* 51, no. 5 (May 2013): 395-400.

Djindjian, M., A. Ribeiro, E. Ortega, A. Gaston, and J. Poirier. "The normal vascularization of the intradural filum terminale in man." *Surg Radiol Anat* 10, no. 3 (1988): 201-9.

Djindjian, R. "Angiography of the spinal cord." *Surg Neurol* 2, no. 3 (May 1974): 179-85.

Dobkin, B., H. Barbeau, D. Deforge, J. Ditunno, R. Elashoff, D. Apple, M. Basso*, et al.* "The evolution of walking-related outcomes over the first 12 weeks of rehabilitation for incomplete traumatic spinal cord injury: the multicenter randomized Spinal Cord Injury Locomotor Trial." *Neurorehabil Neural Repair* 21, no. 1 (Jan-Feb 2007): 25-35.

Dobson, A. W., K. M. Erikson, and M. Aschner. "Manganese neurotoxicity." *Ann N Y Acad Sci* 1012 (Mar 2004): 115-28.

Dohrmann, G. J., F. C. Wagner, Jr., K. M. Wick, and P. C. Bucy. "Fine structural alterations in transitory traumatic paraplegia." *Proc Veterans Adm Spinal Cord Inj Conf* 18 (1971): 6-8.

Dohrmann, G. J., K. M. Wick, and P. C. Bucy. "Spinal cord blood flow patterns in experimental traumatic paraplegia." *J Neurosurg* 38, no. 1 (Jan 1973): 52-8.

Dolan, E. J., and C. H. Tator. "The effect of blood transfusion, dopamine, and gamma hydroxybutyrate on posttraumatic ischemia of the spinal cord." *J Neurosurg* 56, no. 3 (Mar 1982): 350-8.

Dong, C. C., D. B. MacDonald, and M. T. Janusz. "Intraoperative spinal cord monitoring during descending thoracic and thoracoabdominal aneurysm surgery." *Ann Thorac Surg* 74, no. 5 (Nov 2002): S1873-6; discussion S92-8.

Drapeau, P., and D. A. Nachshen. "Manganese fluxes and manganese-dependent neurotransmitter release in presynaptic nerve endings isolated from rat brain." *J Physiol* 348 (Mar 1984): 493-510.

Ducker, T. B., and P. L. Perot, Jr. "Spinal cord oxygen and blood flow in trauma." *Surg Forum* 22 (1971): 413-5.

Ducker, T. B., M. Salcman, J. T. Lucas, W. B. Garrison, and P. L. Perot, Jr. "Experimental spinal cord trauma, II: Blood flow, tissue oxygen, evoked potentials in both paretic and plegic monkeys." *Surg Neurol* 10, no. 1 (Jul 1978): 64-70.

Ducker, T. B., M. Salcman, P. L. Perot, Jr., and D. Ballantine. "Experimental spinal cord trauma, I: Correlation of blood flow, tissue oxygen and neurologic status in the dog." *Surg Neurol* 10, no. 1 (Jul 1978): 60-3.

Ek, C. J., M. D. Habgood, J. K. Callaway, R. Dennis, K. M. Dziegielewska, P. A. Johansson, A. Potter, B. Wheaton, and N. R. Saunders. "Spatio-temporal progression of grey and white matter damage following contusion injury in rat spinal cord." *PLoS One* 5, no. 8 (2010): e12021.

Elmore, J. R., P. Gloviczki, C. M. Harper, P. C. Pairolero, M. J. Murray, R. G. Bourchier, T. C. Bower, and J. R. Daube. "Failure of motor evoked potentials to predict neurologic outcome in experimental thoracic aortic occlusion." *J Vasc Surg* 14, no. 2 (Aug 1991): 131-9.

Erbayraktar, Z., N. Gokmen, O. Yilmaz, and S. Erbayraktar. "Experimental traumatic spinal cord injury." *Methods Mol Biol* 982 (2013): 103-12.

Fairholm, D., and I. Turnbull. "Microangiographic study of experimental spinal injuries in dogs and rabbits." *Surg Forum* 21 (1970): 453-5.

Fehlings, M. G., C. H. Tator, and R. D. Linden. "The relationships among the severity of spinal cord injury, motor and somatosensory evoked potentials and spinal cord blood flow." *Electroencephalogr Clin Neurophysiol* 74, no. 4 (Jul-Aug 1989): 241-59.

Fehlings, M. G., A. Vaccaro, J. R. Wilson, A. Singh, W. Cadotte D, J. S. Harrop, B. Aarabi*, et al.* "Early versus delayed decompression for traumatic cervical spinal cord injury: results of the Surgical Timing in Acute Spinal Cord Injury Study (STASCIS)." *PLoS One* 7, no. 2 (2012): e32037.

Feron, F., C. Perry, J. Cochrane, P. Licina, A. Nowitzke, S. Urquhart, T. Geraghty, and A. Mackay-Sim. "Autologous olfactory ensheathing cell transplantation in human spinal cord injury." *Brain* 128, no. Pt 12 (Dec 2005): 2951-60.

Fix, A. S., J. F. Ross, S. R. Stitzel, and R. C. Switzer. "Integrated evaluation of central nervous system lesions: stains for neurons, astrocytes, and microglia reveal the spatial and temporal features of MK-801-induced neuronal necrosis in the rat cerebral cortex." *Toxicol Pathol* 24, no. 3 (May-Jun 1996): 291-304.

Francel, P. C., B. A. Long, J. M. Malik, C. Tribble, J. A. Jane, and I. L. Kron. "Limiting ischemic spinal cord injury using a free radical scavenger 21-aminosteroid and/or cerebrospinal fluid drainage." *J Neurosurg* 79, no. 5 (Nov 1993): 742-51.

Fried, L. C., and O. Aparicio. "Experimental ischemia of the spinal cord. Histologic studies after anterior spinal artery occlusion." *Neurology* 23, no. 3 (Mar 1973): 289-93.

Gharagozloo, F., R. F. Neville, Jr., and J. L. Cox. "Spinal cord protection during surgical procedures on the descending thoracic and thoracoabdominal aorta: a critical overview." *Semin Thorac Cardiovasc Surg* 10, no. 1 (Jan 1998): 73-86.

Gillilan, L. A. "The arterial blood supply of the human spinal cord." *J Comp Neurol* 110, no. 1 (Aug 1958): 75-103.

Greenberg, G., D. J. Mikulis, K. Ng, D. DeSouza, and R. E. Green. "Use of diffusion tensor imaging to examine subacute white matter injury progression in moderate to severe traumatic brain injury." *Arch Phys Med Rehabil* 89, no. 12 Suppl (Dec 2008): S45-50.

Griffiths, I. R. "Spinal cord blood flow after acute experimental cord injury in dogs." *J Neurol Sci* 27, no. 2 (Feb 1976): 247-59.

Griffiths, I. R., L. H. Pitts, R. A. Crawford, and J. G. Trench. "Spinal cord compression and blood flow. I. The effect of raised cerebrospinal fluid pressure on spinal cord blood flow." *Neurology* 28, no. 11 (Nov 1978): 1145-51.

Guha, A., C. H. Tator, and J. Rochon. "Spinal cord blood flow and systemic blood pressure after experimental spinal cord injury in rats." *Stroke* 20, no. 3 (Mar 1989): 372-7.

Hadley, M. N., B. C. Walters, B. Aarabi, S. S. Dhall, D. E. Gelb, R. J. Hurlbert, C. J. Rozzelle, T. C. Ryken, and N. Theodore. "Clinical assessment following acute cervical spinal cord injury." *Neurosurgery* 72 Suppl 2 (Mar 2013): 40-53.

Hagmann, P., L. Jonasson, P. Maeder, J. P. Thiran, V. J. Wedeen, and R. Meuli. "Understanding diffusion MR imaging techniques: from scalar diffusion-weighted imaging to diffusion tensor imaging and beyond." *Radiographics* 26 Suppl 1 (Oct 2006): S205-23.

Hamamoto, Y., T. Ogata, T. Morino, M. Hino, and H. Yamamoto. "Real-time direct measurement of spinal cord blood flow at the site of compression: relationship between blood flow recovery and motor deficiency in spinal cord injury." *Spine (Phila Pa 1976)* 32, no. 18 (Aug 15 2007): 1955-62.

Hassler, O. "Blood supply to human spinal cord. A microangiographic study." *Arch Neurol* 15, no. 3 (Sep 1966): 302-7.

Hickey, R., M. S. Albin, L. Bunegin, and J. Gelineau. "Autoregulation of spinal cord blood flow: is the cord a microcosm of the brain?". *Stroke* 17, no. 6 (Nov-Dec 1986): 1183-9.

Hitchon, P. W., J. M. Lobosky, T. Yamada, G. Johnson, and R. A. Girton. "Effect of hemorrhagic shock upon spinal cord blood flow and evoked potentials." *Neurosurgery* 21, no. 6 (Dec 1987): 849-57.

Hnath, J. C., M. Mehta, J. B. Taggert, Y. Sternbach, S. P. Roddy, P. B. Kreienberg, K. J. Ozsvath, *et al.* "Strategies to improve spinal cord ischemia in endovascular thoracic aortic repair: Outcomes of a prospective cerebrospinal fluid drainage protocol." *J Vasc Surg* 48, no. 4 (Oct 2008): 836-40.

Holtz, A., B. Nystrom, and B. Gerdin. "Relation between spinal cord blood flow and functional recovery after blocking weight-induced spinal cord injury in rats." *Neurosurgery* 26, no. 6 (Jun 1990): 952-7.

Horn, E. M., N. Theodore, R. Assina, R. F. Spetzler, V. K. Sonntag, and M. C. Preul. "The effects of intrathecal hypotension on tissue perfusion and pathophysiological outcome after acute spinal cord injury." *Neurosurg Focus* 25, no. 5 (2008): E12.

Hsu, S. W., G. Rodesch, C. B. Luo, Y. L. Chen, H. Alvarez, and P. L. Lasjaunias. "Concomitant conus medullaris arteriovenous malformation and sacral dural arteriovenous fistula of the filum terminale." *Interv Neuroradiol* 8, no. 1 (Mar 30 2002): 47-53.

Iwai, A., and W. W. Monafo. "The effects of lumbar sympathectomy on regional spinal cord blood flow in rats during acute hemorrhagic hypotension." *J Neurosurg* 76, no. 4 (Apr 1992): 687-91.

Kalani, M. Y., A. S. Ahmed, N. L. Martirosyan, K. Cronk, K. Moon, F. C. Albuquerque, C. G. McDougall, R. F. Spetzler, and R. E. Bristol. "Surgical and endovascular treatment of pediatric spinal arteriovenous malformations." *World Neurosurg* 78, no. 3-4 (Sep-Oct 2012): 348-54.

Kazama, S., Y. Masaki, S. Maruyama, and A. Ishihara. "Effect of altering cerebrospinal fluid pressure on spinal cord blood flow." *Ann Thorac Surg* 58, no. 1 (Jul 1994): 112-5.

Khan, S. N., and G. Stansby. "Cerebrospinal fluid drainage for thoracic and thoracoabdominal aortic aneurysm surgery." *Cochrane Database Syst Rev* 10 (2012): Cd003635.

Kieffer, E., F. Ammar, J. Chiras, C. Belli, and G. Rochat. "Traumatic rupture of the thoracoabdominal aorta." *Eur J Vasc Surg* 1, no. 5 (Oct 1987): 353-8.

Kim, J. H., D. N. Loy, H. F. Liang, K. Trinkaus, R. E. Schmidt, and S. K. Song. "Noninvasive diffusion tensor imaging of evolving white matter pathology in a mouse model of acute spinal cord injury." *Magn Reson Med* 58, no. 2 (Aug 2007): 253-60.

Kim, L. J., and R. F. Spetzler. "Classification and surgical management of spinal arteriovenous lesions: arteriovenous fistulae and arteriovenous malformations." *Neurosurgery* 59, no. 5 Suppl 3 (Nov 2006): S195-201; discussion S3-13.

Kindt, G. W. "Autoregulation of spinal cord blood flow." *Eur Neurol* 6, no. 1 (1971): 19-23.

Kobrine, A. I., T. F. Doyle, and A. N. Martins. "Autoregulation of spinal cord blood flow." *Clin Neurosurg* 22 (1975): 573-81.

Kobrine, A. I., "Local spinal cord blood flow in experimental traumatic myelopathy." *J Neurosurg* 42, no. 2 (Feb 1975): 144-9.

Kobrine, A. I., D. E. Evans, and H. V. Rizzoli. "The role of the sympathetic nervous system in spinal cord autoregulation." *Acta Neurol Scand Suppl* 64 (1977): 54-5.

Koyanagi, I., C. H. Tator, and E. Theriault. "Silicone rubber microangiography of acute spinal cord injury in the rat." *Neurosurgery* 32, no. 2 (Feb 1993): 260-8; discussion 68.

Krings, T., P. L. Lasjaunias, F. J. Hans, M. Mull, R. J. Nijenhuis, H. Alvarez, W. H. Backes*, et al.* "Imaging in spinal vascular disease." *Neuroimaging Clin N Am* 17, no. 1 (Feb 2007): 57-72.

Kwon, B. K., A. Curt, L. M. Belanger, A. Bernardo, D. Chan, J. A. Markez, S. Gorelik*, et al.* "Intrathecal pressure monitoring and cerebrospinal fluid drainage in acute spinal cord injury: a prospective randomized trial." *J Neurosurg Spine* 10, no. 3 (Mar 2009): 181-93.

Laschinger, J. C., J. N. Cunningham, Jr., I. M. Nathan, E. A. Knopp, M. M. Cooper, and F. C. Spencer. "Experimental and clinical assessment of the adequacy of partial bypass in maintenance of spinal cord blood flow during operations on the thoracic aorta." *Ann Thorac Surg* 36, no. 4 (Oct 1983): 417-26.

Lasjaunias, Pierre L., Alex Berenstein, and C. Raybaud. *Functional vascular anatomy of brain, spinal cord and spine* [in English]. Berlin; New York: Springer-Verlag, 1990.

Lazorthes, G., A. Gouaze, G. Bastide, J. H. Soutoul, O. Zadeh, and J. J. Santini. "[Arterial vascularization of the lumbar elevation. Study of variations and substitutions]." *Rev Neurol (Paris)* 114, no. 2 (Feb 1966): 109-22.

Lazorthes, G., A. Gouaze, J. O. Zadeh, J. J. Santini, Y. Lazorthes, and P. Burdin. "Arterial vascularization of the spinal cord. Recent studies of the anastomotic substitution pathways." *J Neurosurg* 35, no. 3 (Sep 1971): 253-62.

Lazorthes, G., J. Poulhes, G. Bastide, J. Roulleau, and A. R. Chancholle. "[Arterial vascularization of the spine; anatomic research and applications in pathology of the spinal cord and aorta]." *Neurochirurgie* 4, no. 1 (Jan-Mar 1958): 3-19.

Lin, Y. J., and A. P. Koretsky. "Manganese ion enhances T1-weighted MRI during brain activation: an approach to direct imaging of brain function." *Magn Reson Med* 38, no. 3 (Sep 1997): 378-88.

Lindsberg, P. J., T. P. Jacobs, K. U. Frerichs, J. M. Hallenbeck, and G. Z. Feuerstein. "Laser-Doppler flowmetry in monitoring regulation of rapid microcirculatory changes in spinal cord." *Am J Physiol* 263, no. 1 Pt 2 (Jul 1992): H285-92.

Lindsberg, P. J., J. T. O'Neill, I. A. Paakkari, J. M. Hallenbeck, and G. Feuerstein. "Validation of laser-Doppler flowmetry in measurement of spinal cord blood flow." *Am J Physiol* 257, no. 2 Pt 2 (Aug 1989): H674-80.

Lobosky, J. M., P. W. Hitchon, J. C. Torner, and T. Yamada. "Spinal cord autoregulation in the sheep." *Curr Surg* 41, no. 4 (Jul-Aug 1984): 264-7.

Lohse, D. C., H. J. Senter, J. S. Kauer, and R. Wohns. "Spinal cord blood flow in experimental transient traumatic paraplegia." *J Neurosurg* 52, no. 3 (Mar 1980): 335-45.

Margolis, G., and J. P. Pickett. "New applications of the Luxol fast blue myelin stain." *Lab Invest* 5, no. 6 (Nov-Dec 1956): 459-74.

Martirosyan, N. L., K. M. Bennett, N. Theodore, and M. C. Preul. "Manganese-enhanced magnetic resonance imaging in experimental spinal cord injury: correlation between T1-weighted changes and Mn(2+) concentrations." *Neurosurgery* 66, no. 1 (Jan 2010): 131-6.

Martirosyan, N. L., J. S. Feuerstein, N. Theodore, D. D. Cavalcanti, R. F. Spetzler, and M. C. Preul. "Blood supply and vascular reactivity of the spinal cord under normal and pathological conditions." *J Neurosurg Spine* 15, no. 3 (Sep 2011): 238-51.

Mathe, J. F., I. Richard, J. C. Roger, C. Potagas, W. S. el Masry, and B. Perrouin-Verbe. "Ischaemic myelopathy following aortic surgery or traumatic laceration of the aorta." *Spinal Cord* 36, no. 2 (Feb 1998): 110-6.

Mauney, M. C., L. H. Blackbourne, S. E. Langenburg, S. A. Buchanan, I. L. Kron, and C. G. Tribble. "Prevention of spinal cord injury after repair of the thoracic or thoracoabdominal aorta." *Ann Thorac Surg* 59, no. 1 (Jan 1995): 245-52.

McCullough, J. L., L. H. Hollier, and M. Nugent. "Paraplegia after thoracic aortic occlusion: influence of cerebrospinal fluid drainage. Experimental and early clinical results." *J Vasc Surg* 7, no. 1 (Jan 1988): 153-60.

Mesquita, R. C., A. D'Souza, T. V. Bilfinger, R. M. Galler, A. Emanuel, S. S. Schenkel, A. G. Yodh, and T. F. Floyd. "Optical monitoring and detection of spinal cord ischemia." *PLoS One* 8, no. 12 (2013): e83370.

Modi, H. N., S. W. Suh, J. Y. Hong, and J. H. Yang. "The effects of spinal cord injury induced by shortening on motor evoked potentials and spinal cord blood flow: an experimental study in Swine." *J Bone Joint Surg Am* 93, no. 19 (Oct 5 2011): 1781-9.

Mokri, B. "The Monro-Kellie hypothesis: applications in CSF volume depletion." *Neurology* 56, no. 12 (Jun 26 2001): 1746-8.

Molina, J. E., J. Cogordan, S. Einzig, R. W. Bianco, T. Rasmussen, R. M. Clack, and B. Borgwardt. "Adequacy of ascending aorta-descending aorta shunt during cross-clamping of the thoracic aorta for prevention of spinal cord injury." *J Thorac Cardiovasc Surg* 90, no. 1 (Jul 1985): 126-36.

Mulcahey, M. J., A. Samdani, J. Gaughan, N. Barakat, S. Faro, R. R. Betz, J. Finsterbusch, and F. B. Mohamed. "Diffusion tensor imaging in pediatric spinal cord injury: preliminary examination of reliability and clinical correlation." *Spine (Phila Pa 1976)* 37, no. 13 (Jun 1 2012): E797-803.

Naftchi, N. E., M. Demeny, V. DeCrescito, J. J. Tomasula, E. S. Flamm, and J. B. Campbell. "Biogenic amine concentrations in traumatized spinal cords of cats. Effect of drug therapy." *J Neurosurg* 40, no. 1 (Jan 1974): 52-7.

Nossin-Manor, R., R. Duvdevani, and Y. Cohen. "q-Space high b value diffusion MRI of hemi-crush in rat spinal cord: evidence for spontaneous regeneration." *Magn Reson Imaging* 20, no. 3 (Apr 2002): 231-41.

Ohashi, T., T. Morimoto, K. Kawata, T. Yamada, and T. Sakaki. "Correlation between spinal cord blood flow and arterial diameter following acute spinal cord injury in rats." *Acta Neurochir (Wien)* 138, no. 3 (1996): 322-9.

Olive, J. L., K. K. McCully, and G. A. Dudley. "Blood flow response in individuals with incomplete spinal cord injuries." *Spinal Cord* 40, no. 12 (Dec 2002): 639-45.

Palleske, R. Kivelitz, and F. Loew. "Experimental investigation on the control of spinal cord circulation. IV. The effect of spinal or cerebral compression on the blood flow of the spinal cord." *Acta Neurochir (Wien)* 22, no. 1 (Apr 21 1970): 29-41.

Parke, W. W. "Arteriovenous glomeruli of the human spinal cord and their possible functional implications." *Clin Anat* 17, no. 7 (Oct 2004): 558-63.

Parke, W. W., K. Gammell, and R. H. Rothman. "Arterial vascularization of the cauda equina." *J Bone Joint Surg Am* 63, no. 1 (Jan 1981): 53-62.

Parke, W. W., J. L. Whalen, P. C. Bunger, and H. E. Settles. "Intimal musculature of the lower anterior spinal artery." *Spine (Phila Pa 1976)* 20, no. 19 (Oct 1 1995): 2073-9.

Pautler, R. G. "In vivo, trans-synaptic tract-tracing utilizing manganese-enhanced magnetic resonance imaging (MEMRI)." *NMR Biomed* 17, no. 8 (Dec 2004): 595-601.

Pautler, R. G., and A. P. Koretsky. "Tracing odor-induced activation in the olfactory bulbs of mice using manganese-enhanced magnetic resonance imaging." *Neuroimage* 16, no. 2 (Jun 2002): 441-8.

Pautler, R. G., A. C. Silva, and A. P. Koretsky. "In vivo neuronal tract tracing using manganese-enhanced magnetic resonance imaging." *Magn Reson Med* 40, no. 5 (Nov 1998): 740-8.

Piano, G., and B. L. Gewertz. "Mechanism of increased cerebrospinal fluid pressure with thoracic aortic occlusion." *J Vasc Surg* 11, no. 5 (May 1990): 695-701.

Ploumis, A., N. Yadlapalli, M. G. Fehlings, B. K. Kwon, and A. R. Vaccaro. "A systematic review of the evidence supporting a role for vasopressor support in acute SCI." *Spinal Cord* 48, no. 5 (May 2010): 356-62.

Reed, J. E., W. E. Allen, 3rd, and G. J. Dohrmann. "Effect of mannitol on the traumatized spinal cord. Microangiography, blood flow patterns, and electrophysiology." *Spine (Phila Pa 1976)* 4, no. 5 (Sep-Oct 1979): 391-7.

Rivlin, A. S., and C. H. Tator. "Regional spinal cord blood flow in rats after severe cord trauma." *J Neurosurg* 49, no. 6 (Dec 1978): 844-53.

Robertazzi, R. R., and J. N. Cunningham, Jr. "Intraoperative adjuncts of spinal cord protection." *Semin Thorac Cardiovasc Surg* 10, no. 1 (Jan 1998): 29-34.

Ross, J. F., R. C. Switzer, M. R. Poston, and G. T. Lawhorn. "Distribution of bismuth in the brain after intraperitoneal dosing of bismuth subnitrate in mice: implications for routes of entry of xenobiotic metals into the brain." *Brain Res* 725, no. 2 (Jul 1 1996): 137-54.

Rowland, J. W., G. W. Hawryluk, B. Kwon, and M. G. Fehlings. "Current status of acute spinal cord injury pathophysiology and emerging therapies: promise on the horizon." *Neurosurg Focus* 25, no. 5 (2008): E2.

Ryken, T. C., R. J. Hurlbert, M. N. Hadley, B. Aarabi, S. S. Dhall, D. E. Gelb, C. J. Rozzelle, N. Theodore, and B. C. Walters. "The acute cardiopulmonary management of patients with cervical spinal cord injuries." *Neurosurgery* 72 Suppl 2 (Mar 2013): 84-92.

Sandler, A. N., and C. H. Tator. "Effect of acute spinal cord compression injury on regional spinal cord blood flow in primates." *J Neurosurg* 45, no. 6 (Dec 1976): 660-76.

Sasaki, S. "Vascular change in the spinal cord after impact injury in the rat." *Neurosurgery* 10, no. 3 (Mar 1982): 360-3.

Schepens, M. A., J. J. Defauw, R. P. Hamerlijnck, and F. E. Vermeulen. "Use of left heart bypass in the surgical repair of thoracoabdominal aortic aneurysms." *Ann Vasc Surg* 9, no. 4 (Jul 1995): 327-38.

Schwartz, E. D., and D. B. Hackney. "Diffusion-weighted MRI and the evaluation of spinal cord axonal integrity following injury and treatment." *Exp Neurol* 184, no. 2 (Dec 2003): 570-89.

Senter, H. J., and J. L. Venes. "Loss of autoregulation and posttraumatic ischemia following experimental spinal cord trauma." *J Neurosurg* 50, no. 2 (Feb 1979): 198-206.

Silva, A. C., and N. A. Bock. "Manganese-enhanced MRI: an exceptional tool in translational neuroimaging." *Schizophr Bull* 34, no. 4 (Jul 2008): 595-604.

Singh, U., J. R. Silver, and N. C. Welply. "Hypotensive infarction of the spinal cord." *Paraplegia* 32, no. 5 (May 1994): 314-22.

Sliwa, J. A., and I. C. Maclean. "Ischemic myelopathy: a review of spinal vasculature and related clinical syndromes." *Arch Phys Med Rehabil* 73, no. 4 (Apr 1992): 365-72.

Smith, A. J., D. B. McCreery, J. R. Bloedel, and S. N. Chou. "Hyperemia, CO2 responsiveness, and autoregulation in the white matter following experimental spinal cord injury." *J Neurosurg* 48, no. 2 (Feb 1978): 239-51.

Smith, A. L., J. W. Pender, and S. C. Alexander. "Effects of PCO2 on spinal cord blood flow." *Am J Physiol* 216, no. 5 (May 1969): 1158-63.

Soubeyrand, M., E. Laemmel, A. Dubory, E. Vicaut, C. Court, and J. Duranteau. "Real-time and spatial quantification using contrast-enhanced ultrasonography of spinal cord perfusion during experimental spinal cord injury." *Spine (Phila Pa 1976)* 37, no. 22 (Oct 15 2012): E1376-82.

Spetzler, R. F., P. W. Detwiler, H. A. Riina, and R. W. Porter. "Modified classification of spinal cord vascular lesions." *J Neurosurg* 96, no. 2 Suppl (Mar 2002): 145-56.

Stein, S. C., A. K. Ommaya, J. L. Doppman, and G. Di Chiro. "Arteriovenous malformation of the cauda equina with arterial supply from branches of the internal iliac arteries. Case report." *J Neurosurg* 36, no. 5 (May 1972): 649-51.

Stieltjes, B., S. Klussmann, M. Bock, R. Umathum, J. Mangalathu, E. Letellier, W. Rittgen*, et al.* "Manganese-enhanced magnetic resonance imaging for in vivo assessment of damage and functional improvement following spinal cord injury in mice." *Magn Reson Med* 55, no. 5 (May 2006): 1124-31.

Svensson, L. G., E. S. Crawford, K. R. Hess, J. S. Coselli, and H. J. Safi. "Experience with 1509 patients undergoing thoracoabdominal aortic operations." *J Vasc Surg* 17, no. 2 (Feb 1993): 357-68; discussion 68-70.

Svensson, L. G., R. W. Stewart, D. M. Cosgrove, 3rd, B. W. Lytle, M. D. Antunes, E. G. Beven, A. J. Furlan*, et al.* "Intrathecal papaverine for the prevention of paraplegia after operation on the thoracic or thoracoabdominal aorta." *J Thorac Cardiovasc Surg* 96, no. 5 (Nov 1988): 823-9.

Tabayashi, K. "Spinal cord protection during thoracoabdominal aneurysm repair." *Surg Today* 35, no. 1 (2005): 1-6.

Taira, Y., and M. Marsala. "Effect of proximal arterial perfusion pressure on function, spinal cord blood flow, and histopathologic changes after increasing intervals of aortic occlusion in the rat." *Stroke* 27, no. 10 (Oct 1996): 1850-8.

Tator, C. H., and I. Koyanagi. "Vascular mechanisms in the pathophysiology of human spinal cord injury." *J Neurosurg* 86, no. 3 (Mar 1997): 483-92.

Tindemans, I., M. Verhoye, J. Balthazart, and A. Van Der Linden. "In vivo dynamic ME-MRI reveals differential functional responses of RA- and area X-projecting neurons in the HVC of canaries exposed to conspecific song." *Eur J Neurosci* 18, no. 12 (Dec 2003): 3352-60.

Turnbull, I. M. "Chapter 5. Blood supply of the spinal cord: normal and pathological considerations." *Clin Neurosurg* 20 (1973): 56-84.

Turnbull, I. M., "Microvasculature of the human spinal cord." *J Neurosurg* 35, no. 2 (Aug 1971): 141-7.

Turnbull, I. M., A. Brieg, and O. Hassler. "Blood supply of cervical spinal cord in man. A microangiographic cadaver study." *J Neurosurg* 24, no. 6 (Jun 1966): 951-65.

Tveten, L. "Spinal cord vascularity. III. The spinal cord arteries in man." *Acta Radiol Diagn (Stockh)* 17, no. 3 (May 1976): 257-73.

Vale, F. L., J. Burns, A. B. Jackson, and M. N. Hadley. "Combined medical and surgical treatment after acute spinal cord injury: results of a prospective pilot study to assess the merits of aggressive medical resuscitation and blood pressure management." *J Neurosurg* 87, no. 2 (Aug 1997): 239-46.

Van der Linden, A., V. Van Meir, I. Tindemans, M. Verhoye, and J. Balthazart. "Applications of manganese-enhanced magnetic resonance imaging (MEMRI) to image brain plasticity in song birds." *NMR Biomed* 17, no. 8 (Dec 2004): 602-12.

Vlajic, I. "Microangiographic observations of morphological vessel changes after experimental spinal cord trauma." *Adv Neurol* 20 (1978): 451-60.

Walder, N., A. H. Petter-Puchner, M. Brejnikow, H. Redl, M. Essig, and B. Stieltjes. "Manganese enhanced magnetic resonance imaging in a contusion model of spinal cord injury in rats: correlation with motor function." *Invest Radiol* 43, no. 5 (May 2008): 277-83.

Wallace, M. C., and C. H. Tator. "Successful improvement of blood pressure, cardiac output, and spinal cord blood flow after experimental spinal cord injury." *Neurosurgery* 20, no. 5 (May 1987): 710-5.

Wallace, M. C., C. H. Tator, and P. Frazee. "Relationship between posttraumatic ischemia and hemorrhage in the injured rat spinal cord as shown by colloidal carbon angiography." *Neurosurgery* 18, no. 4 (Apr 1986): 433-9.

Watanabe, T., O. Natt, S. Boretius, J. Frahm, and T. Michaelis. "In vivo 3D MRI staining of mouse brain after subcutaneous application of $MnCl_2$." *Magn Reson Med* 48, no. 5 (Nov 2002): 852-9.

Wilson, D. A., A. A. Abla, T. D. Uschold, C. G. McDougall, F. C. Albuquerque, and R. F. Spetzler. "Multimodality treatment of conus medullaris arteriovenous malformations: 2 decades of experience with combined endovascular and microsurgical treatments." *Neurosurgery* 71, no. 1 (Jul 2012): 100-8.

Winnerkvist, A., S. Bartoli, D. C. Iliopoulos, K. R. Hess, C. C. Miller, and H. J. Safi. "Spinal cord protection during aortic cross clamping: retrograde venous spinal cord perfusion, distal aortic perfusion, and cerebrospinal fluid drainage." *Scand Cardiovasc J* 36, no. 1 (Feb 2002): 6-10.

Young, W., V. DeCrescito, and J. J. Tomasula. "Effect of sympathectomy on spinal blood flow autoregulation and posttraumatic ischemia." *J Neurosurg* 56, no. 5 (May 1982): 706-10.

Zeitlin, H., and B. W. Lichtenstein. "Occlusion of the anterior spinal artery: Clinicopathologic report of a case and a review of the literature." *Archives of Neurology & Psychiatry* 36, no. 1 (1936): 96-111.

APPENDIX A

BLOOD SUPPLY AND REACTIVITY OF THE SPINAL CORD UNDER NORMAL

AND PATHOLOGICAL CONDITIONS

Blood supply and vascular reactivity of the spinal cord under normal and pathological conditions

A review

Nikolay L. Martirosyan, M.D., Jeanne S. Feuerstein, B.A., Nicholas Theodore, M.D., Daniel D. Cavalcanti, M.D., Robert F. Spetzler, M.D., and Mark C. Preul, M.D.

Division of Neurological Surgery, Barrow Neurological Institute, St. Joseph's Hospital and Medical Center, Phoenix, Arizona

The authors present a review of spinal cord blood supply, discussing the anatomy of the vascular system and physiological aspects of blood flow regulation in normal and injured spinal cords. Unique anatomical functional properties of vessels and blood supply determine the susceptibility of the spinal cord to damage, especially ischemia. Spinal cord injury (SCI), for example, complicating thoracoabdominal aortic aneurysm repair is associated with ischemic trauma. The rate of this devastating complication has been decreased significantly by instituting physiological methods of protection. Traumatic SCI causes complex changes in spinal cord blood flow, which are closely related to the severity of injury. Manipulating physiological parameters such as mean arterial blood pressure and intrathecal pressure may be beneficial for patients with an SCI. Studying the physiopathological processes of the spinal cord under vascular compromise remains challenging because of its central role in almost all of the body's hemodynamic and neurofunctional processes. (DOI: 10.3171/2011.4.SPINE10543)

KEY WORDS • spinal cord blood supply • autoregulation • spinal cord injury • vascular disorders

DEFINITIVE management of SCI remains illusory, despite intense research efforts and the ongoing development of technology. Ischemia is recognized as one of the most important factors determining the severity of SCI and clinical outcome.[66] The following review discusses the current understanding of the structure and function of the vasculature in normal and injured spinal cords.

Spinal Cord Vasculature

Arteries of the Spinal Cord

The intrinsic arteries of the spinal cord can be separated into a central and a peripheral system. The central system, which supplies two-thirds of the spinal cord, is derived from the ASA and its blood flow is centrifugal.[83] This system supplies the anterior gray matter, anterior portion of the posterior gray matter and posterior white columns, inner half of the anterior and lateral white columns, and base of the posterior white columns.[80] In the peripheral system, the blood flows centripetally from the

PSAs and pial arterial plexus.[83] This system supplies the outer portion of the anterior and lateral white columns and the posterior portion of the posterior gray matter and posterior white columns (Fig. 1).[80]

The central and peripheral arterial systems have no precapillary interconnections. Their terminal branches overlap, however, allowing regions of the spinal cord to receive blood from both systems. This overlap occurs within the inner first one-quarter to first one-third of the white matter and within the outer edge of the gray matter. The exceptions are the posterior halves of the posterior horns, which are supplied entirely by the peripheral system. The widest internal overlap occurs in the posterior and lateral columns.[82] Extrinsically, the anastomosis between the systems is greatest around the tip of the cauda equina (Fig. 2).[71] Although there is some overlap between the systems, because blood flows away from the center in the central system and toward the center in the peripheral systems, their relationship is not truly compensatory.

The various regions of the spinal cord are disproportionately vascularized, and the ratio of blood supplied by the central system to the peripheral system is not constant throughout the cord: The cervical region has a large peripheral and large central arterial supply, the thoracic region has large peripheral and small central supply, and the lumbar and upper sacral regions have a small peripheral and large central supply.[37]
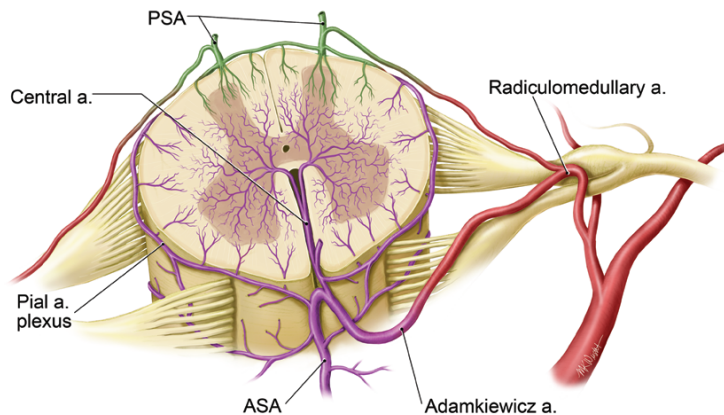

Fig. 1. Vascularization of lumbar spinal cord. Contribution of the ASA and PSA in supplying the blood to the spinal cord. a. = artery/arterial. Used with permission from Nicholas Theodore, M.D.

Obstruction of an artery feeding the cervical and lumbosacral regions seldom results in an infarction, as these areas are well vascularized. The radicular (radiculomedullary) arteries reaching the upper cervical region are fed by intervertebral branches of the vertebral arteries and their descending rami.[50] In the lower cervical region, the segmental arteries, which feed the radiculomedullary arteries, arise from the deep cervical artery, the costocervical artery (from the subclavian artery), or the ascending cervical artery. The many interconnections between these arteries and others in the neck allow blood flow despite occlusion in another area. In the lumbar region, arteries extend from the aorta and into the vertebral body wall where radicular arteries arise from them, some of which may be radiculomedullary arteries. The segmental arteries in the sacral region are supplied with blood from the lateral sacral arteries. These pelvic arteries form numerous anastomoses with other arteries of the pelvis. Therefore, not unlike in the cervical region, a single occlusion of an artery is unlikely to result in ischemia.[80] Because none of the sacral radicular arteries contribute to the ASA or PSA, their obstruction is less threatening.[50]

Due to poor collateralization in the thoracic vascular region, however, compromise of blood flow potentially creates a great risk of ischemia. In the thoracic cord, the distance between sources of blood supply is considerable. The radiculomedullary arteries feeding the thoracic spinal cord originate from a few intercostal arteries (from the subclavian artery and aorta), and anastomotic connections between the extraspinal arteries supplying this region are scarce.[80] The compensatory support provided in the lumbar and cervical regions does not exist in the thoracic region; consequently, compromise of these arteries results in discreet regions of ischemia.

Extrinsic Spinal Cord Arteries

The ASA. The ASA, the trunk of the central arterial system, supplies most of the intrinsic spinal vasculature. Occlusion of this artery results in infarction of the anterior two-thirds of the spinal cord (Figs. 1 and 2).[89]

Before the vertebral arteries unite to form the basilar artery, both give off a branch and join together and then descend on the surface of the anterior spinal cord as the ASA. Usually, these branches fuse within 2 cm of their origins, but they can remain separated until around the C-5 level.[82] The ASA extends over the length of the spinal cord, ventrally to the anterior median fissure.[80]

The diameter of the ASA usually decreases gradually from its origin until it reaches the thoracic region. From the thoracic region down, the diameter of the ASA remains fairly constant. At the lower end of the sacral or coccygeal region, branches from the ASA loop caudally around the conus medullaris and join each limb of the PSA. The trunk of the ASA is then reduced to a tiny vessel, which extends along the conus and the filum terminale (Fig. 2).[83]

Because the ASA is an anastomotic channel consisting of terminal branches of successive radiculomedullary arteries, its size varies in response to its conjunctions. The most striking example is at its junction with the great radicular artery (artery of Adamkiewicz), often at L-1 or L-2 on the left. In the lower thoracic region, before the vessels merge, the ASA becomes so small that it may be indistinguishable from other arteries. At its juncture with the artery of Adamkiewicz, however, the ASA reaches its greatest diameter (Figs. 1 and 2).[32] Although rare, 2 radiculomedullary arteries may enter a single segment of the ASA from both sides. In this scenario, the shape of the ASA is often rhomboidal, a feature often noted in the cervical region.[83] The ASA is frequently duplicated for short distances in the lower cervical region and is singular in other regions.[80]

The PSA. The paired PSAs run longitudinally along the posterolateral surface of the spinal cord medial to the
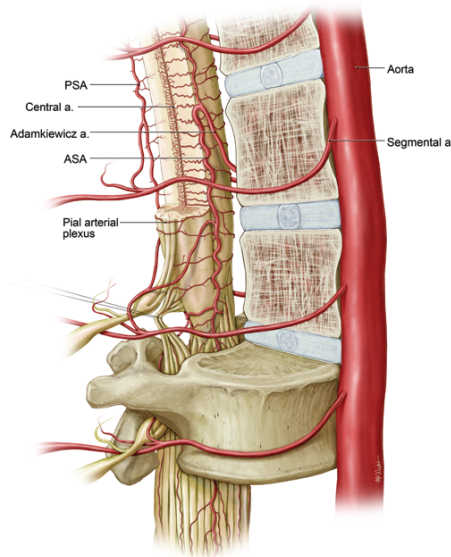
FIG. 2. Anterolateral view of lumbar spinal cord. Used with permission from Nicholas Theodore, M.D.

posterior nerve roots. The PSA can arise from the vertebral arteries or the posterior inferior cerebellar arteries. Much more rarely, it branches from the posterior radicular artery at C-2. The PSAs swing laterally around the brainstem and then veer posteriorly along the surface of the cervical spinal cord.[80] They are identified as distinct single vessels only at their origin. Thereafter, they become anastomosing channels, largely retaining their embryonic plexiform design.[32]

At the lower end of the spinal cord, the PSAs send out small branches to the proximal part of the posterior rootlets and nerve roots, most often in the roots of the cauda equina.[83] The size of the PSAs varies. At times they become incredibly small, making them impossible to identify.

Pial Arterial Plexus. Surface vessels branching from both the ASA and the PSA form an anastomosing network—a pial arterial plexus (vasa coronae)—that encircles the spinal cord.[32] Most of the branches from the pial arterial plexus penetrate the dorsal midline of the spinal cord. All of the penetrating branches run directly inward, perpendicular to the surface of the spinal cord. These branches supply the outer portion of the spinal cord, including the greater part of the posterior horns, and extend to the substantia gelatinosa (Fig. 1).[82]

Radicular Arteries. Among the 31 pairs of radicular arteries, there are 3 distinct types: 1) some radicular arteries end within the roots or on the dura mater before reaching the spinal cord; some radicular arteries do not penetrate beyond the surrounding arterial systems of the spinal cord;

and some radicular arteries actually vascularize the spinal cord (that is, medullary or radiculomedullary arteries). The diversity in the paths of the radicular arteries illustrates their various levels of supply. Radicular arteries supply blood to the dura mater, to the nerve roots that they accompany, to the spinal ganglia, and to the ASA and PSA.[50]

Radiculomedullary arteries are often located on the left side of the thoracic and lumbar regions (where the aorta is left of midline) and are more equally distributed in the cervical region. Left-sidedness size dominance is more pronounced among the anterior radiculomedullary arteries than the posterior radiculomedullary arteries, which nonetheless are still more dominant on the left.[80]

The typical segmental artery, which can originate from various sources (for example, subclavian, aorta), divides into anterior and posterior rami. The posterior ramus splits into a spinal arterial branch and a muscular arterial branch. The spinal branch crosses the intervertebral foramen and divides into anterior and posterior radicular arteries.[72] As noted, not all of these radicular arteries reach the surface arteries of the spinal cord. The radicular arteries that traverse the nerve roots course on the anterior surface. After they reach the nerve root, they become encased in perineurium and enter the subarachnoid space, where they are loosely attached to the nerve roots. A single radicular artery can become an anterior or a posterior radicular (radiculomedullary) artery or, although rare, divide to become both.[80]

The number of anterior radicular arteries that contribute to the ASA ranges from a minimum of 2 to a maximum of 17 (mean 10). The mean diameter of the anterior radicular artery ranges from 0.2 to 0.8 mm. When the diameter of the artery is smaller than 0.2 mm, it seldom reaches the ASA and usually serves to supply the root.[80]

Each region of the ASA receives different numbers of anterior radicular arteries. The cervical ASA receives a mean number of 0–6, the thoracic ASA receives 1–4, and the lumbar ASA receives 1 or 2. The smaller arteries accompanying the roots of the cauda equina are thought to become more important when large radicular arteries enter the spinal cord at a relatively high position or when they become narrowed. Again, the scarcity of anterior radicular arteries and the extensive distance between them indicate that occlusion of a single artery in the thoracic region can result in ischemia.[80]

Posterior radicular arteries, of which there can be 10–23 (average range 12–16), divide on the posterolateral surface of the spinal cord to supply the ipsilateral PSA. These arteries are smaller than their anterior counterparts. Their diameters range from 0.2–0.5 mm. Posterior radicular arteries can originate as superiorly as C-2 and are more frequent on the caudal portion of the spinal cord, where they are usually narrower. The posterior radicular arteries extend to feed the pial arterial plexus on the lateral aspect of the spinal cord, in addition to the nerve roots, dura mater, spinal ganglia, and PSA.[72]

The number and position of the posterior radicular arteries do not appear to be related to the number and position of the anterior radicular arteries. When anterior and posterior radicular arteries occur at the same level and side, they unite to form a common stem outside the dura.[37]

240

Blood supply of spinal cord

The artery of Adamkiewicz (also called the arteria radicularis magna, the great radicular artery, or the artery of lumbar enlargement) is the largest vessel that reaches the spinal cord. It is 1.0–1.3 mm in diameter, and it supplies a quarter of the spinal cord in 50% of people.[72] In 75% of people, this artery travels with the T9–12 roots. In 10% it follows roots L-1 or L-2, and in 15% it has a high origin at posterior roots T5–8. In this final case, a more caudal supplementary artery called the arteria conus medullaris is always present.[50] The artery of Adamkiewicz is found on the left side 80% of the time. When it joins the ASA, it branches into a small ascending branch (0.231 mm) and into a large descending branch (0.941 mm) (Figs. 1 and 2).[61,80]

Fried and Aparicio[30] ligated the artery of Adamkiewicz and the ASA just above and just below the entrance of Adamkiewicz in monkeys to determine how the location of the blockage would alter perfusion of the spinal cord and neurological outcome. When the artery of Adamkiewicz was ligated just above the union of the vessels, neurological deficits were slight. However, ligations above the artery of Adamkiewicz produced mild to moderate chromatolysis and hyperchromatism. When a ligation was placed below the entrance, however, 82% of monkeys became paraplegic.[30] These findings indicate that more caudal regions of the spinal cord rely heavily on the artery of Adamkiewicz for perfusion.

Central Arteries. Adults have a mean of 210 central arteries.[37] The central arteries feed the central area of the spinal cord, which consists of the white matter bordering the central sulcus, the gray matter of anterior horn, and the deep gray matter of posterior horn.[50] Central arteries arise from the ASA and penetrate the spinal cord posteriorly in the anterior median fissure. When central arteries stem from a duplicated portion of the ASA (often in the lower cervical region), they only pass to the side of the ASA from which they arise. Otherwise, when the artery reaches the anterior white commissure, it continues to either side of the spinal cord. Less commonly, it bifurcates and each limb of the vessel retreats to the contralateral side of the spinal cord.[72] Successive central arteries usually alternate sides, but they also can extend to the same side. On reaching the anterior gray matter, the arteries divide into short ascending and descending branches and into horizontal branches, which often traverse the periphery of the gray matter before they transition into capillaries (Fig. 1).[83]

If the central artery bifurcates, it always does so in the sagittal plane. It cannot be seen in transverse sections. Such bifurcations are least common in the cervical and thoracic regions (9% and 7%, respectively) and slightly more common in the lumbar and upper sacral regions (14% and 13%, respectively) (Fig. 2).[37]

The dispersal and configuration of the central arteries, much like the radicular arteries, can be explained by the relative paucity of gray matter in the thoracic spinal region.[81] There are fewer central arteries in the thoracic region, and they are smaller than those in the cervical and lumbosacral regions. The cervical region has 5–8 central arteries/cm of ASA compared with 2–6 and 5–12 in the

lumbosacral region.[81] The mean diameter of the central arteries is 0.21 ± 0.05 mm in the cervical region, 0.14 ± 0.04 mm in the thoracic region, 0.23 ± 0.6 mm in the lumbar region, and 0.2 ± 0.5 mm in the upper sacral region.[37]

In the less crowded cervical and thoracic regions, an acute angle is formed by the emerging central arteries and the ASA. In the lumbosacral region, a right angle is formed. As a result the central arteries in the lumbosacral region extend both horizontally and deeper into the spinal cord than the central arteries in the other regions. This difference is the result of the angles, because the lengths of the central arteries are almost the same (cervical 4.5 ± 1.0 mm, thoracic 4.3 ± 0.9 mm, lumbar 4.7 ± 1.2 mm, and upper sacral 4.4 ± 1.1 mm).[37] In the cervical region, and even more so in the thoracic region, the trunks of the central arteries traverse the spinal cord at an angle, covering the considerable longitudinal distance between arteries. Terminal branches of the central arteries stretch along the length of the spinal cord, overlapping with the territories of neighboring arteries. In the thoracic region, the central arteries send most of their branches longitudinally, whereas those in the cervical and lumbosacral region mainly branch horizontally.[83] A central artery in the thoracic region can cover as much as 3.0 cm in distance. In contrast, it can cover no more than 1.2 cm in the cervical region and no more than 1.7 cm in the lumbosacral region.[81]

Capillaries of the Spinal Cord

As is common in the vasculature of the spinal cord, the white matter is not served by capillary beds as abundantly as is the gray matter. In fact, the density of the capillary bed is 5 times greater in gray matter than in white matter. The capillary beds in white matter are also fairly uniform, stretching longitudinally in the direction of the nerve fibers. Where the gray and white matter meet, the capillary beds are denser than those in white matter alone. Within the gray matter, the density of the beds depends on the location of the cell bodies. This arrangement reflects the greater metabolic requirements of cell bodies compared with axons.[81]

The lateral horns, anterior horns, and base of the posterior horns (especially the substantia gelatinosa) have the thickest capillary beds, although the remainder of the posterior horns is not well supplied.[80]

Direction of Arterial Blood Flow

The watershed effect occurs when 2 streams of blood flowing in opposite directions meet, as is common in the vascular system of the spinal cord. In a watershed area, the likelihood of the surrounding tissues suffering from occlusion increases. Local pressure from a space-occupying lesion, which may not cause any vascular compromise elsewhere, can result in ischemia in the watershed region.[6]

At the union of a radicular artery and the ASA, the blood courses upward and downward from the entry point. Therefore, in the area of the ASA between neighboring radicular arteries, there is a dead point where blood flows in neither direction, that is, a watershed area. The location of this dead point fluctuates constantly. In the midthoracic area, where the distance between radicular arteries is the greatest, the watershed effect is at its maximum.[72]

The blood flow in the PSA does not mirror that of the ASA. The PSA does not narrow like the ASA and thus does not provide a mechanical barrier to upward flow. When Bolton[6] injected a solution with Indian ink into the vertebral arteries of human corpses and followed its path, the blood running down the PSA reached the highest thoracic segments. At this point, the vertebral blood met the blood flowing up from the caudal part of the ASA via 2 terminal branches. These terminal branches pass caudal to the anterior S-5 roots, and each one joins with a single PSA, lateral to the fifth posterior sacral roots (Fig. 2). The ascending blood flow of the caudal portion of the PSA is often reinforced by posterior lumbar radicular arteries.

As noted, the artery of Adamkiewicz, the most notable of the radicular arteries, joins the ASA with a small ascending branch and a larger descending branch. Resistance to flow through the upper branch is 278 times greater than in the downward branch, because the diameter of the ascending branch is much smaller (0.231 mm) than that of the descending branch (0.941 mm).[38] Under normal conditions in humans, the ascending branch of the artery of Adamkiewicz is required to supply the arterial domain of the upper 1–3 thoracolumbar segments, and its relatively small blood flow is sufficient. It is likely, however, that under the collateral demands of aortic cross-clamping during surgery, the quantity of blood flow to the higher midthoracic area is unreliable. In the ASA the blood flow may be modified by contraction of the conventional circular musculature of the tunica media, the generally longitudinally disposed layer of the intimal musculature, and the intimal cushions near and in the critical vascular junction just below the boundary between the thoracolumbar and midthoracic arterial domains.[38]

Autoregulation

Autoregulation is the process that ensures constant blood flow when systemic blood pressure or CO_2 concentrations rise or fall. While the blood flow in the spinal cord is 40%–60% that of the brain, the tissue oxygen levels are the same (35–39 mm Hg).[23] The volume of blood perfusing the spinal cord increases when arterial CO_2 tension increases and falls when it decreases. Vasodilation and constriction enable these changes to occur without altering the SCBF.[74]

Effect of MABP and CO_2 Pressure on SCBF. Research has been done in various animals to determine the ranges of MABP and CO_2 pressure in which autoregulation is maintained. In sheep, blood flow in the gray and white matter in both the cervical and lumbar regions remains steady when MABP ranges between 40 and 100 mm Hg.[51]

Hitchon and associates[38] used lambs to measure SCBF, because the white and gray matter in their spinal cords are markedly distinct. When MABP was between 100 and 40 mm Hg, SCBF in the cervical gray and white matter (124–141 ml/100 g/min and 22–26 ml/100 g/min, respectively) and in the lumbar gray and white matter (74–104 ml/100 g/min and 15–24 ml/100 g/min, respectively) remained fairly stable. When MABP fell below 40 mm Hg, SCBF dropped significantly.[38]

Kobrine and associates[45] found that when CO_2 pressure was between 10 to 50 mm Hg in monkeys, SCBF stayed constant. When the pressure of CO_2 surpassed 50 mm Hg, SCBF increased. Further increases above 90 mm Hg had no effect on SCBF, which had reached a physical maximum.[45] In another study, Kobrine and coworkers[47] found that SCBF remained constant when MABP was between 50 and 135 mm Hg. Below 50 mm Hg, vascular resistance decreased maximally, and SCBF became a function of MABP. When MABP exceeded 135 mm Hg, vascular resistance decreased, vasodilatation occurred, and SCBF increased markedly. These findings are clinically relevant because the capillary endothelium responsible for the normal blood-brain barrier can be disrupted in this hypertensive environment and high SCBF can result in the formation of edema, which can be detrimental to neural function.[47]

Mechanism of Autoregulation. In research by Young and associates,[88] cats received paravertebral sympathectomies, adrenalectomies, or both to determine whether paravertebral sympathetic ganglia or the adrenal gland was involved in autoregulation. There was no autoregulation of SCBF in response to systemic pressure changes in cats with sympathectomies, and there was a linear relationship between MABP and SCBF. In the control and adrenalectomy groups, SCBF did not correlate with MABP between 80 to 160 mm Hg. Therefore, the sympathetic ganglia are a necessary component of spinal cord autoregulation.[88] In contrast, Iwai and Monafo[41] found only moderate effects on regional SCBF after they performed lower lumbar sympathectomies in rats.

Proximal transections have been performed to help determine the location of the sensory control center for autoregulation. These procedures do not influence the response of MABP and CO_2, indicating that the sensory control center for autoregulation lies caudal to the medulla.[44,47] Knots of vessels (glomeruli) exist in and around the capillary beds of the anterior and posterior horns. The capability of these glomeruli to act as sensors to direct autonomic blood flow of the spinal cord is supported by the presence of muscular cushions in the intima of the lower (inferior thoracic and lumbosacral) ASA and their sensory (afferent and efferent) junctions. Glomeruli found in capillary beds within the spinal cord may act as sensors within the spinal cord.[60] One reason for this supposition is that these glomeruli resemble arteriovenous glomerular clumps, which are found in fingers, toes, the penis, and other parts of the body, and act as components of nerve root circulation capable of shunting blood from arteries to veins and bypassing the capillaries. Such shunting can also occur in the spinal cord. Further research is needed to cement this theory.[60]

Spinal Cord Blood Flow After Thoracic Aortic Occlusion

Aortic Cross-Clamping

During repair of thoracoabdominal aortic aneurysms, temporary aortic cross-clamping decreases SCBF and distal organ perfusion.[2] After an hour of aortic cross-clamping, thoracolumbar SCBF has been reported to decrease from 20 to 1.8 ml/100 g/min.[31] Aortic cross-clamping

242

Blood supply of spinal cord

causes distal hypotension (below the clamp), proximal hypertension (above the clamp), left ventricle afterload, and an increase in CSFP and central venous pressure. It also elevates intracranial pressure.[18] The induction of proximal hypertension and intracranial pressure during aortic cross-clamping prompts the autoregulatory mechanisms of the cerebral and spinal vasculature to increase CSFP reflexively, effectively lowering SCPP and diminishing the blood supply to the spinal cord.[65] Systemically, an SCI causes hypotension not only by interrupting sympathetic fibers but also by direct myocardial dysfunction. With its limited blood supply and the most deleterious watershed effect, the thoracolumbar spinal cord is the portion of the spinal cord at greatest risk for ischemic injury.[75]

Understanding the relationships among distal and proximal blood pressure, CSFP, SCPP, and MABP is necessary to solve the problems that can arise during aortic cross-clamping. Spinal cord perfusion pressure is a key measure used to evaluate the circulation of the spinal cord. It is equal to the difference between the mean distal aortic pressure and CSFP.[65] Spinal cord perfusion pressure must stay above 50–60 mm Hg to protect the spinal cord from ischemia.[42,54]

Several studies have supported the notion that SCPP is more relevant in determining SCBF than are CSFP and MABP. Griffiths and associates[34] exemplified this point when they raised SCPP significantly (from 5 to 123 mm Hg) in dogs while maintaining CSFP, and they observed a stealthy rebound of the SCBF. In this study SCBF autoregulation was lost when SCPP fell below 50 mm Hg. As the SCPP was lowered from baseline to 50 mm Hg, the vascular resistance decreased. Below 50 mm Hg, the resistance was unchanged, perhaps because the vessels were fully dilatated and compressed due to CSFP.[34]

Taira and Marsala[77] correlated proximal aortic pressure with distal aortic pressure during aortic cross-clamping and, after the aorta was unclamped, with proportional decreases in distal aortic pressure and SCBF. When proximal aortic pressure was maintained above 100 mm Hg during aortic cross-clamping, distal aortic pressure was 19 ± 4 mm Hg. When proximal aortic pressure was held at 40 mm Hg, distal aortic pressure fell to 7 ± 1 mm Hg. After the clamp was released while proximal aortic pressure slowly decreased, SCBF also decreased. The decrease in SCBF was 8% ± 4% of baseline values when proximal aortic pressure was held above 100 mm Hg and 2.5% ± 1.6% of baseline values when proximal aortic pressure was 40 mm Hg. Therefore, SCBF can increase as a result of increasing proximal aortic pressure during and after aortic cross-clamping. This point is clinically relevant because at lower proximal aortic pressures neurological deficits were incurred more quickly than at higher proximal aortic pressures.[77] In dogs, Laschinger et al.[49] showed that a distal aortic pressure of 60–70 mm Hg was adequate to maintain spinal cord function during aortic cross-clamping. When distal aortic pressure fell below 40 mm Hg, SSEPs were often lost and an SCI was incurred (66% paraplegia). Maintaining distal aortic pressure above 70 mm Hg uniformly preserved SCBF as long as critical intercostal arteries remained intact.

The direct relationship between CSFP and central venous pressure has been shown in various studies.[12] In dogs, Piano and Gewertz[62] showed that although CSFP and central venous pressure both increased significantly with aortic cross-clamping, the increase in CSFP was always equal to or greater than the venous increase. With volume loading this trend continued, supporting the relationship between CSFP and central venous pressure. The mechanism that links the CSFP and central venous pressure relies on the structure of the venous system of the spinal cord. Radicular veins extend from the sinusoidal channels of the spinal cord and travel through dural space, dura, and epidural fat before joining the larger veins. As the veins traverse this labyrinthine route, they narrow. When CSFP within the tissue of the spinal cord becomes higher than venous pressure, the vein collapses. Outflow resistance and venous pressure then increase.[62]

In humans the normal range of CSFP is 13–15 mm Hg, whereas its range during aortic cross-clamping is 21–25 mm Hg. Berendes et al.[3] found that when CSFP remained below 20 mm Hg in patients during thoracic aortic operations (87.5% [8 patients]), no postoperative neurological deficits were evident. When CSFP exceeded 40 mm Hg during the operation (12.5%), paraparesis developed postoperatively.[42] Blaisdell and Cooley[5] found that when the CSFP was higher than the distal aortic pressure, the incidence of paraplegia increased by 17%.

Molina and associates[56] observed that when the clamp was released after an hour of aortic cross-clamping, CSFP remained elevated for 5 minutes and returned to normal only after another 25 minutes. After the clamp was released, hyperemia was observed in both the gray and white matter from T-12 down. The degree of hyperemia, however, was much greater in the gray matter.

Risks and Neurological Deficits

Much has been learned about vascular reactivity in the spinal cord from thoracoabdominal aortic surgery experience. Neurological deficits are a considerable risk associated with surgeries that employ aortic cross-clamping. Svensson and colleagues[75] reviewed 1509 patients who underwent repairs to treat thoracoabdominal aortic disease of varied severity. Among these patients, the incidence of paraplegia or paraparesis was 16%. In a study of 121 cases of thoracoabdominal aortic aneurysm repair by Cinà and associates,[11] neurological deficits were recorded in 6.2% of patients, and the hospital mortality rate was 21.4%.

The complexity of the repair is a significant predictor of SCI. The Crawford classification system[16] organizes thoracoabdominal aortic aneurysm repairs based on the extent and position: Type I aneurysms extend from the proximal descending thoracic aorta to the upper abdominal aorta; Type II aneurysms from the proximal descending thoracic aorta to below the renal arteries; Type III aneurysms from the distal half of the descending thoracic aorta into the abdomen; and Type IV aneurysms involve most or all of the abdominal aorta. Repairs of Types I, II, III, and IV were associated with rates of paraplegia or paraparesis of 15%, 31%, 7%, and 4%, respectively.[16] In a randomized study, Crawford and associates[16] found that there was a 32% incidence of neurological deficits (of

117

varied severity and duration) affecting the legs associated with Type I and II repairs.

In the 1970s the first attempts at improving thoracoabdominal aortic aneurysm surgery focused on decreasing the duration of surgery.[87] Time is clearly an important indicator of neurological outcome. Repairs requiring more than 60 minutes of aortic occlusion were reported to carry a 20% risk of paraplegia and paraparesis, whereas the risk for a 30-minute occlusion was less than 10%.[54] When spinal cord ischemia was sustained for 50 minutes, the incidence of spastic paraplegia in dogs was 87.5%.[12]

During the last 40 years, however, it has become clear that numerous factors influence the neurological outcome of thoracoabdominal aortic aneurysm repairs in addition to the duration of aortic cross-clamping: the extent of the aneurysm, acute dissection, and preoperative problems (that is, renal condition, previous aortic surgery, and diabetes).[13] Preoperative hypotension, distal aortic hypotension after aortic occlusion, the interruption of critical intercostal arteries, and postoperative hypotension or hypoxia can all result in injury.[54] Each of these factors can affect SCBF, the oxygen delivery system to the spinal cord, which is crippling to neurological function. Gharagozloo and colleagues[31] found that SCBF held at 10 ml/100 g/min during aortic cross-clamping resulted in no paraplegia, whereas SCBF reduced to 4 ml/100 g/min resulted in universal paraplegia. This finding illustrates the neurological impact of decreased SCBF.

Not all neurological deficits reveal themselves immediately. The incidence of postoperative paraplegia was 10% in a study by Schepens et al.,[69] 21% in a study by Cox et al.,[14] and 13% in a report by Crawford et al.[16,17] Crawford and associates[15] found that 68% of patients who had undergone Type I and II repairs developed neurological deficits. In 32% of the patients with neurological deficits, the paralysis did not manifest for several days. Immediate neurological deficits are a result of the hypoxic environment induced by prolonged aortic cross-clamping and minimal SCBF. Delayed neurological deficits can materialize 1–21 days after surgery. These deficits may be a result of ischemia arising from low SCBF as a result of high vascular resistance and regional hypotension restricting blood flow through the high-resistance vascular plexus of spinal cord or a result of reperfusion hyperemia and free radicals causing spinal cord edema.[53,65] Barone and associates[2] compared the SCBF and blood pressure of paraplegic and normal dogs during and after surgery. They found that thoracolumbar SCBF in both paraplegic and nonparaplegic dogs was 10%–20% of baseline after 30 minutes of aortic cross-clamping. Thirty minutes after the cross-clamp was released, significant hyperemia was present. After aortic cross-clamping, reperfusion flow in the nonparaplegic dogs was approximately twice that of baseline, whereas in the paraplegic dogs flow was approximately eight times that of baseline.

Avoiding Complications

Various methods have been conceived to improve the neurological outcomes of aortic cross-clamping, although on their own, none of these methods can address all the possible causes of SCI and neurological deficits.

Monitoring and Imaging. Monitoring spinal cord function and using imaging to avoid displacing key radicular arteries are important factors in improving the outcomes of thoracoabdominal aortic aneurysm repair. In patients undergoing surgery to treat thoracoabdominal aortic artery disease and aneurysms, Dong and colleagues[22] found that the use of MEPs to follow spinal cord function was more effective than using SSEPs. The MEPs in 28.6% of their 56 patients showed evidence of SCI, whereas the SSEPs showed such signs in only 25%. In 81.3% of the 28.6% patients, ischemic changes in MEPs were reversed by reimplanting segmental arteries, increasing distal aortic pressure, or using hypothermic conditions.

Kieffer and colleagues[43] found that using spinal cord arteriography to identify the location of the artery of Adamkiewicz before thoracoabdominal aortic surgeries was very useful. When the artery of Adamkiewicz was visualized and originated above or below the clamp area, the duration of surgery decreased and no spinal cord complications occurred. When the artery of Adamkiewicz originated in the clamped section, revascularization was attempted. When revascularization was successful, only 5% of the cases sustained ischemic injury. When it was unsuccessful, 50% developed ischemic injuries. Of the group in which the artery of Adamkiewicz could not be visualized, 60% became paraplegic.

Distal Aortic Perfusion. Distal aortic shunting, as provided by left atrium–to–femoral artery bypass or a simpler artery-to-artery shunt aims to provide effective control of proximal blood pressure and to avoid a decrease in distal aortic flow.[65] Still ischemia can occur if the arteries supplying the ASA rely on excluded segments of the aorta.[76]

Cerebrospinal Fluid Drainage

Manipulating the CSF compartment whether by pressure or content alteration remains an enticing goal for its potential effect on SCIs. Cerebrospinal fluid drainage has been heavily investigated to identify whether drainage is effective and, if so, when it should be initiated and in conjunction with what other protection mechanisms. Proximal hypertension induced by aortic cross-clamping prompts the spinal cord vasculature to increase CSFP reflexively, lowering SCPP and thereby diminishing blood supply to the spinal cord. Drainage of CSF reduces CSFP, offsetting the gradient and improving SCPP.[65]

In dogs, Kazama and associates[42] found that draining CSF 1 hour into a 2-hour aortic cross-clamping procedure was of limited efficacy. It only increased SCPP by 8–10 mm Hg, not enough to ensure the safety of the spinal cord. Only when CSFP was elevated abnormally (40 mm Hg) did drainage of CSF significantly increase SCBF (from 12 to 17 ml/100 g/min) and prevent damage to the spinal cord.[42] Blaisdell and Cooley[5] found that the incidence of paraplegia associated with aortic cross-clamping in dogs decreased from 50% to 8% when CSF drainage was performed during the operation.

McCullough and associates[55] found that draining CSF before 40 minutes of aortic cross-clamping had elapsed increased SCPP from 22 to 30 mm Hg during

244

aortic occlusion and that the incidence of paraplegia decreased by 90%.

Elmore and colleagues[27] found that draining CSF before a 1-hour period of aortic cross-clamping had elapsed eliminated paraplegia in dogs, although 44% of the animals were paraparetic after surgery. Bower and associates[7] showed that draining CSF before a 1-hour period of aortic cross-clamping had elapsed improved SCPP (from 13.5 mm Hg without CSF drainage to 21.1 mm Hg) and improved SCBF (from 2.5 ml/100 g/min without CSF drainage to 15.1 ml/100 g/min) in the gray matter of the lumbar spinal cord. Furthermore, reperfusion hyperemia in the lower portions of the spinal cord was not present when CSF was drained (34.1 ml/100 g/min) but was present when CSF was not drained (136.6 ml/100 g/min). Of the 7 dogs undergoing CSF drainage, 57.1% exhibited no neurological deficit and none became paraplegic. Of the dogs not undergoing CSF drainage, 62.5% developed spastic paraplegia and none was neurologically normal. In contrast, when Horn and associates[40] drained CSF in rabbits after inducing an SCI, there was no indication that perfusion of the spinal cord improved. The different outcomes may reflect different methods: complete SCI versus aortic cross-clamping.

Pathophysiology of Spinal Cord Blood Flow After Trauma

Basics of SCI

To address spinal cord injuries and how to minimize their deleterious effects, an understanding of the pathophysiological mechanisms that follow SCI must first be achieved. Two types of zone define the spinal cord after injury. One zone completely lacks vasculature able to perfuse the tissue, whereas the other is capable of capillary perfusion within a week of injury. The zone with worthless vasculature often consists of the posterior central gray matter and posterior columns at and below the trauma site. The size and extent of the zones vary, depending on the severity of the trauma.[28]

Microangiograms showing vascular changes over various time frames have been used to construct a fairly consistent postinjury timeline. During compression, the extrinsic arteries (ASA and PSA) remain intact, whereas the arteries within the traumatized region become constricted.[84] Five minutes after injury, muscular venules in the gray matter appear distorted and develop holes. Muscular venules in white matter, however, appear to be unaffected.[19] Hemorrhages emerge from capillaries and venules in the border zone between gray and white matter and in the gray matter itself.[68] In these hemorrhagic areas the vessels do not perfuse blood. Fifteen minutes after injury, there is further leakage from gray matter venules and less than one-third of the gray matter vessels perfuse properly. As a result, hemorrhagic areas in the gray matter continue to grow. Although white matter hemorrhages become more pronounced, the number of functioning vessels increases after 30 minutes.[19,20] One hour after injury, the hemorrhages in the gray matter coalesce and neurons are clearly damaged.[28] Furthermore,

most of the vessels near the gray-white matter border cannot perfuse blood. The larger extrinsic vessels (ASA and PSA), however, continue to remain functional. Four hours after injury, vessel leakage is considerable in both the gray and white matter. The only functional intrinsic vessels are limited to the peripheral half of the white matter.[19,20] After 24 hours, the central arteries at the site of injury and adjacent areas are markedly displaced, often occluded, and become narrowed.[48] Reports on the state of white matter vessels 24 hours after injury have differed. In rats Sasaki[68] found that hemorrhages originating from ruptured vessels in the dorsal white matter were present. In contrast, Dohrmann et al.[20] found that the white matter vessels in cats were almost restored to normal.

Still, the implications are fairly clear. Gray matter is severely injured soon after injury, while damage in white matter is slower to appear and more likely to recover. The predominance of hemorrhages in gray matter may be the result of its rich capillary network, which is highly susceptible to mechanical stress because of its complex texture.[78] This stress can induce clotting, which decreases or halts blood flow, and causes venous hypertension, which can disrupt vessel walls.[48] Edema, a result of vessel leakage, may increase interstitial fluid pressure, causing vessel closures, and creating a snowball effect.[64] Damage to central arteries and their branches causes hemorrhaging and ischemia in their areas of distribution, which includes the gray matter.[48] The pia mater is a strong membrane. Therefore, the large vessels on the surface of the spinal cord and in the anterior median sulcus are relatively spared from major damage due to mechanical stress. The ASA and PSA possess heavier mesenchymal-supporting investment, and electron microscopic studies suggest that white matter vasculature possesses denser glial packing than vessels of gray matter.[4]

Autoregulation With Injury. Spinal cord injury is associated with marked vasculature changes. To further understand chronic changes as a result of spinal injury, cats with various degrees of SCI (control, mild 200 g/cm; severe, 400 g/cm) were observed over a 14-day period after injury. In cats with mild trauma, SCBF and CO_2 responsiveness were not significantly different from those of uninjured cats, although there was a trend toward hyperemia. In cats with severe spinal cord trauma, the hyperemia was significantly different from that of uninjured cats on the 11th and 14th days postinjury. In this group, CO_2 responsiveness was strikingly impaired (0.03 ml/min/100 g/torr compared with 0.47 ml/min/100 g/torr in the controls).[73] One explanation for this delayed increase in SCBF is that hypotension causes transient ischemia leading to a local decrease in pH, both intra- and extracellularly. The hydrogen ions then act directly on blood vessels, causing vasodilation. Other ions and substances, such as potassium and histamine, could employ a similar mechanism.[45]

Postinjury Relations Among MABP, SCBF, and Spinal Cord Function

To better understand how treatments should address spinal cord trauma, considerable research has been directed toward defining relationships among MABP,

SCBF, SSEPs, and neurological outcomes after injury, both at and around the trauma site.

Guha et al.[35] investigated autoregulation of SCBF at an MABP of 81–180 mm Hg in rats at the site of SCI (T-1) and adjacent to the injured sites. The results confirmed normal autoregulation in the control group. Autoregulation was present in the mildly injured group but differed from that of the control group: SCBF was lower, and the lower limit of autoregulation was increased to 101–120 mm Hg. In contrast, autoregulation was lost at both T-1 and C-6 in the severely injured group.

Various studies have examined the effect of changing MABP after trauma in an attempt to normalize SCBF. Dolan and Tator[21] found that by increasing the MABP in rats after trauma (175-g cord clip-compression for 1 minute), SCBF also increased. Thirty minutes after injury, SCBF in the white and gray matter were a fraction of control values (3.42 from 18.7 ± 6.7 and 15.6 from 74.2 ± 22.3 ml/100 g/min, respectively). After MABP was increased by blood transfusion, SCBF almost doubled in both white (6.3 ± 6.4 ml/100 g/min) and gray (25.6 ± 30.2 ml/100 g/min) matter.[21]

The results of Guha and associates' study[35] of rats implied that restoring MABP to its baseline after severe injury was the best option when altering MABP. With hypotension, posttraumatic ischemia persisted and worsened, whereas with extreme hypertension (180 mm Hg), SCBF increased to 31.3 ± 3.5 ml/100 g/min (from 16.2 ± 4.4 ml/100 g/min). Raising MABP this much, however, could be deleterious to less injured portions of the spinal cord. Consequently, normotension was identified as the ideal pressure after trauma.[35] Wallace and Tator[85] found that by increasing MABP in rats after trauma by adding whole blood or dextran to the system, SCBF also increased. The dextran decreased the hematocrit by about 50% and was twice as effective as whole blood in increasing SCBF. This finding implied that hemodilution improved perfusion after injury. The combination of restoration to normotension and hemodilution improved SCBF optimally.

Currently we are investigating relationships between SCBF, arterial blood pressure, CSFP, and tissue oxygen partial pressure in moderate SCI model in swine (Martirosyan et al., unpublished data, 2010). Preliminary results show significant hypoperfusion using laser Doppler flowmetry after contusion injury in comparison with the immediate preinjury state. Slight increase in CSFP as well as spike of arterial blood pressure in response to SCI was noted. Indirect measurements of spinal cord tissue oxygen partial pressure showed significant hypo-oxygenation during the first 3 minutes after injury (decrease from 88.2 mm Hg to 69.4 mm Hg). Over the next 7 minutes tissue oxygen partial pressure significantly increased to 176.5 mm Hg. During the next 50 minutes, a decreasing trend in tissue oxygen partial pressure value was observed. At 60 minutes after injury, it reached steady state but was at a higher than immediate preinjury steady state level (measurements over 5 minutes preinjury averaged 88.2 ± 1.35 mm Hg, whereas in a 60–65-minute period after injury the average was 104.2 ± 0.8 mm Hg, $p < 0.001$) (Fig. 3). The ability to monitor and affect tissue oxygen partial pressure may have benefit in predicting ischemia as well as hyperperfusion injury and thus in instituting treatment.

Spinal cord blood flow can differ above and below the trauma site.[21] Ohashi and associates[58] found a potential correlation between arterial diameter and autoregulation when they examined differences between zones distal and proximal to the trauma site in rats after trauma (50-g spinal cord clip compression for 1 minute). Although arterial diameter decreased overall, it did so most significantly distally. In contrast, SCBF decreased to a greater extent proximally. CO_2 reactivity and autoregulation also were both impaired, although more so distally; perhaps, this finding indicates that arterial diameter affects CO_2 reactivity and autoregulation more so than SCBF after injury.

After trauma, SCBF and SSEPs can be used to distinguish between extreme neurological outcomes (uninjured or paraplegic animals); identification of partially injured animals is more difficult. Ducker and associates' research[24] in monkeys supports this idea. The SCBF in monkeys with slight or no neurological deficits steadily increased for a week after injury, reaching 170% of normal SCBF (from 15 to 25.5 ml/min/100 g) and SSEPs reappeared within 5–120 minutes. When monkeys became paraplegic, their SCBF fell to 30% of baseline values in a week (from 15 to 4.5 ml/min/100 g). The SSEPs rarely returned with stability. Partially injured animals maintained their baseline SCBF, and SSEPs returned in 60% of the cases, perhaps as a result of white matter hyperemia. Similarly, Carlson and associates[8] found that neurological recovery in dogs was related to higher SCBF during spinal cord compression.

Severity and Duration of Trauma

After injury, MABP first quickly increases and then falls. Depending on the severity of the trauma, hypotensive tissue is reperfused. Based on the reperfusion and on the effect of the initial impact, the microscopic appearance of the spinal cord can vary. Such variations can be used to illustrate the resulting neurological deficits.

Lohse and associates[52] found that MABP spiked and then fell below baseline values after light (100 g/cm) and moderate (260 g/cm) trauma in cats. After light trauma, MABP immediately increased to 137% of pretrauma values. After 15 minutes, it decreased to 77% of the pretrauma value and remained low for the 6 hours of the experiment. After moderate trauma, the MABP rose to 144% of its pretrauma value, decreased to 72% of that value, and remained low for the duration of the experiment. Five minutes after severe trauma (300 g/cm) in monkeys, SCBF in the gray matter fell to 62% of baseline, whereas in the white matter it fell to 93% of baseline. After 15 minutes, SCBF in gray and white matter rose (to 92% and 141%, respectively). During the next 45 minutes, SCBF in the gray and white matter again fell (to 21% and 90%, respectively). After this point, SCBF in white matter increased slowly, whereas the SCBF of gray matter did not. These data show that as severity of trauma increases so do fluctuations in SCBF.[4]

Another obvious result of increasing the SCI force is depression of SCBF gray matter.[29] Holtz and associates' research[39] supports this finding. They showed that posttrauma motor function likewise declines. Griffiths[33] reported similar results using CO_2 sensitivity as a measure
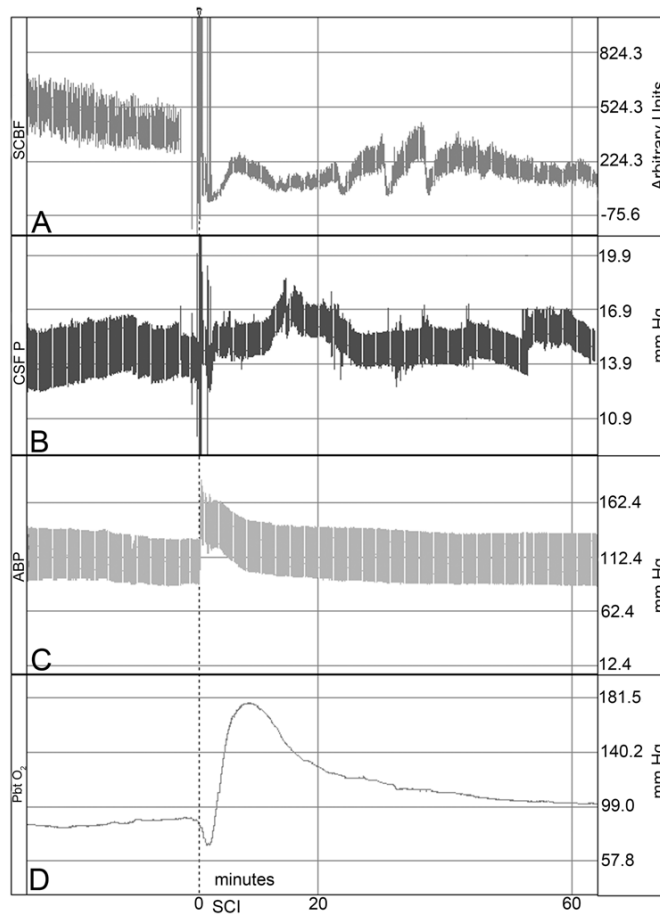
120

FIG. 3. Relationships among SCBF (**A**), CSFP (**B**), arterial blood pressure (ABP, **C**), and spinal cord tissue oxygen partial pressure (PbtO$_2$, **D**) before and after moderate SCI. See comments in text.

of neurological dysfunction. After moderate injury (300 g/cm), CO$_2$ sensitivity was considerably reduced and was nonexistent after severe injury (500 g/cm).

Carlson and associates[9] addressed the question of reperfusion after injury in dogs and found that duration of spinal cord compression (30, 60, and 180 minutes) and reperfusion after decompression were inversely related. Five minutes after compression, SCBF increased from baseline (21.4 ± 2.2 ml/100 g/min) in both the 30-minute group (49.1 ± 3.1 ml/100 g/min) and 60-minute group (~ 44 ml/100 g/min) but fell slightly in the 180-minute group (19.8 ± 6.2 ml/100 g/min). Fifteen minutes after compres-

sion, the 30- and 60-minute groups remained above baseline (32.3 ± 4 and 32.4 ± 3.7 ml/100 g/min, respectively), whereas SCBF in the 180-minute group did not change significantly. Similar results have been observed in other animals, including pigs and monkeys.[4,59]

These differences in SCBF after trauma have a direct impact on vascular resistance. After trauma, SCBF, vascular resistance, and MABP all depend on one another (SCBF = MABP/vascular resistance). Therefore, when moderate and light trauma decrease MABP and increase SCBF, vascular resistance will decrease. Because severe trauma decreases SCBF, vascular resistance increases.

This is a clear distinction between traumatic injuries that do and do not cause paraplegia. The mechanisms that might mediate such changes in local vascular resistance are unknown, but several possibilities exist. Changes in hydrogen and potassium ions, the release of biologically active substances, or primary injury to the microvasculature could affect vascular resistance.[52]

Using contrast material to capture extravasation, Allen and associates[1] evaluated microangiograms obtained in cats after moderate and severe injury (300 g/cm and 500 g/cm, respectively). Immediately after moderate injury, several small areas of extravasation were present in the central gray matter of the traumatized region. Fifteen minutes after injury, blood flow was markedly reduced in the gray matter arterial network, as were the size and number of the peripheral arteries serving the posterior horns, especially in the posterior columns. Thirty minutes after injury, the appearance of the peripheral arteries began to approach normal and continued to improve. Over time the degree of extravasation in the central gray matter became more pronounced. After severe injury there were more areas of extravasation than after moderate trauma. Leakage again appeared in the gray matter, but there were also areas of extravasation in the gray and white border region. Fifteen minutes after injury, the SCBF of both gray and white matter was reduced markedly. Over time the central gray matter filled with extravasated contrast material as it had after moderate injury. Perfusion of the white matter improved after 1 hour but remained below control values.[1] Reed et al.[63] found that 90 minutes after severe (500 g/cm) trauma, microangiography showed severe narrowing of vessels in the gray and white matter. After 2 hours, there was almost no filling of the peripheral vessels supplying the white matter. After 3 hours, the entire gray matter was hemorrhagic and there was no blood flow.

Gray to White Injury

Primary damage directly inflicts injury on neurons and axons. Edema, ischemia, and inflammatory responses are common mechanisms that accelerate damage. Ischemia and reperfusion induce the release of inflammatory cytokines, free radicals, and excitatory amino acids.[36] Vascular disruption and local tissue ischemia are features of secondary damage.

In the mid 1970s, the prevailing theory concerning the pathophysiology of acute spinal cord injuries relied on 2 steps. First, there was hemorrhage in the central gray matter, which specifically included endothelium separating from the basement membranes, recanalization, blood clotting, and disruption of vessel walls. Ischemia in the lateral white matter followed but included no changes comparable to those in the gray matter. Consequently, gray matter was thought to be the origin of the damage, which slowly spread to the surrounding white matter.[4] Wallace and associates[86] found that ischemia in the white matter of rats, especially in the dorsal columns and anterior and lateral funiculi, was common when fed by arteries that traversed hemorrhagic gray matter. This finding further supports the secondary nature of injury in the white matter, stemming from trauma to the gray matter.

Kobrine and associates' experimental study[46] investigating the impact of severe (600 g/cm) injury in monkeys opposes this theory. In the lateral white matter SCBF more than doubled ($p < 0.01$) within 1 hour of injury and returned to normal after 8 hours. In the central gray matter SCBF fell for 4 hours after injury. Cawthon and associates[10] reported similar results in cats after severe trauma (500 g/cm). White matter SCBF almost rebounded to baseline values within 8 hours. An hour after trauma, SCBF in the white matter at the trauma site was near control values (10.99 ± 0.89 ml/min/100 g), whereas rostral and caudal blood flow was depressed for approximately 1 cm. Four hours after trauma, blood flow through white matter was depressed at the trauma site. Two centimeters rostral and caudal to the site, blood flow was also depressed to a lesser extent. Eight hours after trauma, blood flow through white matter was 90% that of the controls 3 mm caudal to the trauma center, and 16 mm caudal to the trauma center it was 97%.[10]

These findings suggest that the initial trauma disrupts the ability of the white matter to function and that injury is not simply a result of spreading from gray to white matter. These data show that autoregulation in white matter is maintained through the 1st hour after injury and then lost. The reappearance of normal blood flow 5–7 hours later indicates that autoregulation is regained. The return of blood flow may depend on clearing the tissue of toxins, vasospasm, or other mechanisms that restore vasoconstriction.[70] The increase in SCBF in white matter after injury also could be a response to increased metabolic demand or loss of autoregulation and subsequent vascular dilation as a direct result of trauma.[46] A documented increase in histamine levels at the site of trauma, known to cause vascular dilation by weakening vascular tone, also explains the increased blood flow in white matter.[57]

Segmental loss of gray matter is functionally tolerated because it involves only a small portion of the total neuronal pool in gray matter. Loss of segmental white matter, however, is more serious because all distal functioning neurons cannot operate and neurological deficit occurs. If treatment could be initiated before white matter is destroyed (within 3–4 hours of severe injury), paralysis might be avoided in some cases.[25]

White Matter Issues

The severity of trauma within white and gray matter varies but is greatest in the white matter. Understanding how specific areas of the spinal cord react to traumatic injury clarifies the ability of the vasculature to function. Sandler and Tator[67] found that after moderate trauma was induced in monkeys by inflating an extradural cuff to 400 mm Hg for 5 minutes, the SCBF in the dorsal columns and dorsolateral white matter rebounded slower than in other areas of the white matter. In the lateral ventral areas, SCBF was significantly different from that of the controls for 30 minutes after trauma, but the SCBF in the dorsal columns and in the left lateral dorsal white matter was still significantly lower after 6 hours compared with controls. After 24 hours, blood flow in all of the white matter was significantly higher than in the controls.

Blood supply of spinal cord

Conclusions

Spinal cord vasculature has unique anatomical and physiological properties. Variability in the direction of blood flow and in the diameter of arteries ensures a constant and sufficient blood supply, but there are regions of the spinal cord that can be readily made ischemic. The pathophysiology of SCBF under normal conditions has been investigated, and it seems that consensus has been reached on the key mechanisms of the blood supply to the normal spinal cord. Although numerous experiments have attempted to investigate the principles elucidating the blood supply in the injured spinal cord, these mechanisms remain unclear. Techniques that would allow continuous precise measurement of blood flow in different spinal cord regions could potentially answer many of the questions regarding how the blood flow is altered. Further optimization of Doppler ultrasonography[79] and arterial spin labeling MR imaging[26] could potentially meet these requirements. Manipulating physiological parameters such as MABP and intrathecal pressure may have potential benefit in improving the blood supply to ischemic areas of the injured spinal cord.

Disclosure

Acknowledgments

References

1. Allen WE III, D'Angelo CM, Kier EL: Correlation of microangiographic and electrophysiologic changes in experimental spinal cord trauma. **Radiology 111:**107–115, 1974
2. Barone GW, Joob AW, Flanagan TL, Dunn CE, Kron IL: The effect of hyperemia on spinal cord function after temporary thoracic aortic occlusion. **J Vasc Surg 8:**535–540, 1988
3. Berendes JN, Bredée JJ, Schipperheyn JJ, Mashhour YA: Mechanisms of spinal cord injury after cross-clamping of the descending thoracic aorta. **Circulation 66:**I112–I116, 1982
4. Bingham WG, Goldman H, Friedman SJ, Murphy S, Yashon D, Hunt WE: Blood flow in normal and injured monkey spinal cord. **J Neurosurg 43:**162–171, 1975
5. Blaisdell FW, Cooley DA: The mechanism of paraplegia after temporary thoracic aortic occlusion and its relationship to spinal fluid pressure. **Surgery 51:**351–355, 1962
6. Bolton B: The blood supply of the human spinal cord. **J Neurol Psychiatrist 2:**137–148, 1939
7. Bower TC, Murray MJ, Gloviczki P, Yaksh TL, Hollier LH, Pairolero PC: Effects of thoracic aortic occlusion and cerebrospinal fluid drainage on regional spinal cord blood flow in dogs: correlation with neurologic outcome. **J Vasc Surg 9:**135–144, 1989
8. Carlson GD, Gorden CD, Nakazawa S, Wada E, Smith JS, LaManna JC: Sustained spinal cord compression: part II: effect of methylprednisolone on regional blood flow and recovery of somatosensory evoked potentials. **J Bone Joint Surg Am 85-A:**95–101, 2003
9. Carlson GD, Minato Y, Okada A, Gorden CD, Warden KE, Barbeau JM, et al: Early time-dependent decompression for spinal cord injury: vascular mechanisms of recovery. **J Neurotrauma 14:**951–962, 1997
10. Cawthon DF, Senter HJ, Stewart WB: Comparison of hydrogen clearance and 14C-antipyrine autoradiography in the measurement of spinal cord blood flow after severe impact injury. **J Neurosurg 52:**801–807, 1980
11. Cinà CS, Laganà A, Bruin G, Ricci C, Doobay B, Tittley J, et al: Thoracoabdominal aortic aneurysm repair: a prospective cohort study of 121 cases. **Ann Vasc Surg 16:**631–638, 2002
12. Clark FJ, Mutch WA, Sutton IR, Teskey JM, McCutcheon K, Thiessen DB, et al: Treatment of proximal aortic hypertension after thoracic aortic cross-clamping in dogs. Phlebotomy versus sodium nitroprusside/isoflurane. **Anesthesiology 77:**357–364, 1992
13. Coselli JS, Lemaire SA, Köksoy C, Schmittling ZC, Curling PE: Cerebrospinal fluid drainage reduces paraplegia after thoracoabdominal aortic aneurysm repair: results of a randomized clinical trial. **J Vasc Surg 35:**631–639, 2002
14. Cox GS, O'Hara PJ, Hertzer NR, Piedmonte MR, Krajewski LP, Beven EG: Thoracoabdominal aneurysm repair: a representative experience. **J Vasc Surg 15:**780–788, 1992
15. Crawford ES, Crawford JL, Safi HJ, Coselli JS: Redo operations for recurrent aneurysmal disease of the ascending aorta and transverse aortic arch. **Ann Thorac Surg 40:**439–455, 1985
16. Crawford ES, Crawford JL, Safi HJ, Coselli JS, Hess KR, Brooks B, et al: Thoracoabdominal aortic aneurysms: preoperative and intraoperative factors determining immediate and long-term results of operations in 605 patients. **J Vasc Surg 3:**389–404, 1986
17. Crawford ES, Hess KR, Cohen ES, Coselli JS, Safi HJ: Ruptured aneurysm of the descending thoracic and thoracoabdominal aorta. Analysis according to size and treatment. **Ann Surg 213:**417–426, 1991
18. D'Ambra MN, Dewhirst W, Jacobs M, Bergus B, Borges L, Hilgenberg A: Cross-clamping the thoracic aorta. Effect on intracranial pressure. **Circulation 78:**III198–III202, 1988
19. Dohrmann GJ, Wagner FC Jr, Wick KM, Bucy PC: Fine structural alterations in transitory traumatic paraplegia. **Proc Veterans Adm Spinal Cord Inj Conf 18:**6–8, 1971
20. Dohrmann GJ, Wick KM, Bucy PC: Spinal cord blood flow patterns in experimental traumatic paraplegia. **J Neurosurg 38:**52–58, 1973
21. Dolan EJ, Tator CH: The effect of blood transfusion, dopamine, and gamma hydroxybutyrate on posttraumatic ischemia of the spinal cord. **J Neurosurg 56:**350–358, 1982
22. Dong CC, MacDonald DB, Janusz MT: Intraoperative spinal cord monitoring during descending thoracic and thoracoabdominal aneurysm surgery. **Ann Thorac Surg 74:**S1873–S1898, 2002
23. Ducker TB, Perot PL Jr: Spinal cord oxygen and blood flow in trauma. **Surg Forum 22:**413–415, 1971
24. Ducker TB, Salcman M, Lucas JT, Garrison WB, Perot PL Jr: Experimental spinal cord trauma, II: blood flow, tissue oxygen, evoked potentials in both paretic and plegic monkeys. **Surg Neurol 10:**64–70, 1978
25. Ducker TB, Salcman M, Perot PL Jr, Ballantine D: Experimental spinal cord trauma, I: correlation of blood flow, tissue oxygen and neurologic status in the dog. **Surg Neurol 10:**60–63, 1978

26. Duhamel G, Callot V, Cozzone PJ, Kober F: Spinal cord blood flow measurement by arterial spin labeling. **Magn Reson Med 59:**846–854, 2008

27. Elmore JR, Gloviczki P, Harper CM, Pairolero PC, Murray MJ, Bourchier RG, et al: Failure of motor evoked potentials to predict neurologic outcome in experimental thoracic aortic occlusion. **J Vasc Surg 14:**131–139, 1991

28. Fairholm D, Turnbull I: Microangiographic study of experimental spinal injuries in dogs and rabbits. **Surg Forum 21:** 453–455, 1970

29. Fehlings MG, Tator CH, Linden RD: The relationships among the severity of spinal cord injury, motor and somatosensory evoked potentials and spinal cord blood flow. **Electroencephalogr Clin Neurophysiol 74:**241–259, 1989

30. Fried LC, Aparicio O: Experimental ischemia of the spinal cord. Histologic studies after anterior spinal artery occlusion. **Neurology 23:**289–293, 1973

31. Gharagozloo F, Neville RF Jr, Cox JL: Spinal cord protection during surgical procedures on the descending thoracic and thoracoabdominal aorta: a critical overview. **Semin Thorac Cardiovasc Surg 10:**73–86, 1998

32. Gillilan LA: The arterial blood supply of the human spinal cord. **J Comp Neurol 110:**75–103, 1958

33. Griffiths IR: Spinal cord blood flow after acute experimental cord injury in dogs. **J Neurol Sci 27:**247–259, 1976

34. Griffiths IR, Pitts LH, Crawford RA, Trench JG: Spinal cord compression and blood flow. I. The effect of raised cerebrospinal fluid pressure on spinal cord blood flow. **Neurology 28:** 1145–1151, 1978

35. Guha A, Tator CH, Rochon J: Spinal cord blood flow and systemic blood pressure after experimental spinal cord injury in rats. **Stroke 20:**372–377, 1989

36. Hamamoto Y, Ogata T, Morino T, Hino M, Yamamoto H: Real-time direct measurement of spinal cord blood flow at the site of compression: relationship between blood flow recovery and motor deficiency in spinal cord injury. **Spine (Phila Pa 1976) 32:**1955–1962, 2007

37. Hassler O: Blood supply to human spinal cord. A microangiographic study. **Arch Neurol 15:**302–307, 1966

38. Hitchon PW, Lobosky JM, Yamada T, Johnson G, Girton RA: Effect of hemorrhagic shock upon spinal cord blood flow and evoked potentials. **Neurosurgery 21:**849–857, 1987

39. Holtz A, Nyström B, Gerdin B: Relation between spinal cord blood flow and functional recovery after blocking weight-induced spinal cord injury in rats. **Neurosurgery 26:**952–957, 1990

40. Horn EM, Theodore N, Assina R, Spetzler RF, Sonntag VK, Preul MC: The effects of intrathecal hypotension on tissue perfusion and pathophysiological outcome after acute spinal cord injury. **Neurosurg Focus 25(5):**E12, 2008

41. Iwai A, Monafo WW: The effects of lumbar sympathectomy on regional spinal cord blood flow in rats during acute hemorrhagic hypotension. **J Neurosurg 76:**687–691, 1992

42. Kazama S, Masaki Y, Maruyama S, Ishihara A: Effect of altering cerebrospinal fluid pressure on spinal cord blood flow. **Ann Thorac Surg 58:**112–115, 1994

43. Kieffer E, Ammar F, Chiras J, Belli C, Rochat G: Traumatic rupture of the thoracoabdominal aorta. **Eur J Vasc Surg 1:** 353–358, 1987

44. Kindt GW: Autoregulation of spinal cord blood flow. **Eur Neurol 6:**19–23, 1971–1972

45. Kobrine AI, Doyle TF, Martins AN: Autoregulation of spinal cord blood flow. **Clin Neurosurg 22:**573–581, 1975

46. Kobrine AI, Doyle TF, Martins AN: Local spinal cord blood flow in experimental traumatic myelopathy. **J Neurosurg 42:** 144–149, 1975

47. Kobrine AI, Evans DE, Rizzoli HV: The role of the sympathetic nervous system in spinal cord autoregulation. **Acta Neurol Scand Suppl 64:**54–55, 1977

48. Koyanagi I, Tator CH, Theriault E: Silicone rubber microangiography of acute spinal cord injury in the rat. **Neurosurgery 32:**260–268, 1993

49. Laschinger JC, Cunningham JN Jr, Nathan IM, Knopp EA, Cooper MM, Spencer FC: Experimental and clinical assessment of the adequacy of partial bypass in maintenance of spinal cord blood flow during operations on the thoracic aorta. **Ann Thorac Surg 36:**417–426, 1983

50. Lazorthes G, Gouaze A, Zadeh JO, Santini JJ, Lazorthes Y, Burdin P: Arterial vascularization of the spinal cord: recent studies of anastomotic substitution pathways. **J Neurosurg 35:**253–262, 1971

51. Lobosky JM, Hitchon PW, Torner JC, Yamada T: Spinal cord autoregulation in the sheep. **Curr Surg 41:**264–267, 1984

52. Lohse DC, Senter HJ, Kauer JS, Wohns R: Spinal cord blood flow in experimental transient traumatic paraplegia. **J Neurosurg 52:**335–345, 1980

53. Mathé JF, Richard I, Roger JC, Potagas C, el Masry WS, Perrouin-Verbe B: Ischaemic myelopathy following aortic surgery or traumatic laceration of the aorta. **Spinal Cord 36:**110–116, 1998

54. Mauney MC, Blackbourne LH, Langenburg SE, Buchanan SA, Kron IL, Tribble CG: Prevention of spinal cord injury after repair of the thoracic or thoracoabdominal aorta. **Ann Thorac Surg 59:**245–252, 1995

55. McCullough JL, Hollier LH, Nugent M: Paraplegia after thoracic aortic occlusion: influence of cerebrospinal fluid drainage. Experimental and early clinical results. **J Vasc Surg 7:** 153–160, 1988

56. Molina JE, Cogordan J, Einzig S, Bianco RW, Rasmussen T, Clack RM, et al: Adequacy of ascending aorta-descending aorta shunt during cross-clamping of the thoracic aorta for prevention of spinal cord injury. **J Thorac Cardiovasc Surg 90:**126–136, 1985

57. Naftchi NE, Demeny M, DeCrescito V, Tomasula JJ, Flamm ES, Campbell JB: Biogenic amine concentrations in traumatized spinal cords of cats. Effect of drug therapy. **J Neurosurg 40:**52–57, 1974

58. Ohashi T, Morimoto T, Kawata K, Yamada T, Sakaki T: Correlation between spinal cord blood flow and arterial diameter following acute spinal cord injury in rats. **Acta Neurochir (Wien) 138:**322–329, 1996

59. Palleske KR, Kivelitz R, Loew F: Experimental investigation on the control of spinal cord circulation. IV. The effect of spinal or cerebral compression on the blood flow of the spinal cord. **Acta Neurochir (Wien) 22:**29–41, 1970

60. Parke WW: Arteriovenous glomeruli of the human spinal cord and their possible functional implications. **Clin Anat 17:**558–563, 2004

61. Parke WW, Whalen JL, Bunger PC, Settles HE: Intimal musculature of the lower anterior spinal artery. **Spine (Phila Pa 1976) 20:**2073–2079, 1995

62. Piano G, Gewertz BL: Mechanism of increased cerebrospinal fluid pressure with thoracic aortic occlusion. **J Vasc Surg 11:** 695–701, 1990

63. Reed JE, Allen WE III, Dohrmann GJ: Effect of mannitol on the traumatized spinal cord. Microangiography, blood flow patterns, and electrophysiology. **Spine (Phila Pa 1976) 4:** 391–397, 1979

64. Rivlin AS, Tator CH: Regional spinal cord blood flow in rats after severe cord trauma. **J Neurosurg 49:**844–853, 1978

65. Robertazzi RR, Cunningham JN Jr: Intraoperative adjuncts of spinal cord protection. **Semin Thorac Cardiovasc Surg 10:** 29–34, 1998

66. Rowland JW, Hawryluk GW, Kwon B, Fehlings MG: Current status of acute spinal cord injury pathophysiology and emerging therapies: promise on the horizon. **Neurosurg Focus 25(5):**E2, 2008

67. Sandler AN, Tator CH: Effect of acute spinal cord compression injury on regional spinal cord blood flow in primates. **J Neurosurg 45:**660–676, 1976

124

68. Sasaki S: Vascular change in the spinal cord after impact injury in the rat. **Neurosurgery 10:**360–363, 1982
69. Schepens MA, Defauw JJ, Hamerlijnck RP, Vermeulen FE: Use of left heart bypass in the surgical repair of thoracoabdominal aortic aneurysms. **Ann Vasc Surg 9:**327–338, 1995
70. Senter HJ, Venes JL: Loss of autoregulation and posttraumatic ischemia following experimental spinal cord trauma. **J Neurosurg 50:**198–206, 1979
71. Singh U, Silver JR, Welply NC: Hypotensive infarction of the spinal cord. **Paraplegia 32:**314–322, 1994
72. Sliwa JA, Maclean IC: Ischemic myelopathy: a review of spinal vasculature and related clinical syndromes. **Arch Phys Med Rehabil 73:**365–372, 1992
73. Smith AJ, McCreery DB, Bloedel JR, Chou SN: Hyperemia, CO2 responsiveness, and autoregulation in the white matter following experimental spinal cord injury. **J Neurosurg 48:** 239–251, 1978
74. Smith AL, Pender JW, Alexander SC: Effects of PCO2 on spinal cord blood flow. **Am J Physiol 216:**1158–1163, 1969
75. Svensson LG, Crawford ES, Hess KR, Coselli JS, Safi HJ: Experience with 1509 patients undergoing thoracoabdominal aortic operations. **J Vasc Surg 17:**357–370, 1993
76. Tabayashi K: Spinal cord protection during thoracoabdominal aneurysm repair. **Surg Today 35:**1–6, 2005
77. Taira Y, Marsala M: Effect of proximal arterial perfusion pressure on function, spinal cord blood flow, and histopathologic changes after increasing intervals of aortic occlusion in the rat. **Stroke 27:**1850–1858, 1996
78. Tator CH, Koyanagi I: Vascular mechanisms in the pathophysiology of human spinal cord injury. **J Neurosurg 86:**483–492, 1997
79. Tsuji T, Matsuyama Y, Sato K, Iwata H: Evaluation of spinal cord blood flow during prostaglandin E1-induced hypotension with power Doppler ultrasonography. **Spinal Cord 39:**31–36, 2001
80. Turnbull IM: Chapter 5. Blood supply of the spinal cord: normal and pathological considerations. **Clin Neurosurg 20:**56–84, 1973
81. Turnbull IM: Microvasculature of the human spinal cord. **J Neurosurg 35:**141–147, 1971
82. Turnbull IM, Brieg A, Hassler O: Blood supply of cervical spinal cord in man. A microangiographic cadaver study. **J Neurosurg 24:**951–965, 1966
83. Tveten L: Spinal cord vascularity. III. The spinal cord arteries in man. **Acta Radiol Diagn (Stockh) 17:**257–273, 1976
84. Vlajić I: Microangiographic observations of morphological vessel changes after experimental spinal cord trauma. **Adv Neurol 20:**451–460, 1978
85. Wallace MC, Tator CH: Successful improvement of blood pressure, cardiac output, and spinal cord blood flow after experimental spinal cord injury. **Neurosurgery 20:**710–715, 1987
86. Wallace MC, Tator CH, Frazee P: Relationship between posttraumatic ischemia and hemorrhage in the injured rat spinal cord as shown by colloidal carbon angiography. **Neurosurgery 18:**433–439, 1986
87. Winnerkvist A, Bartoli S, Iliopoulos DC, Hess KR, Miller CC, Safi HJ: Spinal cord protection during aortic cross clamping: retrograde venous spinal cord perfusion, distal aortic perfusion, and cerebrospinal fluid drainage. **Scand Cardiovasc J 36:**6–10, 2002
88. Young W, DeCrescito V, Tomasula JJ: Effect of sympathectomy on spinal blood flow autoregulation and posttraumatic ischemia. **J Neurosurg 56:**706–710, 1982
89. Zeitin H, Lichtenstein BW: Occlusion of the anterior spinal artery: clinicopathologic report of a case and a review of the literature. **Arch Neurol Psychiatry 36:**96–111, 1936

Address correspondence to: Nicholas Theodore, M.D., Neuroscience Publications, Barrow Neurological Institute, 350 West Thomas Road, Phoenix, Arizona 85013. email: neuropub@chw.edu.

125

APPENDIX B

MICROSURGICAL ANATOMY OF THE ARTERIAL BASKET OF THE CONUS

MEDULLARIS

Microsurgical anatomy of the arterial basket of the conus medullaris

Nikolay L. Martirosyan, MD,[1,2] M. Yashar S. Kalani, MD, PhD,[1] G. Michael Lemole Jr., MD,[2] Robert F. Spetzler, MD,[1] Mark C. Preul, MD,[1] and Nicholas Theodore, MD[1]

[1]Division of Neurological Surgery, Barrow Neurological Institute, St. Joseph's Hospital and Medical Center, Phoenix; and [2]Division of Neurological Surgery, University of Arizona, Tucson, Arizona

OBJECT The arterial basket of the conus medullaris (ABCM) consists of 1 or 2 arteries arising from the anterior spinal artery (ASA) and circumferentially connecting the ASA and the posterior spinal arteries (PSAs). The arterial basket can be involved in arteriovenous fistulas and arteriovenous malformations of the conus. In this article, the authors describe the microsurgical anatomy of the ABCM with emphasis on its morphometric parameters and important role in the intrinsic blood supply of the conus medullaris.

METHODS The authors performed microsurgical dissections on 16 formalin-fixed human spinal cords harvested within 24 hours of death. The course, diameter, and branching angles of the arteries comprising the ABCM were then identified and measured. In addition, histological sections were obtained to identify perforating vessels arising from the ABCM.

RESULTS The ASA tapers as it nears the conus medullaris (mean preconus diameter 0.7 ± 0.12 mm vs mean conus diameter 0.38 ± 0.08 mm). The ASA forms an anastomotic basket with the posterior spinal artery (PSA) via anastomotic branches. In most of the specimens (n = 13, 81.3%), bilateral arteries formed connections between the ASA and PSA. However, in the remaining specimens (n = 3, 18.7%), a unilateral right-sided anastomotic artery was identified. The mean diameter of the right ABCM branch was 0.49 ± 0.13 mm, and the mean diameter of the left branch was 0.53 ± 0.14 mm. The mean branching angles of the arteries forming the anastomotic basket were $95.9° \pm 36.6°$ and $90° \pm 34.3°$ for the right- and left-sided arteries, respectively. In cases of bilateral arterial anastomoses between the ASA and PSA, the mean distance between the origins of the arteries was 4.5 ± 3.3 mm. Histological analysis revealed numerous perforating vessels supplying tissue of the conus medullaris.

CONCLUSIONS The ABCM is a critical anastomotic connection between the ASA and PSA, which play an important role in the intrinsic blood supply of the conus medullaris. The ABCM provides an important compensatory function in the blood supply of the spinal cord. Its involvement in conus medullaris vascular malformations makes it a critical anatomical structure.

http://thejns.org/doi/abs/10.3171/2014.10.SPINE131081

KEY WORDS conus medullaris; arterial basket; anterior spinal artery; posterior spinal artery; microsurgical anatomy

DURING embryonic development, the vascular supply of the spinal cord undergoes significant modification and pruning. The differential growth of the spinal cord and spinal column results in the descent of the spinal nerve roots and ascent of the spinal cord into its adult configuration by the 1st year of life.[4] The blood supply to the spinal cord consists of an anterior spinal artery (ASA) and paired smaller posterior spinal arteries (PSAs).[17,22,23] The arterial blood supply to the spinal cord consists of several anastomoses that allow for redundancy of supply to the spinal cord.[15,17,22–24] One critical anasto-

motic connection is the arterial basket of the conus medullaris (ABCM). Initially described by Adamkiewicz in the 1880s, it has subsequently been studied using angiography by Djindjian and Lasjaunias.[1,2,5–7,13,14,16]

The ABCM consists of 1 or 2 arterial branches connecting the ASA and PSAs at the level of the conus medullaris. Although initially thought of as a fail-safe mechanism for providing alternative vascular supply to the conus, the ABCM has also been noted to be a critical component of vascular malformations of the conus medullaris.[6,18,21] To the best of our knowledge, this is the first detailed micro-

Methods

Study Material

We used 16 human cadaveric thoracolumbar spines up to 24 hours postmortem with no known vascular disease of the spinal cord. The anterior corpectomies and foraminotomies were performed utilizing a high-speed drill and rongeurs. The ventral aspect of the entire thoracolumbar spinal thecal sac and nerve root were fully exposed. Utilizing an operating microscope, a longitudinal midline durotomy was performed and the ventral spinal cord and cauda equina were defined. The artery of Adamkiewicz was identified and cannulated with a 32-gauge plastic cannula. Continuous room-temperature normal saline irrigation was used to purge the vascular system until no gross blood clots could be observed in vessels. Next, a red-colored silicone-rubber mixture was injected into the artery of Adamkiewicz.[3] This injection was performed under moderate pressure to avoid contrast extravasation and ensure adequate latex filling into distal small caliber vessels. Macroscopically, there was no evidence of vascular malformations or pathology involving the spinal cords (including atherosclerosis that could alter the latex injection). The specimens were fixed in a 5% formalin solution. One week after formalin fixation, we performed microsurgical dissection of the samples.[6,18] We identified and measured the course, diameter, and branching angle of the arteries comprising the ABCM. After all measurements were obtained, spinal cords sections were sent for histological analysis to identify smaller caliber perforating vessels arising from the ABCM.

Histological Analysis

Embedding and Sectioning

Spinal cords were treated with 20% glycerol and 2% dimethylsulfoxide to prevent freeze artifacts. Spinal cords were embedded in a gelatin matrix using MultiCord Technology (NeuroScience Associates) as used in previous studies.[8,19] The block of embedded spinal cord was allowed to cure and was then rapidly frozen by immersion in isopentane chilled with crushed dry ice. The block was mounted on a freezing stage of an AO 860 sliding microtome and sectioned in the coronal and sagittal plane at 40 μm. All sections cut were collected sequentially into a 4 × 6 array of containers. These containers were filled with Antigen Preserve solution (50% phosphate-buffered saline [pH 7.0], 50% ethylene glycol, and 1% polyvinyl pyrrolidone) for sections to be stained immunohistochemically. At the completion of sectioning, each container held a serial set of 1 of every 24th section (or, 1 section every 960 μm). Each of the large sections cut from the block was actually a composite section holding individual sections from the spinal cord embedded in each block. With such composite sections, uniformity of staining was achieved.

Nissl (Thionine) Stain

Every sixth section (every 240 μm) was used for staining. For Nissl staining, 40-μm sections were first mounted onto gelatinized slides. They were then dehydrated through alcohol rinses prior to defatting in a chloroform/ether/alcohol solution. The slides were then rehydrated and stained in 0.05% thionine/0.08 M acetate buffer, at a pH of 4.5. Following deionized water rinses, the slides were differentiated in 95% alcohol/acetic acid and dehydrated in a standard alcohol series, cleared in xylene, and coverslipped.

Results

Characteristics of the ABCM

The ASA tapers distally at the level of the conus medullaris. The mean preconus diameter of the ASA measured 0.7 ± 0.12 mm. At the level of the conus, the mean diameter of the artery narrowed to 0.38 ± 0.08 mm. The ASA forms an anastomotic basket with the PSA via 1 or 2 anastomotic branches (see Table 1 for measurements). In most specimens (n = 13, 81.3%), we identified 2 anastomotic branches connecting the ASA and PSA (Fig. 1). In the remaining specimens (n = 3, 18.7%), a unilateral right-sided anastomotic artery was identified (Fig. 2D). We measured the diameter of the anastomotic arteries in all specimens. The mean diameter of the right anastomotic branch was 0.49 ± 0.13 mm, and the mean diameter of the left anastomotic branch was 0.53 ± 0.14 mm. The branching angle of the arteries forming the anastomotic basket was $95.9° \pm 36.6°$ on the right side, and $90° \pm 34.3°$ on the left side.

Branching Orientation and Anastomosis Between the ASA and PSA

In most specimens, the arterial basket connecting the ASA and PSA consisted of 2 arterial connection points. In these instances, we noted that in 6 cases the right vessel branched first (Fig. 2A), in 5 cases the left vessel branched first (Fig. 2B), and in 2 cases both vessels branched simultaneously (Fig. 2C). These 3 differing branching orientations constitute the spectrum of patterns noted in the ABCM. In cases of bilateral arterial anastomoses between the ASA and PSA, the mean distance between the origins of the arteries was 4.5 ± 3.3 mm.

Histological Results

We were able to identify small caliber (< 0.5 mm) centripetal perforating branches arising from the ABCM (Fig. 3). Due to limitations of histological sections, we were not able to identify precisely the number of these branches and their lengths.

Discussion

Anastomotic Contribution of the ABCM

The ABCM functions as an anastomotic connection between the ASA and PSA. The arterial basket was symmetric in most specimens (n = 13), meaning that the ASA was connected to paired PSAs via right and left branches. This symmetric configuration allows for continuity of circulation between the anterior and posterior spinal circulations. In rare cases (n = 3), the anastomotic network was asymmetrical with a dominant artery connecting the ASA to one of the PSAs. This rare arrangement resulted in 1

TABLE 1. Morphometric parameters of ABCM branches

Spinal Cord No.	ASA Above Origin (mm)	ASA Below Origin (mm)	Right Branch (mm)	Right Angle (°)	Left Branch (mm)	Left Angle (°)	Distance Between Origins (mm)
1	0.8	0.3	0.4	120	0.5	85	2
2	0.5	0.4	0.4	115	NA	NA	NA
3	0.6	0.4	0.15	100	0.25	130	6.4
4	0.75	0.5	0.5	85	0.45	120	6.1
5	0.55	0.35	0.5	160	NA	NA	NA
6	0.55	0.4	0.5	50	NA	NA	NA
7	0.75	0.3	0.6	90	0.5	85	2.5
8	0.9	0.45	0.75	90	0.8	150	0
9	0.8	0.35	0.5	77	0.6	55	6.3
10	0.55	0.4	0.5	85	0.5	35	5
11	0.8	0.4	0.6	155	0.6	120	12.7
12	0.8	0.5	0.55	30	0.5	90	0.9
13	0.65	0.5	0.4	47	0.4	80	2.4
14	0.8	0.4	0.4	140	0.7	100	6
15	0.7	0.2	0.6	90	0.65	40	2.45
16	0.75	0.3	0.5	100	0.4	80	5.3
Mean	0.70	0.38	0.49	95.88	0.53	90.00	4.47
SD	0.12	0.08	0.13	36.57	0.14	34.28	3.31

NA = not applicable.

PSA receiving all of the ASA flow. This arrangement may result in a watershed zone on the contralateral dorsal surface of the spinal cord. Given the limitations of our current technique, it is possible that in these asymmetrical cases, finer anastomotic networks between the ASA and the other PSA exist but are not visualized with the injection technique.

Branching Orientation and Anastomosis Between the ASA and PSA

We identified 3 branching orientations connecting the ASA and PSAs. In the 2 most common scenarios, the ASA was connected to the PSA via bilateral branching arteries, which branched from the ASA at different levels of the conus (Fig. 2A and B). In a more uncommon orientation, the bilateral branching arteries branched simultaneously from the ASA to connect to the paired PSAs. These branching orientations do not appear to have functional significance, but the anatomical description of these branching patterns is novel and has not been previously described.

Conus Medullaris Arteriovenous Malformations and the ABCM

The ABCM is frequently involved in vascular malformations of the conus medullaris (Figs. 4 and 5).[9–12,20,25] The angiography provides a robust means of obtaining anatomical information about vasculature at the conus. However, spinal angiography is a rarely performed, time-consuming procedure that is only performed to evaluate pathological conditions. For this reason we were not able to perform additional correlations between anatomical findings with angiographic data.
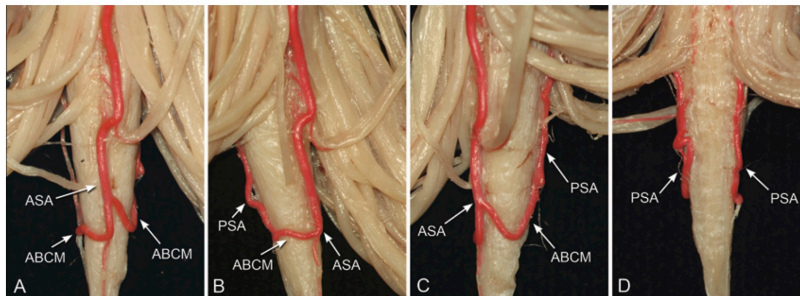
FIG. 1. Gross anatomical specimens. **A:** Anterior view demonstrating bilateral networks connecting the ASA to the paired PSAs. **B and C:** Lateral right (B) and left (C) views at the level of the conus medullaris demonstrating the connection of the ASA to the PSAs via the arterial branches of the ABCM. **D:** Posterior view of the arterial branches of the basket draining into the PSA.

129
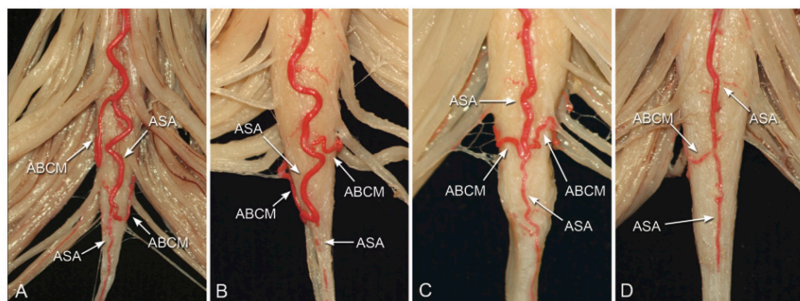
FIG. 2. Anterior gross anatomical specimen at the level of the conus medullaris. **A and B:** Early right- (A) and left-sided (B) ABCM branching from the ASA. **C:** Alternatively, ABCM bilateral branches from the ASA may occur simultaneously, although this is a rare arrangement. **D:** Unilateral right-sided branching from the ASA.
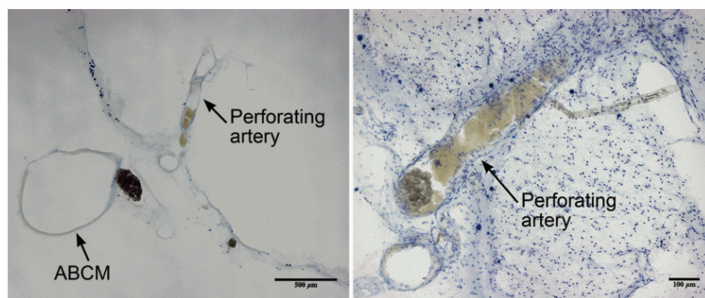
FIG. 3. Nissl stain images. **Left:** The axial section through the conus medullaris shows a perforator branch arising from the ABCM. **Right:** Small perforator branch of the ABCM surrounded with spinal cord tissue.

We reviewed one of the senior authors' experience (R.F.S.) with resection of arteriovenous malformations (AVMs) of the conus and noted that in complex cases, the ABCM is ill defined or undefinable on spinal angiogra-

FIG. 4. Anteroposterior angiograms at the level of the conus medullaris demonstrate the involvement of the ABCM in a conus medullaris AVM. The ASA, PSA, and ABCM can be identified.

phy.[25] In many cases of AVMs of the conus, the large size of the nidus obscures proper delineation of the ABCM (Fig. 5).

Understanding of the anatomy of the ABCM and its variations is critical for addressing vascular malformations in this location. The presence of perforating vessels feeding the conus that arise from this ABCM has clinical implications for the resection of vascular lesions as well as other pathologies in this region. This anatomy is often not well described or studied; our study adds a new dimension, highlighting the importance of perforating vessels arising from the ABCM to the vasculature of the conus medullaris.

Conclusions

The ABCM is an anastomotic network connecting the ASA and PSAs. We identified 3 different branching patterns connecting the ASA and PSAs. In the majority of the cases, bilateral arteries connected the ASA and PSA, allowing for redundancy in vascular supply to the spinal cord and conus medullaris. Small perforating arteries arising from the ABCM provide blood supply to the conus medullaris tissue. The ABCM is involved in vascular malformations and tumors at the level of the conus. The physi-

130

FIG. 5. Anteroposterior angiograms of complex cases of AVMs of the conus medullaris involving the ABCM. The large size of the nidus obscures proper delineation of the ASA, PSA, and ABCM.

ological role of the ABCM in the vascular malformation of the conus is unclear and requires further investigation. Practitioners treating vascular lesions and tumors of the conus medullaris must have a solid understanding of the anatomy of this critical anastomotic network.

References

1. Adamkiewicz A: Die Blutgefasse des menschlichen ruckenmarkes II: Theil. die gefasse der ruckenmarksoberflache. **S B Heidelberg Akad Wiss 85:**101–130, 1882
2. Adamkiewicz A: I. Die Gefasse der Ruckenmarkersubstanz. **Sitzungsb Akad Wissench Wien Math-Naturw 84:**469, 1881
3. Alleyne CH Jr, Cawley CM, Shengelaia GG, Barrow DL: Microsurgical anatomy of the artery of Adamkiewicz and its segmental artery. **J Neurosurg 89:**791–795, 1998
4. Altman J, Bayer SA: **Development of the Human Spinal Cord: An Interpretation Based on Experimental Studies in Animals.** New York: Oxford University Press, 2001
5. Bolton B: The blood supply of the human spinal cord. **J Neurol Psychiatry 2:**137–148, 1939
6. Djindjian M, Ribeiro A, Ortega E, Gaston A, Poirier J: The normal vascularization of the intradural filum terminale in man. **Surg Radiol Anat 10:**201–209, 1988
7. Djindjian R: Angiography of the spinal cord. **Surg Neurol 2:**179–185, 1974
8. Fix AS, Ross JF, Stitzel SR, Switzer RC: Integrated evaluation of central nervous system lesions: stains for neurons, astrocytes, and microglia reveal the spatial and temporal features of MK-801-induced neuronal necrosis in the rat cerebral cortex. **Toxicol Pathol 24:**291–304, 1996
9. Hsu SW, Rodesch G, Luo CB, Chen YL, Alvarez H, Lasjaunias PL: Concomitant conus medullaris arteriovenous malformation and sacral dural arteriovenous fistula of the filum terminale. **Interv Neuroradiol 8:**47–53, 2002
10. Kalani MY, Ahmed AS, Martirosyan NL, Cronk K, Moon K, Albuquerque FC, et al: Surgical and endovascular treatment of pediatric spinal arteriovenous malformations. **World Neurosurg 78:**348–354, 2012
11. Kim LJ, Spetzler RF: Classification and surgical management of spinal arteriovenous lesions: arteriovenous fistulae and arteriovenous malformations. **Neurosurgery 59 (5 Suppl 3):**S3-195–S3-201, 2006
12. Krings T, Lasjaunias PL, Hans FJ, Mull M, Nijenhuis RJ, Alvarez H, et al: Imaging in spinal vascular disease. **Neuroimaging Clin N Am 17:**57–72, 2007
13. Lasjaunias PL, Berenstein A: **Surgical Neuroangiography, Volume 3. Functional Vascular Anatomy of Brain, Spinal Cord, and Spine.** New York: Springer, 1990
14. Lazorthes G, Gouazé A, Bastide G, Soutoul JH, Zadeh O, Santini JJ: [Arterial vascularization of the lumbar elevation. Study of variations and substitutions.] **Rev Neurol (Paris) 114:**109–122, 1966 (Fr)
15. Lazorthes G, Gouaze A, Zadeh JO, Santini JJ, Lazorthes Y, Burdin P: Arterial vascularization of the spinal cord. Recent studies of the anastomotic substitution pathways. **J Neurosurg 35:**253–262, 1971
16. Lazorthes G, Poulhes J, Bastide G, Roulleau J, Chancholle AR: [Arterial vascularization of the spine; anatomic research and applications in pathology of the spinal cord and aorta.] **Neurochirurgie 4:**3–19, 1958 (Fr)
17. Martirosyan NL, Feuerstein JS, Theodore N, Cavalcanti DD, Spetzler RF, Preul MC: Blood supply and vascular reactivity of the spinal cord under normal and pathological conditions. **J Neurosurg Spine 15:**238–251, 2011
18. Parke WW, Gammell K, Rothman RH: Arterial vascularization of the cauda equina. **J Bone Joint Surg Am 63:**53–62, 1981
19. Ross JF, Switzer RC, Poston MR, Lawhorn GT: Distribution of bismuth in the brain after intraperitoneal dosing of bismuth subnitrate in mice: implications for routes of entry of xenobiotic metals into the brain. **Brain Res 725:**137–154, 1996
20. Spetzler RF, Detwiler PW, Riina HA, Porter RW: Modified classification of spinal cord vascular lesions. **J Neurosurg 96 (2 Suppl):**145–156, 2002
21. Stein SC, Ommaya AK, Doppman JL, Di Chiro G: Arteriovenous malformation of the cauda equina with arterial supply from branches of the internal iliac arteries. Case report. **J Neurosurg 36:**649–651, 1972
22. Turnbull IM: Chapter 5. Blood supply of the spinal cord: normal and pathological considerations. **Clin Neurosurg 20:**56–84, 1973
23. Turnbull IM: Microvasculature of the human spinal cord. **J Neurosurg 35:**141–147, 1971
24. Tveten L: Spinal cord vascularity. III. The spinal cord arteries in man. **Acta Radiol Diagn (Stockh) 17:**257–273, 1976
25. Wilson DA, Abla AA, Uschold TD, McDougall CG, Albuquerque FC, Spetzler RF: Multimodality treatment of conus medullaris arteriovenous malformations: 2 decades of experience with combined endovascular and microsurgical treatments. **Neurosurgery 71:**100–108, 2012

Author Contributions

Conception and design: Theodore, Martirosyan, Kalani, Preul. Acquisition of data: Martirosyan, Kalani. Analysis and interpretation of data: Theodore, Martirosyan, Kalani, Preul. Drafting the article: Martirosyan, Kalani. Critically revising the article: Theodore, Lemole, Spetzler, Preul. Reviewed submitted version of manuscript: Theodore, Lemole, Spetzler, Preul. Administrative/technical/material support: Theodore, Lemole, Spetzler, Preul. Study supervision: Theodore, Lemole, Spetzler, Preul.

Correspondence

Nicholas Theodore, c/o Neuroscience Publications, Barrow Neurological Institute, St. Joseph's Hospital and Medical Center, 350 W. Thomas Rd., Phoenix, AZ 85013. email: neuropub@dignityhealth.org.

131

APPENDIX C

CEREBROSPINAL FLUID DRAINAGE AND INDUCED HYPERTENSION

IMPROVE SPINAL CORD PERFUSION AFTER ACUTE SPINAL CORD INJURY IN

PIGS

Cerebrospinal Fluid Drainage and Induced Hypertension Improve Spinal Cord Perfusion After Acute Spinal Cord Injury in Pigs

Nikolay L. Martirosyan, MD*‡

M. Yashar S. Kalani, MD, PhD*

William D. Bichard*

Ali A. Baaj, MD‡

L. Fernando Gonzalez, MD§

Mark C. Preul, MD*

Nicholas Theodore, MD*

*Division of Neurological Surgery, Barrow Neurological Institute, St. Joseph's Hospital and Medical Center, Phoenix, Arizona; ‡Division of Neurosurgery, University of Arizona, Tucson, Arizona; §Division of Neurological Surgery, Thomas Jefferson University, Philadelphia, Pennsylvania

Correspondence:
Nicholas Theodore, MD,
c/o Neuroscience Publications;
Barrow Neurological Institute,
St. Joseph's Hospital and Medical Center,
350 W Thomas Rd;
Phoenix, AZ 85013.
E-mail: Neuropub@dignityhealth.org

BACKGROUND: Acute spinal cord injury (SCI) is commonly treated by elevating the mean arterial pressure (MAP). Other potential interventions include cerebrospinal fluid drainage (CSFD).

OBJECTIVE: To determine the efficacy of aggressive MAP elevation combined with intrathecal pressure (ITP) reduction; our primary objective was to improve spinal cord blood flow (SCBF) after SCI.

METHODS: All 15 pigs underwent laminectomy. Study groups included control (n = 3); SCI only (n = 3); SCI combined with MAP elevation (SCI + MAP) (n = 3); SCI combined with CSFD (SCI + CSFD) (n = 3); and SCI combined with both MAP elevation and CSFD (SCI + MAP + CSFD) (n = 3). SCBF was measured with laser Doppler flowmetry.

RESULTS: In the SCI group, SCBF decreased by 56% after SCI. MAP elevation after SCI resulted in a 34% decrease in SCBF, whereas CSFD resulted in a 59% decrease in SCBF. The combination of CSFD and MAP elevation resulted in a 24% increase in SCBF. The SCI + MAP group had an average ITP increase of 5.45 mm Hg after MAP elevation 1 hour after SCI and remained at that level throughout the experiment.

CONCLUSION: Both MAP elevation alone and CSFD alone led to only short-term improvement of SCBF. The combination of MAP elevation and CSFD significantly and sustainably improved SCBF and spinal cord perfusion pressure. Although laser Doppler flowmetry can provide flow measurements to a tissue depth of only 1.5 mm, these results may represent pattern of blood flow changes in the entire spinal cord after injury.

KEY WORDS: Cerebrospinal fluid drainage, Intrathecal pressure, Mean arterial pressure, Paraplegia, Spinal cord blood flow, Spinal cord injury, Spinal cord perfusion

Acute spinal cord injury (SCI) from blunt trauma affects 10 000 to 14 000 persons per year in the United States.[1,2] The goals of treatment are to overcome the physiological barriers imposed by the SCI itself and to allow patients to regain their preinjury level of neurological function.[3]

The role of ischemia in the secondary injury cascade has been well studied in animal models. The mechanisms of secondary injury after SCI have been well defined; loss of spinal cord

microcirculation, loss of autoregulation, and ischemia are all important in the pathogenesis of secondary spinal cord damage.[4-8] One of the basic tenets of management of acute SCI is the prevention of spinal cord ischemia by avoiding systemic hypotension and hypoxia. Rapid decompression of the compressed spinal cord with stabilization of the spine to prevent further injury and aggressive medical resuscitation with mean arterial pressure (MAP) elevation have become common practice.[9-11] Although no class I evidence supports its effectiveness, MAP elevation is now recommended for routine use after cervical SCI.[12,13]

Other potential nonpharmacological interventions include cerebrospinal fluid drainage (CSFD) and hypothermia.[14,15] The neuroprotective strategy

---

ABBREVIATIONS: CSFD, cerebrospinal fluid drainage; **ITP,** intrathecal pressure; **LDF,** laser Doppler flowmetry; **MAP,** mean arterial pressure; **SCBF,** spinal cord blood flow; **SCI,** spinal cord injury

133

of CSFD has been used in patients undergoing abdominal aortic aneurysm surgery, decreasing the neurological dysfunction after aortic occlusion.[16,17] Furthermore, in animal studies, CSFD has been shown to decrease spinal cord damage following acute injury.[14,18] However, in humans with SCI, CSFD alone did not result in clinical improvement.[19]

Characterizing the physiological changes induced in the spinal cord by MAP elevation and CSFD could help clinicians better understand the mechanisms of ischemia after SCI, with the ultimate goal of ameliorating the detrimental effects of ischemia. In our study, we sought to determine the efficacy, in pigs, of aggressive MAP elevation combined with intrathecal pressure (ITP) reduction via CSFD; our primary objective was to improve spinal cord blood flow (SCBF) after blunt SCI to decrease or even prevent ischemia.

METHODS

Animal Care

All methodologies concerning the use of animals for scientific study have been approved by the Institutional Animal Care and Use Committee at Barrow Neurological Institute in Phoenix and St. Joseph's Hospital and Medical Center.

Study Groups

For these nonsurvival experiments, we used 15 pigs (adult Yorkshire swine). All 15 pigs underwent laminectomy. We divided them evenly into 5 groups: control (n = 3); SCI only (n = 3); SCI combined with MAP elevation (SCI + MAP, n = 3); SCI combined with CSFD (SCI + CSFD, n = 3); and SCI combined with both MAP elevation and CSFD (SCI + MAP + CSFD, n = 3).

Preparation and Monitoring

Each pig was anesthetized with an intramuscular injection of ketamine (40 mg/kg) and xylazine (10 mg/kg). After adequate anesthesia was achieved, the pigs were intubated and maintained under general anesthesia with 2% to 3% isoflurane and propofol (0.1-0.5 mg/kg/min continuous intravenous [IV] infusion). A femoral artery was cannulated for blood pressure recordings, and an ear vein was cannulated for the administration of drugs. Body temperature was maintained with a heating pad and monitored by rectal temperature probe.

For the surgery, the animals were positioned prone on the operating table. To expose the T3-T8 and L5-S1 spinal levels, we made 2 separate midline incisions and performed a subperiosteal dissection. Next, to expose the dura mater at those levels, we performed a laminectomy. A laser Doppler flow-monitoring TSD143 probe (Biopac Systems, Inc, Goleta, California) was then placed over the dura mater at the T5 level. This technology allows measurement of blood flow to a tissue depth of 1.5 mm. During all procedures, we measured SCBF in blood perfusion units and recorded the results. To ensure identical placement of each probe after SCI, we marked the underlying dura mater.

For the pigs with CSFD, we placed a lumbar drain (Medtronic, Inc., Minneapolis, Minnesota)—under direct visualization, using an operating microscope—at the lumbosacral junction level intrathecally. To avoid uncontrolled CSF leakage, we used a minimal durotomy (up to 1 mm). We chose the L5-S1 level because of the anatomy of the pig spinal cord,

which typically terminates just above the lumbosacral junction. Throughout the procedure, we monitored ITP and recorded the total amount of drained CSF.

Next, 1 hour after the laminectomy (in all groups except the control group), we induced mild SCI by delivering a force of 300 g/cm² (20 g weight 15 cm above the spinal cord).

In the pertinent study groups, we also initiated MAP elevation and CSFD 1 hour after SCI, to allow the pigs to recover from the procedural stress. MAP was elevated by a continuous infusion of phenylephrine (at a rate of 0.2 µg/kg/min). This concentration and rate resulted in doubling of MAP.

All relevant physiological parameters (SCBF, ITP, MAP, and body temperature) were monitored in real time for all animals by using the Biopac MP150 unit with additional LDF100C, DA100C, and SKT100C amplifiers. To display and store data, we used a Windows personal computer with AcqKnowledge 3.8.2 software (Biopac Systems, Inc).

Data Analysis

We acquired data immediately before SCI and then 30 minutes and 1, 2, 3, and 4 hours after SCI. In treatment groups, measurements at 1 hour were taken immediately after treatment initiation. For data processing, we used Excel (Microsoft Corp., Redmond, Washington). For data analysis, we used the 1-tailed Student t test, with results considered significant if $P < .05$.

Spinal Cord Blood Flow

To standardize and compare SCBF, we recorded the value immediately before SCI as zero. SCBF was then calculated at the set time points after SCI as the percentage of difference from the value immediately before SCI. Thus, a negative value represented a decrease in SCBF; a positive value represented an increase in SCBF.

Intrathecal Pressure

We analyzed ITP, at the set time points after SCI, by comparing it with the value (in mm Hg) taken immediately before SCI.

Study Design

All 15 pigs underwent T5 laminectomy and monitoring as described above. The control group was not subjected to SCI or any additional interventions (beyond laminectomy and monitoring). In the other 4 study groups, we induced mild SCI 1 hour after the laminectomy. In the 2 MAP groups, a phenylephrine drip was begun 1 hour after SCI. In the 2 CSFD groups, CSFD was begun 1 hour after SCI, with the lumbar drain open at 5 mm Hg. The total experiment time was 6 hours, including 1 hour of preparation and 5 hours of monitoring time. At the end of the procedures, the pigs were euthanized per institutional guidelines.

RESULTS

Spinal Cord Blood Flow

SCBF in the SCI group decreased by 47.5% to 61.1% after SCI compared with baseline (Figure 1; Table). This gradual decrease began 30 minutes after SCI and persisted throughout the experiment. MAP elevation after SCI (the SCI + MAP group) decreased SCBF by 25.5% to 34.0% at 2, 3, and 4 hours after SCI; interestingly, at 1 hour after SCI (when the phenylephrine drip began), SCBF increased by an average of 12.6%. However, the difference in SCBF between the SCI group

134

FIGURE 1. *Percentage of change in SCBF at different time points after SCI compared with baseline for the control and treatment groups. In treatment groups, measurements at 1 hour were taken immediately after treatment initiation. There was overall hypoperfusion in SCI, SCI + MAP, and SCI + CSFD groups after SCI. In contrast, SCBF was elevated in comparison with the pre-SCI level in the SCI + MAP + CSFD group. CSFD, cerebrospinal fluid drainage; MAP, mean arterial pressure; SCBF, spinal cord blood flow; SCI, spinal cord injury. Used with permission from Barrow Neurological Institute.*

and the SCI + MAP group was not statistically significant ($P >$ .05; Table).

In the SCI + CSFD group, SCBF decreased by an average of 16.8% 1 hour after SCI and continued to decrease at later time points (range, 50.3%-60.0%). The difference was not statistically significant ($P = .42$) compared with the SCI + MAP group, but it was statistically significant compared with the SCI + MAP + CSFD group ($P < .05$; Table).

In the SCI + MAP + CSFD group, SCBF increased at 1, 2, 3, and 4 hours after SCI (range, 24.6%-61.6%)—a statistically significant difference compared with the decrease in both the SCI and SCI + MAP groups ($P < .05$; Table). Furthermore, 1 hour after SCI (when both the phenylephrine drip and CSF drainage began), SCBF increased by an average of 61.6% (Figure 1).

SCBF in the control group decreased only slightly, by 2.4% to 5%, throughout the experiment.

Intrathecal Pressure

In the SCI group, ITP decreased by 0.8 to 2.35 mm Hg after SCI (Figure 2). In the SCI + MAP group, ITP increased by 4.9 to 5.45 mm Hg (Figure 2). In the control group, ITP remained stable throughout the experiment. Mean CSFD was 32.3 mL in the SCI + CSFD group and 55.4 mL in the SCI + MAP + CSFD group.

Dynamics

In all 4 study groups (not counting the control group), SCBF increased for a short period immediately after acute SCI (Figures 3, 4). In the SCI group, the SCBF remained low throughout the

experiment (Figure 3B), and ITP varied only slightly, without significant changes.

In the SCI + MAP group, SCBF increased immediately after the phenylephrine drip began, but decreased below the baseline level within the next 1 to 1.5 hours (Figure 3C). The SCBF remained low for the remainder of the experiment. ITP increased immediately after the phenylephrine drip began and remained elevated throughout the experiment.

In the SCI + CSFD group, SCBF increased somewhat. However, as in the SCI + MAP group, this effect was temporary: after CSFD began at 1 hour, SCBF decreased and remained at the level below baseline (Figure 4A, B).

In the SCI + MAP + CSFD group, SCBF increased and remained elevated throughout the experiment (Figure 4C).

In the control group, all parameters remained stable throughout the experiment (Figure 3A).

In a separate test procedure to define dynamic CSF changes with changing ITP, we began MAP elevation and CSFD 1 hour after SCI. As a result, SCBF increased. However, about 40 minutes later, we stopped CSFD; over the next 3 hours, ITP increased and SCBF gradually decreased, despite MAP elevation. After 3 hours, we again began CSFD, which resulted in a noticeable increase in SCBF (Figure 5).

DISCUSSION

This study describes the effects of ITP and MAP changes on SCBF in the setting of mild SCI. The results of our study suggest that a combination of elevated MAP and CSFD improves SCBF.

135

TABLE. Statistical Difference in Changes (Positive or Negative) in SCBF After SCI (%), With Comparison of SCI + MAP + CSFD Group and SCI, SCI + MAP and SCI + CSFD Groups[a,b]

Time After SCI	SCI + MAP + CSFD SCBF	SCI SCBF	P Value	SCI + MAP SCBF	P Value	SCI + CSFD SCBF	P Value
30 min	14.7 ± 32.7	−53.0 ± 35.4	.1	−21.3 ± 58.0	.3	−33.2 ± 37.2	.1
1 h	61.6 ± 61.2	−47.5 ± 44.3	.03	12.6 ± 68.4	.2	−16.8 ± 23.3	.07
2 h	38.4 ± 16.0	−53.9 ± 18.3	.001	−25.5 ± 20.7	.007	−50.3 ± 18.3	.002
3 h	24.6 ± 4.2	−58.0 ± 2.2	<.001	−34.0 ± 28.0	.03	−59.2 ± 17.5	.005
4 h	44.9 ± 18.1	−61.1 ± 11.2	.001	−25.5 ± 37.0	.03	−60.0 ± 19.5	.001

[a]CSFD, cerebrospinal fluid drainage; MAP, mean arterial pressure; SCBF, spinal cord blood flow; SCI, spinal cord injury.
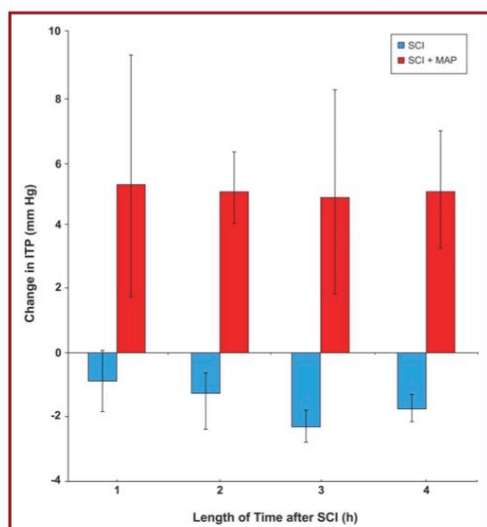[b]$P < .05$ considered significant.

Blood flow in the normal spinal cord is maintained within a normal range (ie, is autoregulated) when the MAP is 60 to 120 mm Hg and the $PaCO_2$ is 10 to 50 mm Hg.[6,20,21] One study has suggested that sympathetic control plays an important role in autoregulation.[22] Loss of autoregulation greatly contributes to ischemia after SCI.[4,23] Moreover, experimental data have demonstrated delayed onset (by 1-2 hours) of ischemia after SCI, which is coincident with the loss of autoregulation.[23] Thus, at least theoretically, MAP elevation should address the hypoperfusion experienced after loss of autoregulation after SCI. We also know that, according to the Monro-Kellie doctrine, any MAP elevation beyond the limit of autoregulation causes

FIGURE 2. *Mean ITP changes at different time points after SCI compared with baseline. ITP, intrathecal pressure; MAP, mean arterial pressure; SCI, spinal cord injury. Used with permission from Barrow Neurological Institute.*

increases in cerebral blood flow, intracranial pressure, and, subsequently, ITP.[24,25] However, CSF is produced via an active secretory process and does not change with alterations in MAP.[26]

Another suggested mechanism of ischemia after SCI is increased vascular resistance. Vascular resistance increases in inverse ratio to SCBF. One of the proposed mechanisms of increased vascular resistance is increased ITP. The spinal cord is encased within the dura mater, which, in turn, is surrounded by rigid bony and ligamentous structures. Thus, increased ITP causes compression of neural elements and vasculature (in a manner analogous to the effects of increased intracranial pressure as predicted by the Monro-Kellie doctrine). Venous outflow compromise results in congestion, increased vascular resistance, and decreased SCBF.[25] Thus, CSFD decreases ITP, and therefore should improve spinal cord perfusion pressure after acute SCI.

In our study, we used a mild injury model. This type of SCI provides more opportunities for successful therapeutic interventions with better functional outcome. With this type of SCI, autoregulation of the spinal cord blood supply is altered. However, elements of autoregulation are still present. In contrast, severe SCI results in significantly decreased SCBF and a potential total loss of autoregulation.[4]

Measurements of SCBF at 30 minutes provided nonconsistent data with no statistically significant difference (Figure 1; Table). This observation could be explained by complex alterations in spinal cord vasculature after injury. Hyperperfusion has been shown to be the first response to SCI, followed by hypoperfusion.[7,27] It is possible that our measurements registered different stages of early post-SCI changes in SCBF in different animals. Similar observations were made for the 1-hour measurements, taken immediately after treatment initiation. However the measurements taken 2, 3, and 4 hours after SCI represent homogeneous and comparable data after stabilization of physiological parameters.

In the SCI group, typical ischemic changes in SCBF occurred after injury; overall, ITP and arterial blood pressure remained stable (Figures 1, 2). In our other 3 study groups (the SCI + MAP group, the SCI + CSFD group, and the SCI + MAP + CSFD group), our interventions were intended to address ischemia. In the SCI + MAP group, elevation of MAP was initiated 1 hour after SCI, which, according to previous research,

136

FIGURE 3. *Snapshot of SCBF in the control group (**A**), SCI group (**B**), and SCI + MAP group (**C**). Arrows indicate the SCI and MAP elevation time points. BPU, blood perfusion unit; SCBF, spinal cord blood flow; SCI, spinal cord injury; MAP, mean arterial pressure.* Used with permission from Barrow Neurological Institute.
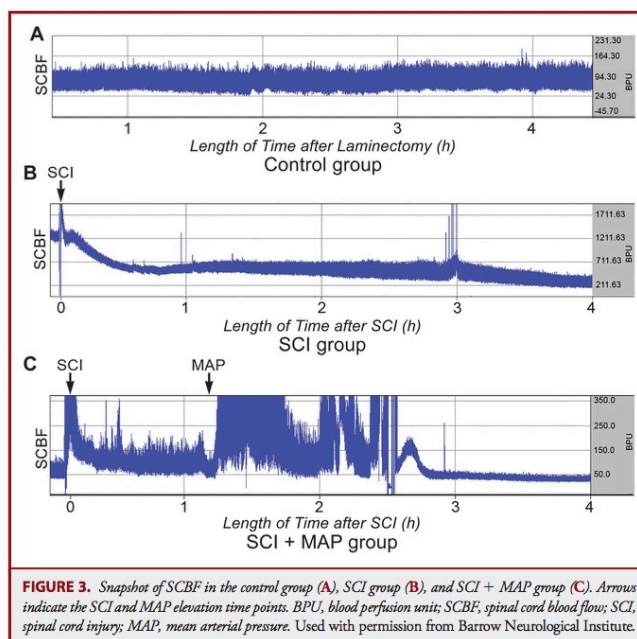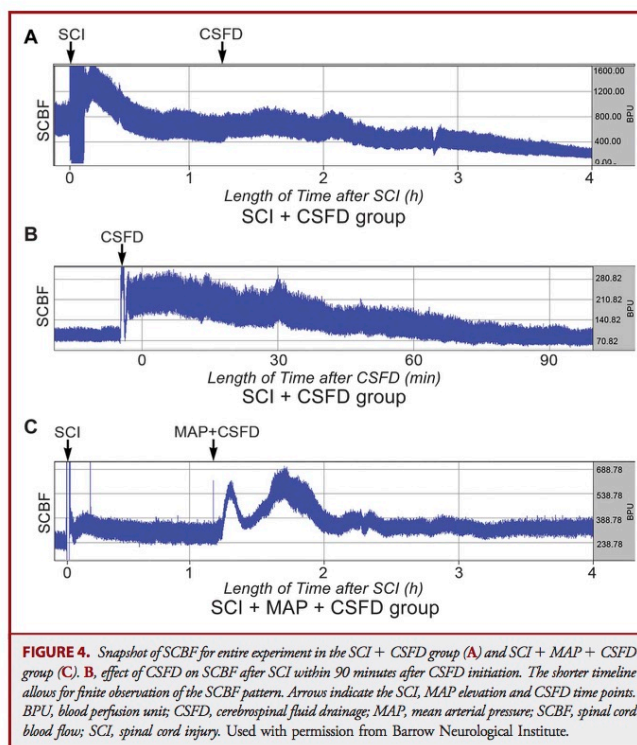
corresponds to the time course of loss of autoregulation and ischemia.[6,23] We implemented aggressive elevation of MAP to reach levels beyond autoregulation limits. This allowed us to maximize the effect on SCBF. However, as described previously, elevation of MAP beyond autoregulation level resulted in elevation of ITP. Overall, treatment with induced hypertension resulted in short-term improvement of SCBF. However, SCBF did not reach pre-SCI levels. As ITP pressure continued to rise, SCBF decreased and the spinal cord was left relatively ischemic (Figures 1, 2, 3C, 5). Addition of CSFD to MAP therapy in the SCI + MAP + CSFD group 1 hour after SCI resulted in significant improvement of SCBF. The SCBF improved and stayed above pre-SCI levels throughout the experiment. Furthermore, there was a statistically significant difference in SCBF between the SCI group and the SCI + MAP and the SCI + MAP + CSFD groups (Figures 1, 3, 4; Table). Analysis of the effect of CSF drainage on SCI (SCI + CSFD) revealed short-term improvement of SCBF without reaching pre-SCI values, similar to the SCI + MAP group (Figures 4C, 5). This effect could be attributed to the decompression of the venous system, improving outflow and decreasing vascular resistance. However, alteration of autoregulation and worsening of ischemia resulted in overall decrease in SCBF. According to our results, neither sustained MAP (SCI group) nor its elevation (SCI + MAP

group) resulted in lasting improvement in SCBF in the setting of acute SCI (Figures 1, 3B and C; Table). Moreover, the spinal cord remained relatively hypoperfused.

The main purpose of this study was to perform an observation of physiological parameters following acute SCI. In our experiments, animals were euthanized 4 hours after SCI (immediate and early acute phase). According to previous reports, we could expect differences on the molecular level.[3] However, given the relatively short time of observation, we did not expect to detect significant histological differences between study groups in this experiment.

Our initial experiment was intended to investigate short-term pathophysiological changes with a combination of CSFD and MAP. These experiments are very cumbersome and require substantial financial and infrastructural resources. It would not be feasible to perform experiments with as long a monitoring time for as many animal groups as was presented in the current investigation. On the basis of the results of this study, we plan to conduct an investigation exploring the long-term effects of CSFD and MAP in pigs. We are planning to monitor animals for 24 hours after injury. The animals will be under general anesthesia for the time of the experiment. This will allow more prominent histological changes to occur in the injured spinal cord. We are planning to use advanced methods of SCBF monitoring in our

137

FIGURE 4. *Snapshot of SCBF for entire experiment in the SCI + CSFD group (**A**) and SCI + MAP + CSFD group (**C**). **B**, effect of CSFD on SCBF after SCI within 90 minutes after CSFD initiation. The shorter timeline allows for finite observation of the SCBF pattern. Arrows indicate the SCI, MAP elevation and CSFD time points. BPU, blood perfusion unit; CSFD, cerebrospinal fluid drainage; MAP, mean arterial pressure; SCBF, spinal cord blood flow; SCI, spinal cord injury.* Used with permission from Barrow Neurological Institute.

future experiments. Very recent advances in technology allow for continuous/repetitive SCBF monitoring deeper into the parenchyma of the spinal cord.[28,29] However, local regulations preclude the performance of long-term survival studies of pigs with SCI.

Limitations

Laser Doppler flowmetry (LDF) was used to assess SCBF in our study. This technique was the only reliable and validated method available for continuous SCBF monitoring when we designed and started our experiments. It has been validated and used in multiple studies previously.[30-39]

Other more precise methods to measure SCBF (eg, hydrogen clearance, microspheres) require animal euthanization and provide data at a single time point.[40,41] The goal of our study was to monitor SCBF changes after each step of the experiment (baseline before SCI, and at 1-hour, 2-hour, 3-hour, and 4-hour time points). To euthanize an animal at each time point would have required using 5 times as many animals (75 pigs instead of 15). Therefore, these methods were not feasible for our study.

Our data represent superficial SCBF, and therefore could not assess the SCBF deep within the parenchyma. LDF allowed measurement of blood flow at a comparably small depth (up to 1.5 mm), which is a limitation of this technology.[42,43] The pattern of superficial SCBF changes that we observed in the treatment groups may potentially be applicable to deep structures. Nevertheless, the majority of the spinal cord contains eloquent tissue and the protection of any tissue from secondary injury may greatly affect a patient's functional recovery.

CONCLUSION

In our study of 15 pigs, we found that SCI did not increase ITP, but that the elevation of MAP did, leading to a decrease in spinal cord perfusion pressure. Both MAP elevation alone and CSFD alone led to only short-term improvement of SCBF followed by hypoperfusion. However, the combination of MAP elevation and CSFD improved SCBF at the injury site—appearing to prevent hypoperfusion of the spinal cord after SCI. Such an outcome, if replicated in human patients, could

138
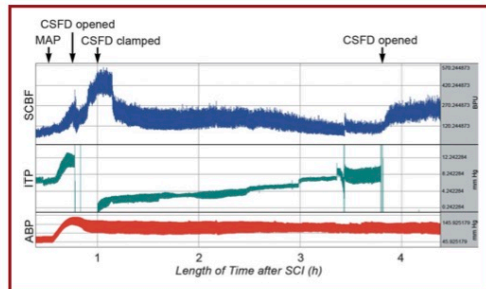
FIGURE 5. *Effect of cerebrospinal fluid drainage (CSFD) and MAP elevation on typical monitoring parameters after SCI. In this test procedure, CSFD was stopped after 40 minutes, and restarted 3 hours later. Arrows indicate the MAP elevation and consecutive initiation and termination of CSFD time points. ABP, arterial blood pressure; BPU, blood perfusion unit; CSFD, cerebrospinal fluid drainage; ITP, intrathecal pressure; MAP, mean arterial pressure; SCBF, spinal cord blood flow; SCI, spinal cord injury. Used with permission from Barrow Neurological Institute.*

potentially decrease spinal cord damage and improve clinical outcomes. Although LDF provides flow measurements to a tissue depth of only 1.5 mm, these results may represent a pattern of blood flow changes in the entire spinal cord after injury. We are currently contemplating a clinical trial based on a review of the literature and the results of our experiments.

Disclosure

The authors have no personal, financial, or institutional interest in any of the drugs, materials, or devices described in this article.

REFERENCES

1. Hadley MN, Walters BC, Aarabi B, et al. Clinical assessment following acute cervical spinal cord injury. *Neurosurgery.* 2013;72(suppl 2):40-53.
2. Burke DA, Linden RD, Zhang YP, Maiste AC, Shields CB. Incidence rates and populations at risk for spinal cord injury: A regional study. *Spinal Cord.* 2001;39(5):274-278.
3. Rowland JW, Hawryluk GW, Kwon B, Fehlings MG. Current status of acute spinal cord injury pathophysiology and emerging therapies: promise on the horizon. *Neurosurg Focus.* 2008;25(5):E2.
4. Guha A, Tator CH, Rochon J. Spinal cord blood flow and systemic blood pressure after experimental spinal cord injury in rats. *Stroke.* 1989;20(3):372-377.
5. Martirosyan NL, Feuerstein JS, Theodore N, Cavalcanti DD, Spetzler RF, Preul MC. Blood supply and vascular reactivity of the spinal cord under normal and pathological conditions. *J Neurosurg Spine.* 2011;15(3):238-251.
6. Kobrine AI, Doyle TF, Martins AN. Autoregulation of spinal cord blood flow. *Clin Neurosurg.* 1975;22:573-581.
7. Smith AJ, McCreery DB, Bloedel JR, Chou SN. Hyperemia, CO2 responsiveness, and autoregulation in the white matter following experimental spinal cord injury. *J Neurosurg.* 1978;48(2):239-251.
8. Dohrmann GJ, Wick KM, Bucy PC. Spinal cord blood flow patterns in experimental traumatic paraplegia. *J Neurosurg.* 1973;38(1):52-58.
9. Casha S, Christie S. A systematic review of intensive cardiopulmonary management after spinal cord injury. *J Neurotrauma.* 2011;28(8):1479-1495.
10. Ploumis A, Yadlapalli N, Fehlings MG, Kwon BK, Vaccaro AR. A systematic review of the evidence supporting a role for vasopressor support in acute SCI. *Spinal Cord.* 2010;48(5):356-362.
11. Fehlings MG, Vaccaro A, Wilson JR, et al. Early versus delayed decompression for traumatic cervical spinal cord injury: results of the Surgical Timing in Acute Spinal Cord Injury Study (STASCIS). *PLoS One.* 2012;7(2):e32037.
12. Ryken TC, Hurlbert RJ, Hadley MN, et al. The acute cardiopulmonary management of patients with cervical spinal cord injuries. *Neurosurgery.* 2013;72(suppl 2):84-92.
13. Vale FL, Burns J, Jackson AB, Hadley MN. Combined medical and surgical treatment after acute spinal cord injury: results of a prospective pilot study to assess the merits of aggressive medical resuscitation and blood pressure management. *J Neurosurg.* 1997;87(2):239-246.
14. Horn EM, Theodore N, Assina R, Spetzler RF, Sonntag VK, Preul MC. The effects of intrathecal hypotension on tissue perfusion and pathophysiological outcome after acute spinal cord injury. *Neurosurg Focus.* 2008;25(5):E12.
15. Dididze M, Green BA, Dietrich WD, Vanni S, Wang MY, Levi AD. Systemic hypothermia in acute cervical spinal cord injury: a case-controlled study. *Spinal Cord.* 2013;51(5):395-400.
16. Svensson LG, Crawford ES, Hess KR, Coselli JS, Safi HJ. Experience with 1509 patients undergoing thoracoabdominal aortic operations. *J Vasc Surg.* 1993;17(2):357-368; discussion 368-370.
17. Khan SN, Stansby G. Cerebrospinal fluid drainage for thoracic and thoracoabdominal aortic aneurysm surgery. *Cochrane Database Syst Rev.* 2012;10:CD003635.
18. Francel PC, Long BA, Malik JM, Tribble C, Jane JA, Kron IL. Limiting ischemic spinal cord injury using a free radical scavenger 21-aminosteroid and/or cerebrospinal fluid drainage. *J Neurosurg.* 1993;79(5):742-751.
19. Kwon BK, Curt A, Belanger LM, et al. Intrathecal pressure monitoring and cerebrospinal fluid drainage in acute spinal cord injury: a prospective randomized trial. *J Neurosurg Spine.* 2009;10(3):181-193.
20. Hickey R, Albin MS, Bunegin L, Gelineau J. Autoregulation of spinal cord blood flow: is the cord a microcosm of the brain? *Stroke.* 1986;17(6):1183-1189.
21. Kindt GW. Autoregulation of spinal cord blood flow. *Eur Neurol.* 1971-1972;6(1):19-23.
22. Kobrine AI, Evans DE, Rizzoli HV. The role of the sympathetic nervous system in spinal cord autoregulation. *Acta Neurol Scand Suppl.* 1977;64:54-55.
23. Senter HJ, Venes JL. Loss of autoregulation and posttraumatic ischemia following experimental spinal cord trauma. *J Neurosurg.* 1979;50(2):198-206.
24. Mokri B. The Monro-Kellie hypothesis: applications in CSF volume depletion. *Neurology.* 2001;56(12):1746-1748.
25. Piano G, Gewertz BL. Mechanism of increased cerebrospinal fluid pressure with thoracic aortic occlusion. *J Vasc Surg.* 1990;11(5):695-701.
26. Brown PD, Davies SL, Speake T, Millar ID. Molecular mechanisms of cerebrospinal fluid production. *Neuroscience.* 2004;129(4):957-970.
27. Kobrine AI, Doyle TF, Martins AN. Local spinal cord blood flow in experimental traumatic myelopathy. *J Neurosurg.* 1975;42(2):144-149.
28. Mesquita RC, D'Souza A, Bilfinger TV, et al. Optical monitoring and detection of spinal cord ischemia. *PLoS One.* 2013;8(12):e83370.
29. Soubeyrand M, Laemmel E, Dubory A, Vicaut E, Court C, Duranteau J. Real-time and spatial quantification using contrast-enhanced ultrasonography of spinal cord perfusion during experimental spinal cord injury. *Spine (Phila Pa 1976).* 2012;37(22):E1376-E1382.
30. Blaser A, Lang J, Henke D, Doherr MG, Adami C, Forterre F. Influence of durotomy on laser-Doppler measurement of spinal cord blood flow in chondrodystrophic dogs with thoracolumbar disk extrusion. *Vet Surg.* 2012;41(2):221-227.
31. Brady KM, Lee JK, Kibler KK, et al. The lower limit of cerebral blood flow autoregulation is increased with elevated intracranial pressure. *Anesth Analg.* 2009;108(4):1278-1283.
32. Lindsberg PJ, Jacobs TP, Frerichs KU, Hallenbeck JM, Feuerstein GZ. Laser-Doppler flowmetry in monitoring regulation of rapid microcirculatory changes in spinal cord. *Am J Physiol.* 1992;263(1 pt 2):H285-H292.
33. Modi HN, Suh SW, Hong JY, Yang JH. The effects of spinal cord injury induced by shortening on motor evoked potentials and spinal cord blood flow: an experimental study in swine. *J Bone Joint Surg Am.* 2011;93(19):1781-1789.
34. Olive JL, McCully KK, Dudley GA. Blood flow response in individuals with incomplete spinal cord injuries. *Spinal Cord.* 2002;40(12):639-645.

139

APPENDIX D

CURRICULUM VITAE

EDUCATION AND POSTGRADUATE TRAINING

09/99-06/05   Doctor of Medicine with Honors, First Moscow State Medical University, Moscow, Russia

06/05-06/08   Resident, Department of Neurological Surgery, Burdenko Neurosurgical Institute, Moscow, Russia

06/08-06/12   Research Fellow, Division of Neurological Surgery, Barrow Neurological Institute, Phoenix, Arizona

07/12-Current Resident, Division of Neurological Surgery, University of Arizona, Tucson, Arizona

07/13-Current Graduate Student in Neuroscience, Arizona State University, Tempe, Arizona

HONORS AND AWARDS

2014   Philip Carter Award, Arizona Neurosurgical Society

2014   Mayfield Award, Congress of Neurological Surgeons/American Association of Neurological Surgeons

2014   DePuy Synthes Award, American Association of Neurosurgical Surgeons

2012   John Green Award, Arizona Neurosurgical Society.

2009   Synthes Resident Spine Award, American Association of Neurosurgical Surgeons

RESEARCH GRANTS

2014-2018 Department of Defense; Investigator (PI-Nicholas Theodore, MD), "A multicenter, randomized, controlled, trial of cerebrospinal fluid drainage in acute spinal cord injury"; Amount: $1,600,000

PATENT

Georges J, **Martirosyan N**, Nakaji P. System and Method for Diagnosis of Astrocytic Brain Tumors: US Patent 20,150,104,395; 2015

BOOK

Gevorkov AR, **Martirosyan NL**, Eliava ShSh, Didikin SS "Microsurgery Basics" (in Russian). Geotar-Media. Moscow. November 2008.

BOOK CHAPTERS

Martirosyan NL, Theodore N. Spinal Cord Transection. Encyclopedia of the Neurological Sciences, 2nd Edition. Elsevier. 2014.

Martirosyan NL, Neckrysh S, Charbel FT, Theodore N, Lemole GM. Vascular lesion of

the spinal cord. Surgical anatomy and techniques to the spine. Elsevier. 2013: 646-660.

SELECT PUBLICATIONS (from over 40)

Martirosyan NL, Skoch JM, Zaninovich O, Zoccali C, Galgiani JN, Baaj AA. A paradigm for the evaluation and management of spinal coccidioidomycosis. Surg Neurol Int. 2015 Jun 17;6:107.

Martirosyan NL, Kalani MY, Lemole GM Jr, Spetzler RF, Preul MC, Theodore N. Microsurgical anatomy of the arterial basket of the conus medullaris. J Neurosurg Spine. 2015 Mar 6:1-5.

Martirosyan NL, Skoch J, Watson JR, Lemole GM Jr, Romanowski M, Anton R. Integration of Indocyanine Green Videoangiography With Operative Microscope: Augmented Reality for Interactive Assessment of Vascular Structures and Blood Flow. Neurosurgery. 2015 Feb 12.

Martirosyan NL, Kalani MY, Bichard WD, Baaj AA, Gonzalez FL, Preul MC, Theodore N. Cerebrospinal Fluid Drainage and Induced Hypertension Improve Spinal Cord Perfusion After Acute Spinal Cord Injury in Pigs. Neurosurgery. 2015 Jan 23.

Kalb S, Zaidi HA, Ribas-Nijkerk JC, Sindhwani MK, Clark JC, **Martirosyan NL,** Theodore N. Persistent Outpatient Hypertension is Independently Associated with Spinal Cord Dysfunction and Imaging Characteristics of Spinal Cord Damage among Patients with Cervical Spondylosis. World neurosurgery. 2015.

Georges J, Zehri A, Carlson E, Nichols J, Mooney MA, **Martirosyan NL,** Ghaffari L, Kalani MY, Eschbacher J, Feuerstein B, Anderson T, Preul MC, Van Keuren-Jensen K, Nakaji P. Label-free microscopic assessment of glioblastoma biopsy specimens prior to biobanking. Neurosurg Focus. 2014 Feb;36(2):E8.

Martirosyan NL, Georges J, Eschbacher JM, Cavalcanti DD, Elhadi AM, Abdelwahab MG, Scheck AC, Nakaji P, Spetzler RF, Preul MC. Potential application of a handheld confocal endomicroscope imaging system using a variety of fluorophores in experimental gliomas and normal brain. Neurosurg Focus. 2014 Feb;36(2):E16.

Fenton KE, **Martirosyan NL,** Abdelwahab MG, Coons SW, Preul MC, Scheck AC. In vivo visualization of GL261-luc2 mouse glioma cells by use of Alexa Fluor-labeled TRP-2 antibodies. Neurosurg Focus. 2014 Feb;36(2):E12.

Maughan P, Ducruet AF, Elhadi AM, **Martirosyan NL,** Garrett M, Mushtaq R, Albuquerque FC, Theodore N. Multimodality Management of Vertebral Artery Injury Sustained During Cervical or Craniocervical Surgery. Neurosurgery. 2013 May 29.

Behbahaninia M, **Martirosyan NL,** Georges J, Udovich JA, Kalani MY, Feuerstein BG, Nakaji P, Spetzler RF, Preul MC. Intraoperative fluorescent imaging of intracranial tumors: a review. Clin Neurol Neurosurg. 2013 May;115(5):517-28.

Martirosyan NL, Kingery MT, Theodore N. Management of Type II Odontoid Fractures. Contemporary Neurosurgery 35 (1), 1-4. 2013

Kalani MY, Kalb S, **Martirosyan NL,** Lettieri SC, Spetzler RF, Porter RW, Feiz-Erfan I. Cerebral revascularization and carotid artery resection at the skull base for treatment of advanced head and neck malignancies. J Neurosurg. 2012 Oct 19.

Eschbacher J, **Martirosyan NL,** Nakaji P, Sanai N, Preul MC, Smith KA, Coons SW, Spetzler RF. In vivo intraoperative confocal microscopy for real-time histopathological imaging of brain tumors. J Neurosurg. 2012 Apr;116(4):854-60. Epub 2012 Jan 27. PMID: 22283191

Kalani MY, **Martirosyan NL,** Eschbacher JM, Nakaji P, Albuquerque FC, Spetzler RF. Large hemangiopericytoma associated with arteriovenous malformations and dural arteriovenous fistulae. World Neurosurg. 2011 Dec;76(6):592.e7-10. PMID: 22251512

Martirosyan NL, Kalb S, Cavalcanti DD, Lochhead RA, Uschold TD, Loh A, Theodore N. Comparative Analysis of Isocentric 3-dimensional C-arm Fluoroscopy and Biplanar Fluoroscopy for Anterior Screw Fixation in Odontoid Fractures. J Spinal Disord Tech. 2011 Dec 5. PMID: 22158300

Kalani MY, **Martirosyan NL,** Little AS, Kakarla UK, Theodore N. Tumoral calcinosis presenting as a deformity of the thoracic spine. J Neurosurg Pediatr. 2011 Dec;8(6):584-7. PMID: 22132916

Kalani MY, Ahmed A, **Martirosyan NL,** Cronk K, Moon K, Albuquerque FC, McDougall CG, Spetzler RF, Bristol RE. Surgical and Endovascular Treatment of Pediatric Spinal Arteriovenous Malformations. World Neurosurg. 2011 Nov 1. PMID: 22120563

Kalani MY, Filippidis A, **Martirosyan NL,** Theodore N. Cerebral Herniation as a Complication of Chest Tube Drainage of Cerebrospinal Fluid After Injury to the Spine. World Neurosurg. 2011 Nov 7. PMID: 22120389

Kalb S, **Martirosyan NL,** Kalani MY, Broc GG, Theodore N. Genetics of the Degenerated Intervertebral Disc. World Neurosurg. 2011 Nov 7. PMID: 22120330

Cavalcanti DD, Kalani MY, **Martirosyan NL,** Eales J, Spetzler RF, Preul MC. Cerebral cavernous malformations: from genes to proteins to disease. J Neurosurg. 2012 Jan;116(1):122-32. Review. PMID: 21962164

Martirosyan NL, Cavalcanti DD, Eschbacher JM, Delaney PM, Scheck AC, Abdelwahab MG, Nakaji P, Spetzler RF, Preul MC. Use of in vivo near-infrared laser

confocal endomicroscopy with indocyanine green to detect the boundary of infiltrative tumor. J Neurosurg. 2011 Dec;115(6):1131-8. PMID: 21923240

Martirosyan NL, Cavalcanti DD, Kalani MY, Maughan PH, Theodore N. Aplasia of the anterior arch of atlas associated with multiple congenital disorders: case report. Neurosurgery. 2011 Dec;69(6):E1317-20. PMID: 21712741

Martirosyan NL, Feuerstein JS, Theodore N, Cavalcanti DD, Spetzler RF, Preul MC. Blood supply and vascular reactivity of the spinal cord under normal and pathological conditions. J Neurosurg Spine. 2011 Sep;15(3):238-51. Review. PMID: 21663407

Kalb S, **Martirosyan NL,** Perez-Orribo L, Kalani MY, Theodore N. Analysis of demographics, risk factors, clinical presentation, and surgical treatment modalities for the ossified posterior longitudinal ligament. Neurosurg Focus. 2011 Mar;30(3):E11. PMID: 21361749

Cavalcanti DD, **Martirosyan NL,** Verma K, Safavi-Abbasi S, Porter RW, Theodore N, Sonntag VK, Dickman CA, Spetzler RF. Surgical management and outcome of schwannomas in the craniocervical region. J Neurosurg. 2011 May;114(5):1257-67. PMID: 20617880

Martirosyan NL, Bennett KM, Theodore N, Preul MC. Manganese-enhanced magnetic resonance imaging in experimental spinal cord injury: correlation between T1-weighted changes and Mn(2+) concentrations. Neurosurgery. 2010 Jan;66(1):131-6. PMID: 20023543

ORAL PRESENTATIONS

Martirosyan NL, Kalani MY, Bichard WD, Baaj AA, Gonzalez LF, Spetzler RF, Preul MC, Theodore N. Cerebrospinal fluid drainage and Induced hypertension improve spinal cord perfusion in the setting of acute Spinal cord injury. American Association of Neurological Surgeons, Spine section 2014

Martirosyan NL, Theodore N, Kalani MY, Bichard WD, Baaj AA, Spetzler RF, Preul MC. Cerebrospinal fluid drainage and increased mean arterial blood pressure improve outcome after spinal cord injury. Arizona Neurosurgical Society, 2012

Martirosyan NL, Eschbacher JM, Delaney PM, Nakaji P, Preul MC, Spetzler RF. Histopathologic features of brain tumors revealed with in vivo intraoperative fiber-optic confocal laser endomicroscopy using fluorescein sodium in humans. AANS 2011.

Martirosyan NL, Cavalcanti DD, Eschbacher JM, Delaney PM, Scheck AC, Abdelwahab MG, Nakaji P, Spetzler RF, Preul MC. Use of Indocyanine Green Near-infrared Laser Confocal Endomicroscopy In Vivo: Potential to Intraoperatively Detect the Boundary of Infiltrative Tumor. (Top Ten CNS abstract). **Neurosurgery;** August 2010:67(2):562.

Martirosyan NL, Cavalcanti DD, Eschbacher JM, Delaney PM, Abdewahab MG, Scheck AC, Hattendorf G, Nakaji P, Spetzler RF, Preul MC. Advances in Handheld Confocal Microscopy. Barrow Neurological Inst. Grand Rounds. March 2010. Phoenix, AZ, USA.

Martirosyan NL, Bennett KM, Theodore N, Preul MC. Manganese enhanced MRI to detect spinal cord injury. International Society for Magnetic Resonance in Medicine. Annual meeting. April. 2009. Honolulu, Hawaii, USA.

APPENDIX E

PERMISSIONS

PERMISSIONS

All articles in this dissertation were used with permission from all co-authors.